Development of OTM Syngas Process and Testing of Syngas Derived Ultra-clean Fuels in Diesel Engines and Fuel Cells

Budget Period 2

Topical Report

For Reporting Period Starting November 1, 2001 and Ending December 31, 2002

Principal Authors:
E.T. (Skip) Robinson, Principal Investigator, Torix
James P. Meagher, Program Administrator, Praxair
Prasad Apte, Ceramic Manufacturing Manager, Praxair
Xingun Gui, Chief Engineer, Advanced Combustion and Control, International Truck and Engine Corp.
Tytus R. Bulicz, Project Development Engineer, International Truck and Engine Corp.
Siv Aasland, Staff Engineer, Statoil
Charles Besecker, Senior Chemist, BP America
Jack Chen, Senior Development Associate, Praxair
Bart A. van Hassel, Senior Development Associate, Praxair
Olga Polevaya, Manager Process Engineering, Nuvera Fuel Cells
Rafey Khan, Senior Engineer, Nuvera Fuel Cells
Piyush Pilaniwalla, Engineer, Nuvera Fuel Cells

Report Issue Date: February 2003

DOE Cooperative Agreement No. DE-FC26-01NT41096

Submitting Organizations:

Primary: Praxair, Inc.
P.O. Box 44
175 East Park Drive
Tonawanda, NY 14150

Subcontractors: BP America Production Company
150 W. Warrenville Road
Mail Code H-5
Naperville, IL 60566

International Truck and Engine Corp.
10400 W. North Avenue
Melrose Park, IL 60160

Statoil
Arkitekt Ebbels veg 10, Rotvoll
N-7005 Trondheim, Norway

Torix, Inc.
7165 Hart St., Suite B
Mentor, OH 44060

Nuvera Fuel Cells
15 Acorn Park
Cambridge, MA 02140

DISCLAIMER

ABSTRACT

This topical report summarizes work accomplished for the Program from November 1, 2001 to December 31, 2002 in the following task areas:

Task 1: Materials Development
Task 2: Composite Development
Task 4: Reactor Design and Process Optimization
Task 8: Fuels and Engine Testing
    8.1 International Diesel Engine Program
    8.2 Nuvera Fuel Cell Program
Task 10: Program Management

Major progress has been made towards developing high temperature, high performance, robust, oxygen transport elements. In addition, a novel reactor design has been proposed that co-produces hydrogen, lowers cost and improves system operability.

Fuel and engine testing is progressing well, but was delayed somewhat due to the hiatus in program funding in 2002. The Nuvera fuel cell portion of the program was completed on schedule and delivered promising results regarding low emission fuels for transportation fuel cells. The evaluation of ultra-clean diesel fuels continues in single cylinder (SCTE) and multiple cylinder (MCTE) test rigs at International Truck and Engine. FT diesel and a BP oxygenate showed significant emissions reductions in comparison to baseline petroleum diesel fuels.

Overall through the end of 2002 the program remains under budget, but behind schedule in some areas.

TABLE OF CONTENTS

List of Tables

List of Figures

List of Acronyms

BPO	BP Oxygenate
BSFC	Brake Specific Fuel Consumption
F-T	Fischer-Tropsch
HCCI	Homogeneous Charge Compression Ignition
LCM	Lead candidate material
MM	Alternative material systems
OTM	Oxygen Transport Membrane
P-0	Small bench scale test reactors capable of testing single OTM tubes up to 8 inches in length at elevated pressures and temperature.
SCTE	Single Cylinder Test Engine
MCTE	Multi-Cylinder Test Engine
TF	Target Flux
TFd	Target flux for dense disks
TFc	Target flux for composite systems
TP	Target Pressure
TT	Target Temperature
ULS	Ultra-low Sulfur
Target A	High severity process conditions
Target B	Low severity process conditions

1.0 Executive Summary

This program has two primary objectives: 1) development of an advanced, low cost syngas technology based on ceramic oxygen transport membranes and 2) the evaluation of syngas derived ultra-clean fuels in Nuvera fuel cells; and the development of advanced compression ignition engines /after- treatment/ultra-clean fuel systems.

This report covers the period November 1, 2001 through December 31, 2002. Under the revised scope of work for this budget period, work will be performed only in Tasks 1, 2, 4, 8 and 10.

Under objective 1, major progress has been made towards developing high performance, robust oxygen transport elements for high temperature operation. The operating window of these new systems has been expanded dramatically, with tests successfully completed at 1.1TT and 2.2TP. In addition, a new flexible, reactor design has been proposed that lowers cost, improves system operability and can co-produce hydrogen.

Under objective 2, the fuel cell portion of the program was completed. The evaluation of ultra-clean diesels continues in the SCTE and MCTE rigs. Both FT diesel and the BP oxygenate dramatically reduce emissions (NOX, unburned hydrocarbon) in comparison to a baseline No.2 diesel and an ultra-low diesel fuel without the BP oxygenate.

Task 1, Materials Development
Two new high temperature robust substrates, LCM29 and MM1, have been discovered. These materials exhibit low creep and excellent strength at high temperature. In addition, a new suite of high flux OTM materials has been developed with thermal expansion characteristics that are compatible with the new high temperature substrates. This new portfolio of substrate and membrane materials is key to developing high performance, long life OTM elements.

Task 2, Composite Element Development
Composite elements based on the two new substrates, LCM29 and MM1, and the advanced OTM materials have been fabricated and tested in disk reactors. Both systems have survived life tests that include multiple thermal cycles and extended operation (over 500 hundred hours) at extremely high temperatures, 1.1TT. Work is now focusing on developing and optimizing the element architecture to maximize oxygen flux and durability. Several new element architectures now under development have survived multiple rapid thermal cycles in an oven thermal cycling test. These designs will be evaluated under full flux conditions in the next quarter.

Task 4, Reactor Design and Process Optimization
Proprietary engineering studies evaluated the impact of porosity, tortuosity and wall thickness on flux rate. Design ranges for tube internal diameter, porosity, tortuosity and material creep rate were derived that satisfy both creep/buckling lifetime targets and oxygen flux targets.

A novel reactor design concept was modeled. This system offers lower capital cost, improved operability, and flexibility to produce hydrogen as well as syngas for FTGL applications.

A new high pressure P-0 rig has been commissioned and operated at BP. A dense LCM1 tube performed well at the extreme conditions of 2.2TP and 1 TT.

Task 8, Fuels and Engine Testing
SCTE evaluations of four fuels were completed: 1) No.2 diesel, 2) FT diesel, 3) an ultra-low sulfur (ULS) petroleum diesel and 4) the same ULS diesel with BP oxygenate blend to 10% oxygen. The test focused on the four modes of the HDFTP emission certification cycle (4, 6, 7, 8) considered to be the most significant contributors to air emissions. The FT diesel showed significant reductions in NOx and unburned hydrocarbon for all four test modes and operating conditions. Soot reductions were achieved for modes 6 and 7 and for most of the operating conditions in 4 and 8.
The effectiveness of a BP oxygenate (BPO) was evaluated in a ULS fuel blended to a 10% level of chemical oxygen. The oxygenated fuel showed significant reductions in soot and NOx at all modes and operating conditions tested. However brake specific fuel consumption increased due to the lower heating value of the fuel and perhaps other inefficiencies. More tests are planned at intermediate levels of oxygen.

The Nuvera fuel cell program was completed. The second phase of this program evaluated effect of three fuel candidates for transportation fuel cells: 1) a California Phase II RFG, 2) a GTL naphtha and 3) a GTL naphtha with BPO blended to 1.74% chemical oxygen. The BPO showed significant reductions in both start-up and steady state NOx levels in comparison to both the GTL naphtha and the RFG. The GTL naphtha was slightly better than the RFG in CO and slightly worse in THC.

Task 10, Project Management
The project remains under budget, but behind schedule in certain tasks.
All reports and briefings were completed on time. Some delays were incurred due to a 5 month hiatus between completion of Budget Period 1 and approval for Budget Period 2. More recently, availability of BPO for fuel blending has impacted schedule. Most tasks should be brought back on schedule in 2003.

2.0 Introduction

The DOE's Office of Fossil Energy created strategic partnerships targeted at the development and verification of advanced fuel-making processes that utilize fossil feedstocks. These processes will enable the production of ultra-clean transportation fuels that improve the environment, while also expanding and diversifying the fossil resource base. In response to the DOE's solicitation for research and development leading to the production of ultra-clean transportation fuels from fossil resources, Cooperative Agreement number DE-FC26-01NT41096 for work entitled "Development of OTM Syngas Process and Testing of Syngas-Derived Ultra-clean Fuels in Diesel Engines and Fuel Cells" was awarded to Praxair.

The objectives of this project are: (1) develop an advanced syngas technology, based on Oxygen Transport Membranes (OTMs), that will provide a step change reduction in the cost of converting natural gas to a spectrum of liquid transportation fuels and thereby improve the prospects for meeting vehicle emissions targets with cost competitive ultra clean transportation fuels (UCTFs); (2) evaluate the performance of, and emissions from selected syngas-derived UCTFs in advanced vehicle propulsion systems, including advanced diesel engines with post treatment and fuel cells; and 3) develop an optimized UCTF/diesel engine/exhaust after treatment system capable of meeting 2007 emission regulations.

The program will follow a systems approach as shown below, encompassing natural gas pre-treatment, syngas generation, liquid fuel production, product work-up/blending, and validation of the UCTF in engine tests including aftertreatment of emissions.

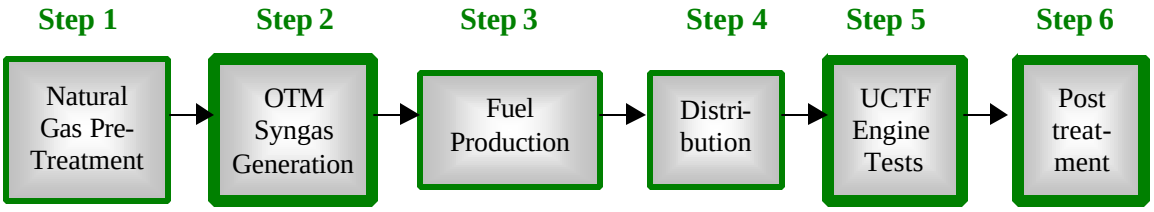

Systems Approach to UCTF

The 60-month project includes three parallel development or testing programs: 1) OTM syngas reactor and reactor components, OTM element fabrication and OTM syngas process development; 2) testing and co-optimization of UCTF in International Truck and Engine advanced diesel engines with exhaust post treatment; and 3) emission testing of UCTFs in a Nuvera transportation fuel cell power system. Performance objectives include:

- OTM Syngas Technology: lower capital costs, lower operating costs, lower emissions and smaller footprint compared to conventional syngas plants.
- UCTF in Advanced Diesel Engines: co-optimized system of syngas derived UCTF, diesel engine and post treatment technology targeting proposed 2007

regulations for light and medium duty engines i.e. diesel fuel sulfur < 15 ppm; light duty engine emissions: NOx < 0.2 g/mi, PM < 0.01 g/mi; and heavy duty engines NOx < 0.2 g/mi and PM < 0.02 g/bhp. UCTF should enable compliance with these objectives and/or lower vehicle costs.

- UCTF in Nuvera fuel cell system: lower air emissions (on a per mile basis) based on UCTF properties such as ultra low sulfur, high aliphatic content and oxygen content.

The program has 10 major tasks, seven of which are focused on syngas technology development, one task is devoted to fuel and engine testing and optimization, one task addresses the marketing and commercialization of an UCTF system, and the final task is for program management and cost control.

The Cooperative Agreement was signed by the DOE's Contracting Officer on May 21, 2001. This Topical Report includes results and discussions for work conducted November 1, 2001 through December 31, 2002.

3.0 Progress and Results by Task

3.1 Task 1: Materials Development

3.1.1 Goal - Task 1

The Recipient shall fabricate, test and characterize OTM film and substrate materials with goal of developing a more robust and cost effective OTM element in comparison to the lead candidate material, LCM1.

3.1.2 Experimental - Task 1

The experimental facilities and methods in Task 1 were described in detail in the Topical Report for Budget Period 1 [Ref. 1].

3.1.3 Results and Discussion – Task 1

The goal of this task is to develop superior materials for fabricating OTM elements. The approach is to focus on two subsets of materials, substrate materials and oxygen transport membrane (OTM) materials, for building composite or laminated elements. The substrate provides a robust foundation for the thin film OTM layer. Key characteristics of the substrate are: high temperature strength, creep resistant, stability in both oxidizing and reducing atmospheres and low reactivity with the OTM materials. The substrate does not have to conduct oxygen ions, but must be sufficiently porous to allow gas species to diffuse to the OTM membrane surface. Thus strength and permeability of the substrate material in porous form are equally important.

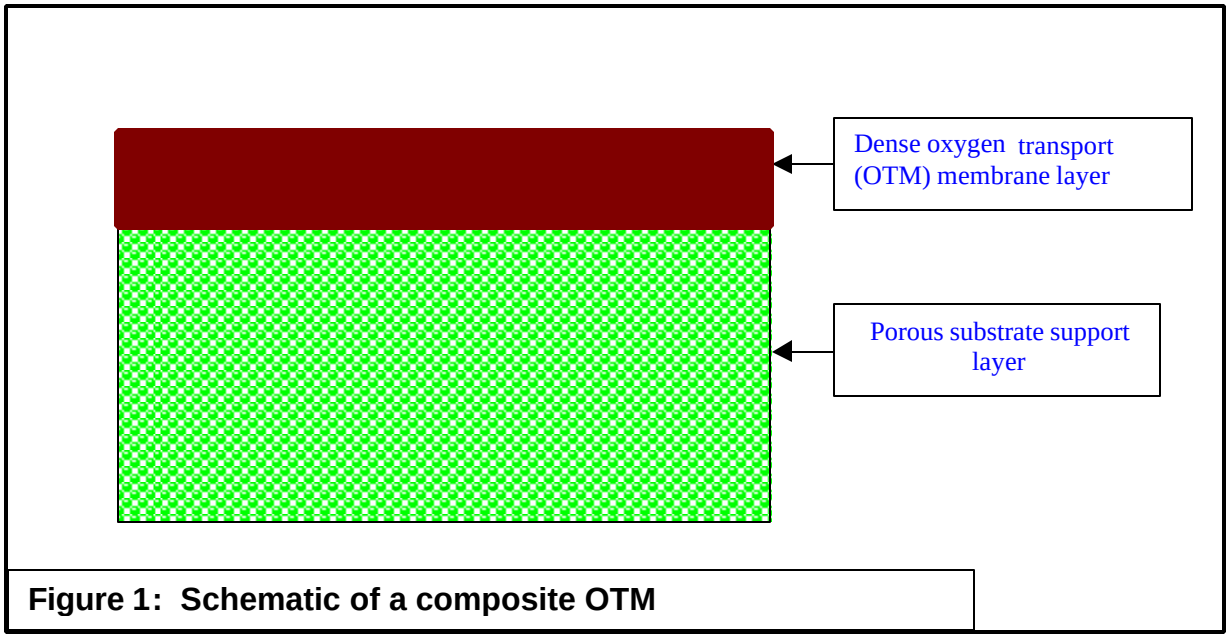

Figure 1: Schematic of a composite OTM

The OTM layer does the work of separating oxygen from air as shown in Figure 2. The dense OTM layer must seal the porous substrate, withstand a pressure differential of 15 to 40 bar and conduct oxygen. The key characteristics of OTM materials are oxygen ion and electronic conductivity (usually measured together and reported as oxygen flux), high temperature stability under both oxidizing and reducing conditions, high temperature strength, volumetric expansion or contraction in response to oxygen partial pressure and high temperature creep. Creep is less important because a proper substrate should provide the required high temperature strength and rigidity.

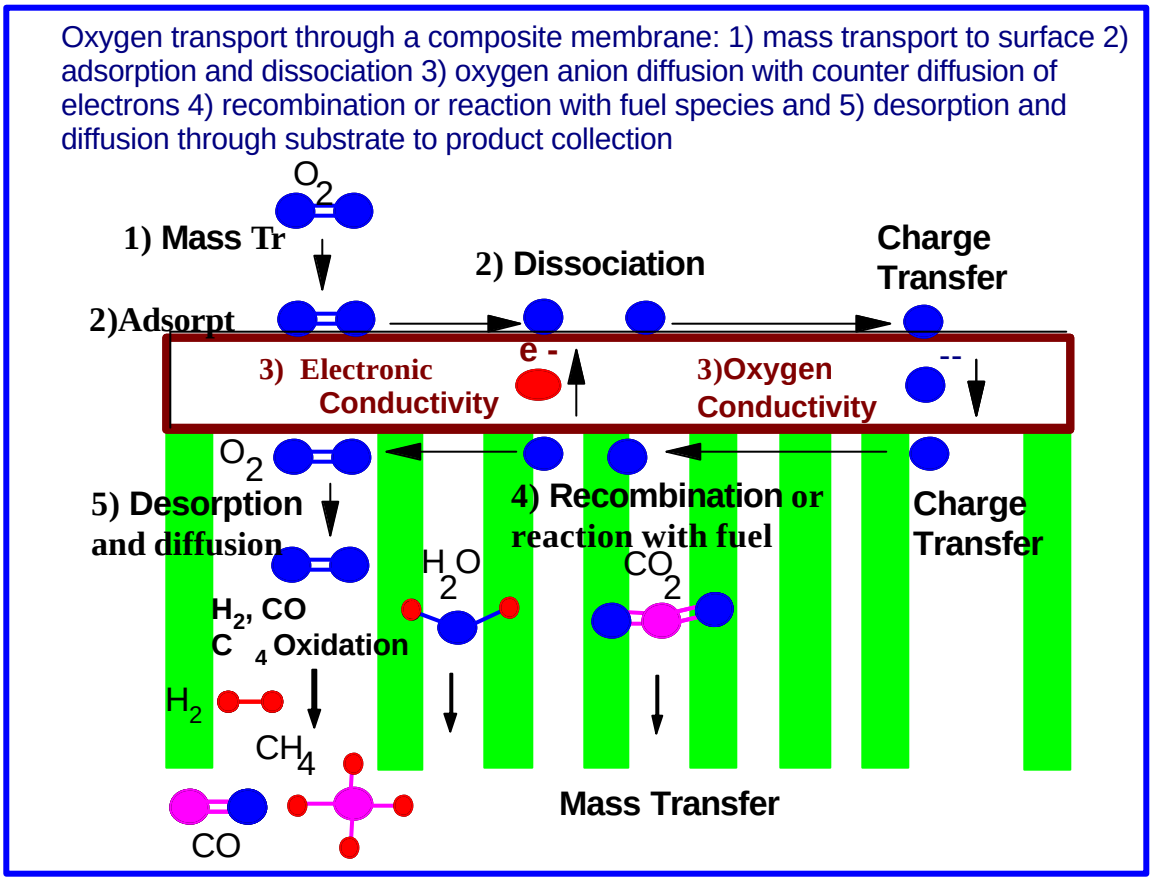

Figure 2: Oxygen transport mechanism through an OTM composite element

The composite element, made of at least two dissimilar materials, must be capable of withstanding rapid changes in temperature and oxygen partial pressure to survive start-up, shutdown or other planned or unplanned process upsets. Ideally both the substrate and membrane materials would change volume in response to temperature in exactly the same way (or not at all) so that stresses caused by thermal expansion are minimized. Thus another important physical property of both membrane and substrate materials is the thermal expansion coefficient (TEC), measured by a dilatometer, over the temperature range of interest.

In Task 1 several new substrate and OTM materials have been developed that meet proprietary criteria for performance, durability and mutual compatibility. Results of this work are discussed below. In addition, another class of substrates materials, designated MM, do not require material development, but require development of compatible OTM materials and an architecture that will permit high oxygen flux while retaining high temperature strength and creep resistance. The development of these MM compatible OTM materials is included in Task 1. However development and testing of the MM substrate and MM composite systems are reported in Task 2, Composite Element Development.

3.1.3.1 Substrate materials

Twenty substrate materials (LCM 7-9, 11, 12, 21-31, 36, 41-43) were either made in-house or obtained from outside sources and evaluated. In 1Q02, LCM29 was selected as the primary substrate candidate. Subsequent work focused on characterization and optimization of this material.

3.1.3.1.1 High Temperature Creep Rates of Substrate Materials

Creep rates as a function of temperature for a number of substrate and membrane candidates are plotted in Figure 3. The red diamonds, A and B, designate target creep rates for a high temperature scenario (1.1TT) and the target temperature scenario (TT), respectively. The open blue squares show the creep rate of a porous LCM29; the dark blue squares are creep rates of dense samples of LCM29. The lines through these data show that porous LCM29 meets the TT target creep rate (within the error of the measurements) and dense LCM exceeds the creep requirements for TT. However neither dense or porous LCM meet creep targets for the extreme temperature case, point A. Note that the creep rates for these materials are so low, that very high temperatures and compressive loads must be used just to obtain a measurable rate within a reasonable time frame (~ 1 to 3 weeks). For dense LCM29, no creep rate could be measured at the target temperature, TT; rates at TT are extrapolated from higher temperature measurements. The low creep rate of LCM29 is one of the main reasons for selecting it as the prime substrate candidate. It is at least 2 to 3 orders of magnitude more creep resistant than LCM1.

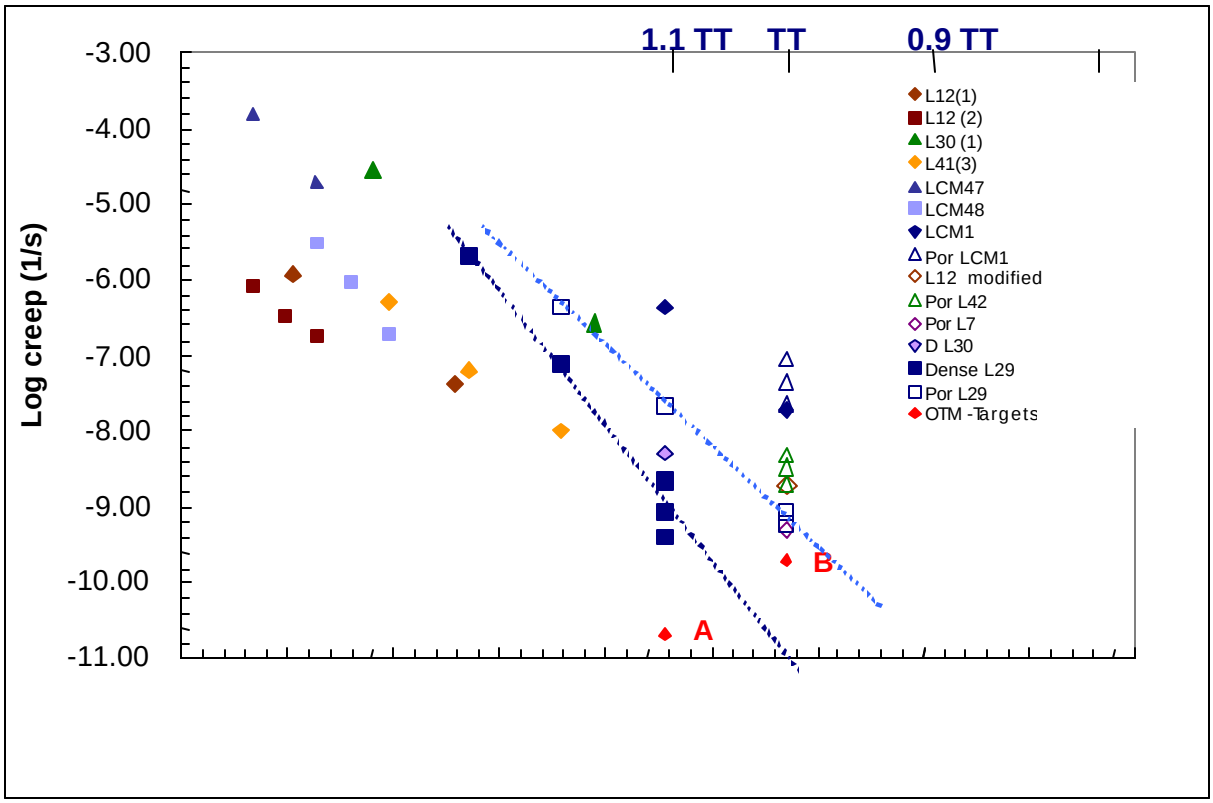

Figure 3: High temperature creep rates of substrate and membrane candidates

3.1.3.1.2 Thermal and chemical expansion of substrate materials

Thermal and chemical expansion behavior of both substrate and membrane materials as a function of temperature and oxygen partial pressure must be known to engineer a robust, low stress, composite element. LCM29 thermal expansion coefficient (TEC) is reported below in Table 1. It was discovered that LCM29 exhibited high volumetric expansion when subjected to low oxygen partial pressures at very high temperature, 1.1TT. Variations of LCM29, LCM 26 and 27, were fabricated and tested. Both of these materials reduced the chemical expansion by a factor of 10 with only a small impact on TEC. These materials will probably replace LCM29 as the substrate of choice for very high temperature applications. LCM23 was also found to have good high temperature chemical expansion behavior. However this material has other issues which preclude its selection as a substrate candidate at this time.

Table 1. Thermal and chemical expansion behavior of substrate candidates

Composition	TEC 100-1.1TT (10^{-6}/K)	CEC at 1.1TT Air- 90CO/10CO_2 %
LCM29	11.9±0.3	0.21
LCM26	11.6	0.02
LCM27	11.6	0.02
LCM23	11.5	0.00

3.1.3.1.3 Substrate fracture strength and slow crack growth

Fracture strength at high temperature is an important property for substrate materials because the membrane system must withstand high external pressure gradients and internal stresses created by thermal and chemical expansion. Slow crack growth has been measured at the target temperature (TT) in air for LCM29 in a 4-point bend apparatus by varying the displacement rate (and thereby the load rate) according to ASTM C1465. The sample sizes were 3x4x45mm and the fracture strength was measured at the deflection rates of 50, 5, 0.5, 0.05 mm/min. The slow crack parameters n= 68.2 and D=208.7 were calculated from the data illustrated in Figure 4. The data indicate that slow crack growth is negligible under the measurement conditions. However, slow crack growth may be different under reactor conditions. To be sure that slow crack growth is not a problem; the measurements should also be done in environments simulating reactor conditions on the fuel side. For example, elevated steam concentrations have been reported to increase the slow crack growth rates in other high temperature ceramics.

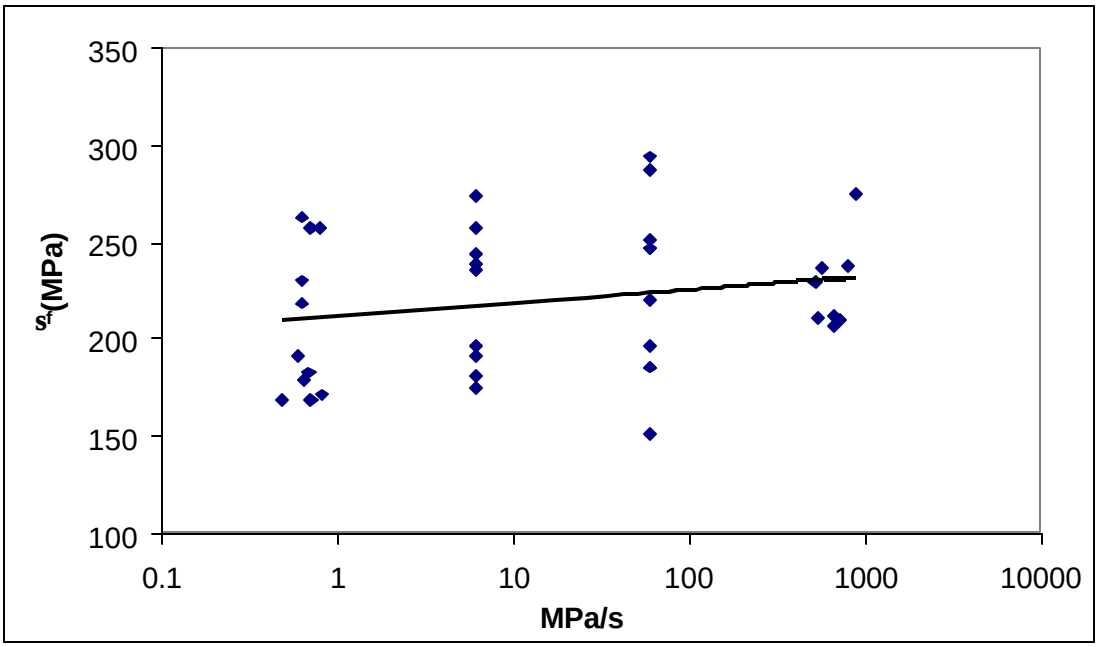

Figure 4: Fracture strength as a function of load rate for LCM29

3.1.3.1.5 Fracture toughness and hardness

Fracture toughness and hardness has been measured for a number of different materials by the Vickers indentation method. These properties are important for gauging the ability of a material to withstand physical shock and resist cracking. The data are summarized in Table 2. All the measured perovskites have fracture toughness values in the region 0.7-1.1 $MPam^{0.5}$, which is very low. The calculated fracture toughness values depend on the estimated Young's modulus and will increase somewhat if the Young's modulus is higher than estimated.

Table 2. Hardness and Fracture Toughness Data Measured at Statoil by the Vickers Indentation Method

Sample (wt%)	Average hardness [GPa]	Fracture toughness [MPa $m^{0.5}$]
LCM20	6.5 (0.5)	0.95 (0.14)*
LCM32	7.1 (0.1)	0.68 (0.06)*
LCM33	7.6 (0.2)	0.76 (0.11)*
LCM16	7.0 (0.3)	1.03 (0.18)*
LCM16 (another batch)	4.5 (0.6)	1.15 (0.26)*
LCM34	5.7 (0.4)	1.02 (0.12)*
LCM35	5.7 (0.3)	0.85 (0.34)*
LCM30	10.6 (1.5)	2.0 (0.5)**
LCM9	8.7 (0.2)	1.2 (0.1)**
LCM29	**8.8 (0.4)**	**> 10**

Estimated Young's modulus of 110* and 200** GPa.

The substrate material candidates LCM12, LCM30, and LCM9 all have fracture toughness values in the range 1-2 $MPam^{0.5}$ (similar crack lengths as the perovskites but higher Young's modulus). The materials which stand out with remarkably higher fracture toughness are LCM25 and LCM29, for which the fracture toughness could not be measured by the Vickers indentation method even with a 30 kg load. Fracture toughness values for LCM29 above 10 $MPam^{0.5}$ have previously been reported.

3.1.3.1.6 Phase stability of substrate materials

A number of different LCM29 samples were examined by XRD before and after heat treatment for 800 h at 1.1TT in order to investigate the phase stability of the materials. XRD analyses of the samples are given in Table 3.

Table 3. XRD analyses of samples before and after heat treatment at 1.1 TT*

Sample	Before*	After*
LCM 29 (Supplier 1)	x	Xx
LCM 29 (Supplier 2)	x	Xxx
LCM29 – variant 1	0	0
LCM29 –variant 2	0	0
LCM29 – variant 3	0	0

* One x marks a trace amount of second phase, the amount of second phase increases with number of x's. Zeros denote no second phase

The data shows the amount of second phase in LCM29 can vary by supplier, and there is some increase in this phase with a high temperature heat soak. However, there is no evidence that other, more deleterious phases are formed. Also, some variations of LCM29 result in no second phase with excellent high temperature stability.

3.1.3.2 Membrane materials

The main objective of the membrane development work is to find robust high flux OTM materials that are compatible with the lead substrate candidates, such as LCM29 and MM1. A systemic approach has been taken that focuses on the LCM_{ABC} system as shown in Figure 5. The points on the tertiary diagram show the compositions that have been synthesized. Each new material is measured for oxygen flux, electrical conductivity, thermal and chemical expansion. Proprietary correlations and trends have been developed that show how these properties are affected by compositional changes, such as atomic substitutions or variations in the A and B sites of the base perovskite material. (Note: A, B and C materials in Figure 5 do not necessarily correspond to the ABO_3 general formula for a perovskite.)

Results of this extensive material synthesis and testing work are summarized in the following sections.

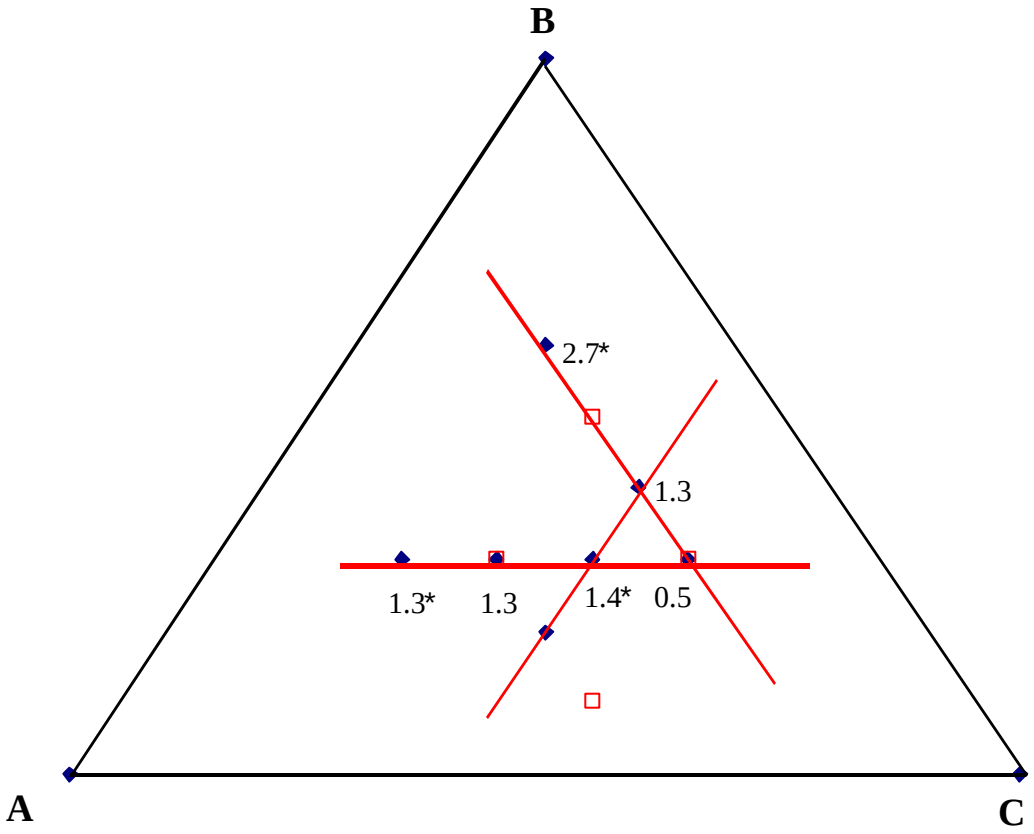

Figure 5: Synthesized compositions & relative flux results in the LCM_{ABC} system

3.1.3.2.1 Oxygen Flux Testing of New Membrane Materials

Oxygen flux tests of a number of membrane material candidates are shown in Figure 5. All of these tests are of dense disk, ~ 1 mm thick, using a standard gas mixture, at the target temperature, TT. The fluxes are normalized to the target flux for a dense disk, TFd. Thus a flux of 2.7 means the flux is 2.7 times the target flux for a dense disk. Note that flux doubles as B increases relative to C or A. For reference, LCM1 flux is ~ 4.3 TFd.

The impact of A/B ratio was also studied for LCM 16. Flux versus A/B ratio is plotted below in Figure 6. Small variances in the A/B ratio can have a very significant impact on flux of a material. A sharp optimum is found exactly at A/B = 1.0

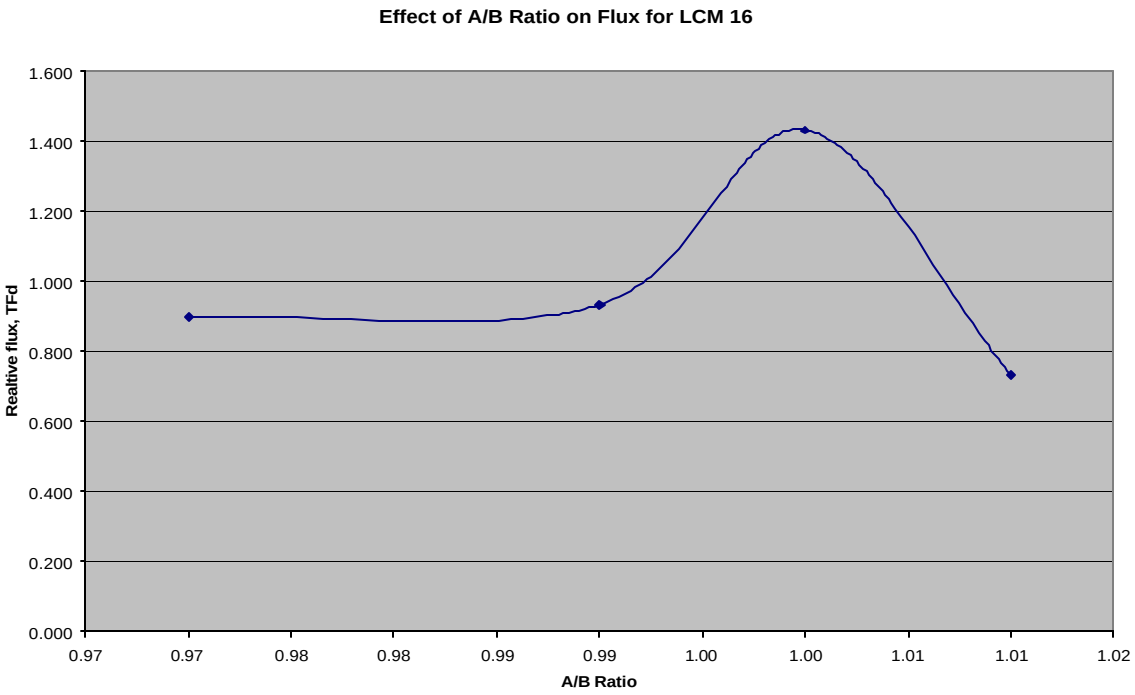

Figure 6: Effect of A/B ratio on the flux of LCM16

In addition to single phase OTM materials, multiphase mixtures of OTM materials were prepared and tested. Fluxes of three mixtures are reported below in Table 4. The goal is to develop materials that at least achieve the minimum flux criteria of 1.0TFd, while improving other properties such as TEC, chemical expansion or strength.

Table 4. Oxygen flux of dual phase materials

Material	70% H2 / 30% CO2	85% H2 / 15%CO2
LCM38	0.87TFd	0.87TFd
LCM39	1.37TFd	1.8TFd
LCM45	0.33TFd	

3.1.3.2.2 Thermal and chemical expansion of membrane materials

Thermal and chemical expansion of both the single phase and dual phase materials were measured using dilatometry. The goal is to develop membrane materials that closely match LCM29, MM1, or MM2 in thermal expansion properties while minimizing the chemical expansion at low pO_2, and achieving a flux of at least 1.0TFd. Several materials have been found that meet these criteria for LCM29 and MM1 as shown in Table 5. For the substrates LCM26 and 29, membrane materials LCM38 and 46 provide fairly good matches. For the substrate MM1, membranes LCM15 and 20 provide excellent TEC match, marginal chemical expansion (CE) and good flux properties.

Table 5. Summary of Expansion and flux properties for lead candidate materials

Material	TEC to 1.1TT (in air) $10^{-6}/^{o}K$	CE @ 1.1TT Air to Fuel, Vol. %	Flux @ TT TFd
LCM29 (S)	**11.9**	**0.21**	**0**
LCM26 (S)	**11..6**	**0.02**	**0**
LCM15	**15.2**	**0.11**	**1.35**
LCM16	15.8	~0.14	1.41
LCM20	**15.8**	**0.09**	**1.75**
LCM38	**11.7**	**TBD**	**0.87**
LCM39	13.5	0.12	1.80
LCM46	**12.6**	**0.06**	**TBD**
LCM1	18.1		4.3
MM1 (S)	**15.3**	**0.0**	**0**

(S) = substrates TBD = To be determined

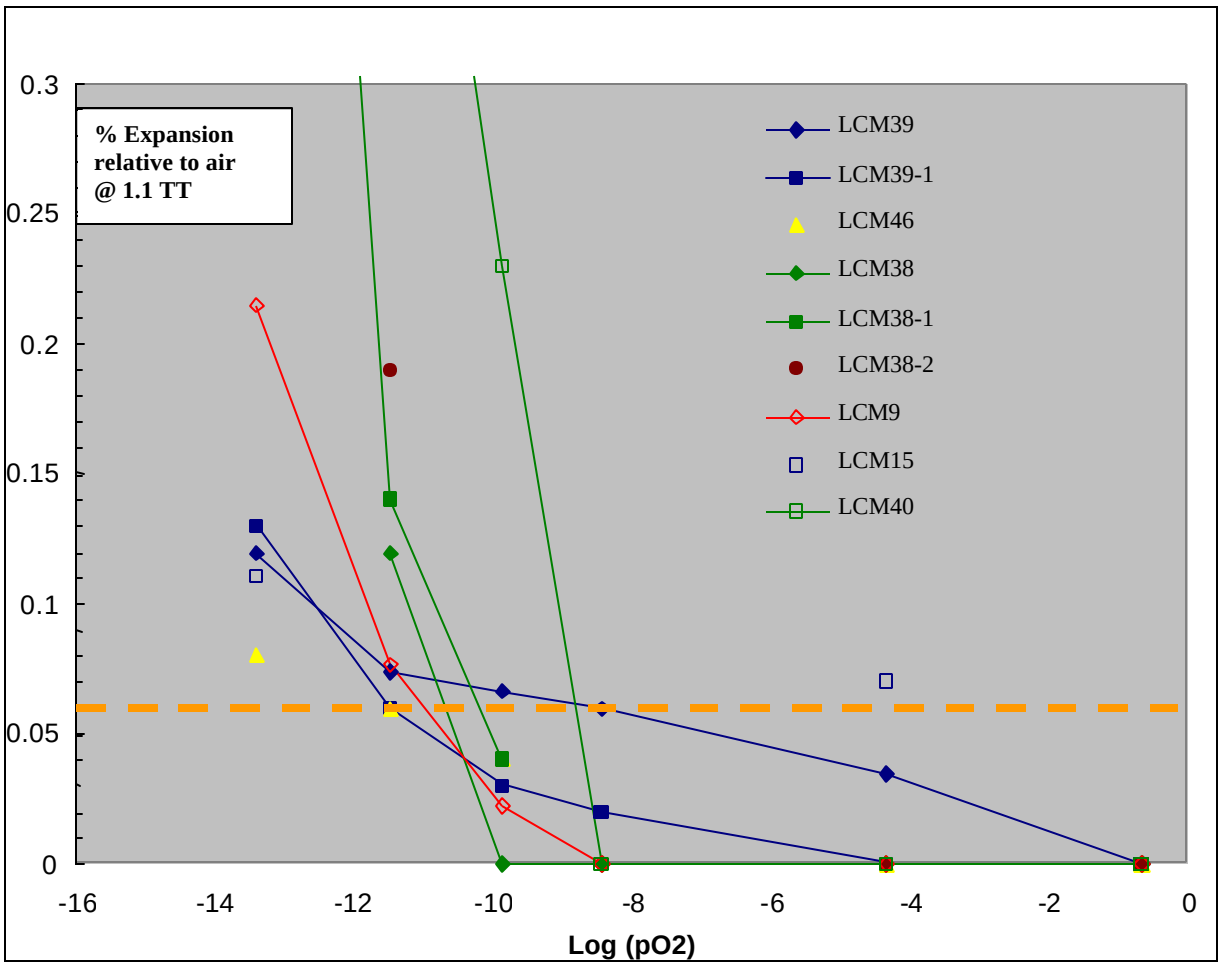

Figure 7: Chemical expansion of substrate and membrane materials versus pO2

The chemical expansion shown above is the change in volume recorded when a sample at 1.1TT is switched from air to a fuel gas containing 75%CO and 25% CO2.
Chemical expansion generally increases as oxygen partial pressure decreases and temperature increase. The effect of oxygen partial pressure at 1.1TT is illustrated in Figure 7 for a number of membrane and substrate materials. This plot also shows that minor variations in composition of the component materials (LCM39 vs. 39-1; LCM 38 vs. 38-1, 38-2) changes can have significant impact on chemical expansion behavior.
Thus at lower temperature and higher oxygen partial pressure chemical expansion may not be an issue for the lead candidates. And with some minor manipulation, it is believed that all of the key physical properties, CE, TEC and oxygen flux, can be improved further.

3.1.3.3 Interaction of Substrate and Membrane Materials

A robust composite system must be chemically stable over long periods of time. At very high temperatures adjacent layers of dissimilar materials can chemically react or inter-diffuse. Other phases can be formed that may physically weaken the substrate materials or adversely affect the membrane's ability to transport oxygen. However some reaction or diffusion is desirable to ensure a strong bond between adjacent layers.

Chemical reactivity of membrane and substrate candidates was determined by preparing diffusion couples of selected pairs of materials. The membrane candidates studied were LCM16, LCM20 and LCM40 versus substrate candidates LCM7, LCM9, CLM36, LCM30 and LCM29. The couples were exposed to stagnant air for 100 hours at 1.2 and 1.3TT. XRD was used to identify secondary phase formation. SEM and EDS analysis were also used to examine polished cross sections of selected samples sputtered with carbon. Results show that LCM16 was the least reactive of the membrane candidates and LCM36 was the least reactive of the substrate candidates.

Table 6. High temperature interaction test results

Material	LCM40	LCM20	LCM16
LCM36	Surface color chance **Diffusion**	Good adherence. **Diffusion**	No visible rx. **Diffusion**
LCM7	Surface color changed **Diffusion**	Good adherence. **Diffusion**	No visible rx. **Diffusion**
LCM9	**Secondary phases** **Diffusion**	Good adherence. **Secondary phases** **Diffusion**	No visible rx. **Diffusion**
LCM30	. **Secondary phases** **Diffusion**	Good adherence. **Secondary phases** **Diffusion**	**Secondary phases** **Diffusion**
LCM29	**Secondary phases** **Diffusion**	**Secondary phases** **Diffusion**	**Secondary phases** **Diffusion**

Material interactions of LCM29 with LCM30, LCM8 and LCM 9 were also studied. No visible reactions were observed for any of the diffusion couples after 100 h at 1.3TT.

3.2 Task 2: Composite Development

3.2.1 Goal - Task 2

Develop advanced composite OTM elements and the techniques for fabricating these elements at the bench scale. The goal is to develop robust, low cost, high flux elements that can survive multiple temperature and fuel composition cycles while maintaining structural integrity at target pressure differentials.

3.2.2 Experimental - Task 2

The experimental facilities and methods in Task 2 were described in detail in the Topical Report for the Period Jan. 1 through Oct. 31, 2001 [Ref. 1].

In addition, an oven thermal cycle test is being employed to test durability of the composite systems subjected to rapid changes in temperature. The procedure is:

- Heat the sample in air from room temperature to TT at 1^{O}C/minute.
- Hold the sample at TT in air for 1 hour.
- Cool at 1^{O}C/minute.
- Leak test sample by applying a differential pressure up to 50 psi and measuring the gas permeability rate, in cc/second. (This may not be performed after every cycle.)
- Repeat.

3.2.3 Results and Discussion - Task 2

In this task, composite elements (disk and tubes) are built using proprietary fabrication techniques and tested. The composite element, shown in Figure 1, consists of a robust porous substrate and a dense oxygen transport membrane. Oxygen flux is primarily controlled by two mechanisms in series: ambipolar diffusion of oxygen across the dense membrane and diffusion of the reaction species through the porous substrate layer. (See also Figure 2) Both material properties, as discussed in Task 1, and element architecture (layer dimensions, pore structure, etc) are important factors affecting the performance and durability of the composite system.

Two types of composite elements are under development: the LCM family of materials and the MM family of materials. Each type requires different fabrication techniques. Both types promise excellent high temperature performance.

3.2.3.1 LCM Composite Systems

Two LCM systems were fabricated and tested. Both systems utilize LCM 29 as the substrate. Each system is discussed below.

3.2.3.1.1 LCM38/LCM29

An LCM 38/LCM29 composite disk was fabricated and cycled in air using the oven cycling procedure. This disk did not exhibit any signs of stress cracking and the layers remained intact. Another 38/29 disk was subjected to a life test that included both

thermal and chemical cycles as shown below in Figure 8. The test ran for over 800 hours. The first 24 hours were run at 1.0TT. Gas compositions were changed to reduce the pO2 in steps three steps. Flux increased as pO2 was reduced as expected. Flux is calculated by two methods and both are shown in the figure as dark blue and mauve. The temperature was increased to 1.1TT for the remainder of the test. This is an extremely high test temperature intended to evaluate OTM syngas conditions in a commercial reactor. The flux increased from ~ 0.3 to ~ 0.5TFc. The flux remained constant for the next 500 hours, showing no significant degradation. Equally important, the fuel leak did not change, indicating the disk did not crack. The disk was then subject to five thermal cycles between 0.65TT and 1.1TT. The fuel leak rate did not change and the flux showed a slight degradation. Finally the disk was subject to a more severe cycling sequence where the end temperature was dropped to 0.2TT and the gas composition was switched to nitrogen. Under these conditions the disk developed a leak and the run was terminated after five severe cycles and over 800 hours at high temperature operation. Post mortem of the disk showed no deleterious interactions between the layers, but some cracks were formed in the membrane. It was also concluded that flux was inhibited by the architecture, which can be readily improved.

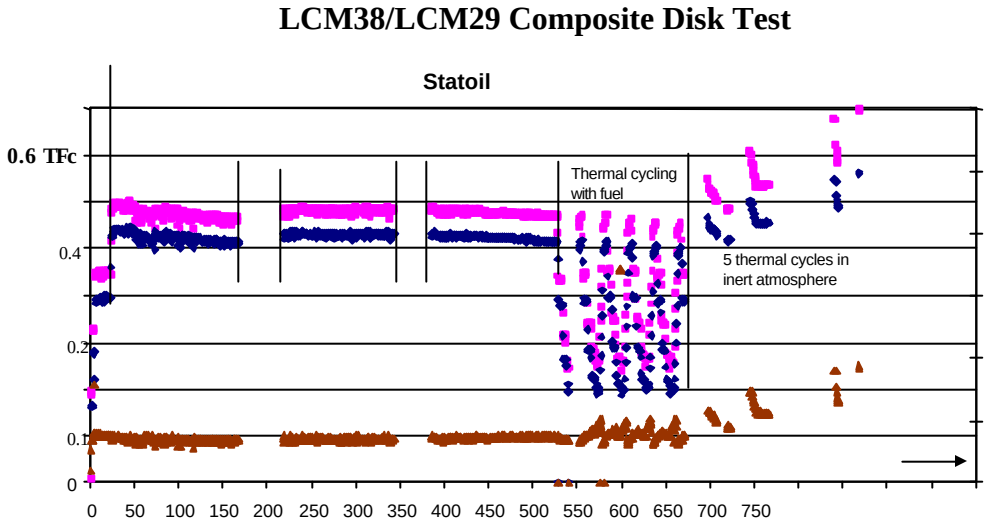

Figure 8: Composite disk LCM38/LCM29 life and cycle test results

3.2.3.1.2 LCM15/LCM29

A composite disk comprised of LCM15 and LCM29 was fabricated by improved techniques. This disk is currently the subject of a life test. At 1.0TT the disk has achieved

a steady flux of ~ 0.8TFc for over 300 hours as shown in Figure 9. The leak rate has not increased and the test is on-going. This demonstrates that learnings from

the prior life test were successfully applied and resulted in a doubling of the flux with no apparent degradation in the robustness of the disk. (Compare fluxes at 1.0 TT)

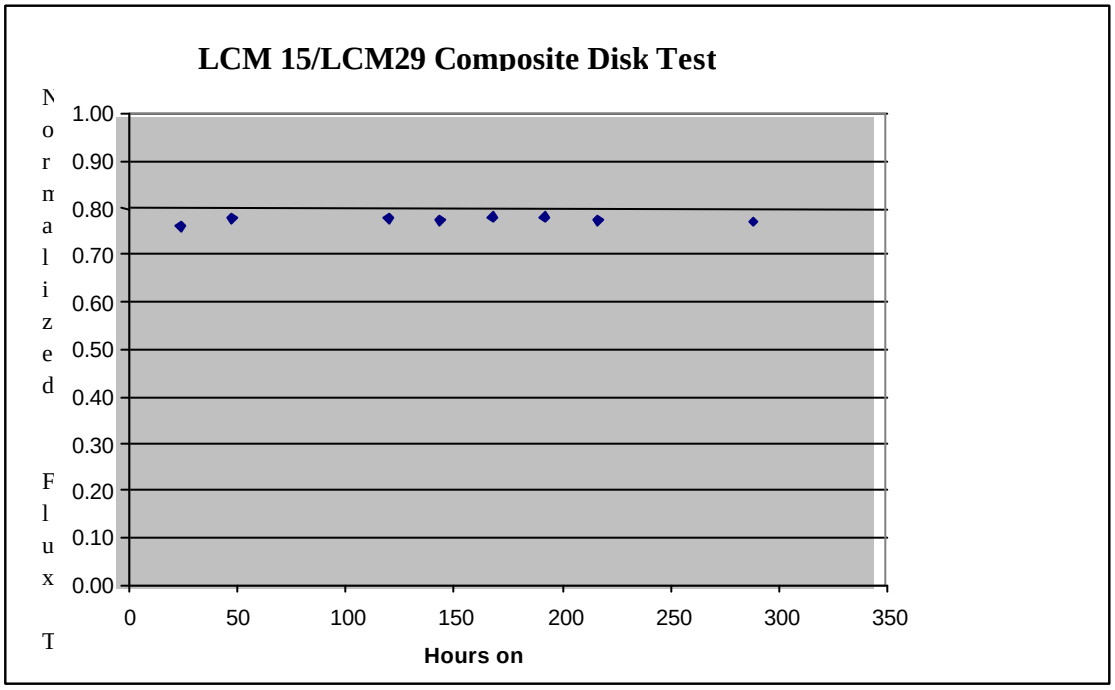

Figure 9: Composite disk LCM15/LCM29 life test results (in-progress)

3.2.3.2 MM Composite Systems

A second type of substrate, designated MM, is being explored that could provide certain fabrication advantages over our LCM materials. These materials are commercially available; work is focused on finding compatible membrane materials and a suitable architecture. Several membrane materials have been identified with similar thermal expansion properties, as shown in Table 5. Test disks of three systems have been fabricated using in-house proprietary techniques. The MM1 and MM2 systems are targeted for very high temperature operation, which are expected in an OTM reactor. The MM3 system is a lower temperature material more suitable for a hydrogen application. Each of these systems is discussed below.

3.2.3.2.1 LCM1/MM3 Composite Disk

Three samples of an LCM1/MM3 composite were fabricated utilizing different architectures and techniques. The performance of the discs, designated Disk 1, Disk 2 and Disk 3 is

shown in Figure 10. Disk 1 and Disk 2 represents two different techniques while Disk 3 combines both of these techniques. All three disks begin with the same flux off ~ 0.7TFc, then performance rapidly diverges. Disk 2 begins to decline immediately while 1 and 3 appear to behave a bit erratically for the first 150 hours.
Disk 1 then begins to decline at ~250 hours while Disk 3 maintains a steady flux for 350 hours. The tests show that the combined techniques are better than either alone, but further improvement is needed to sustain stability.

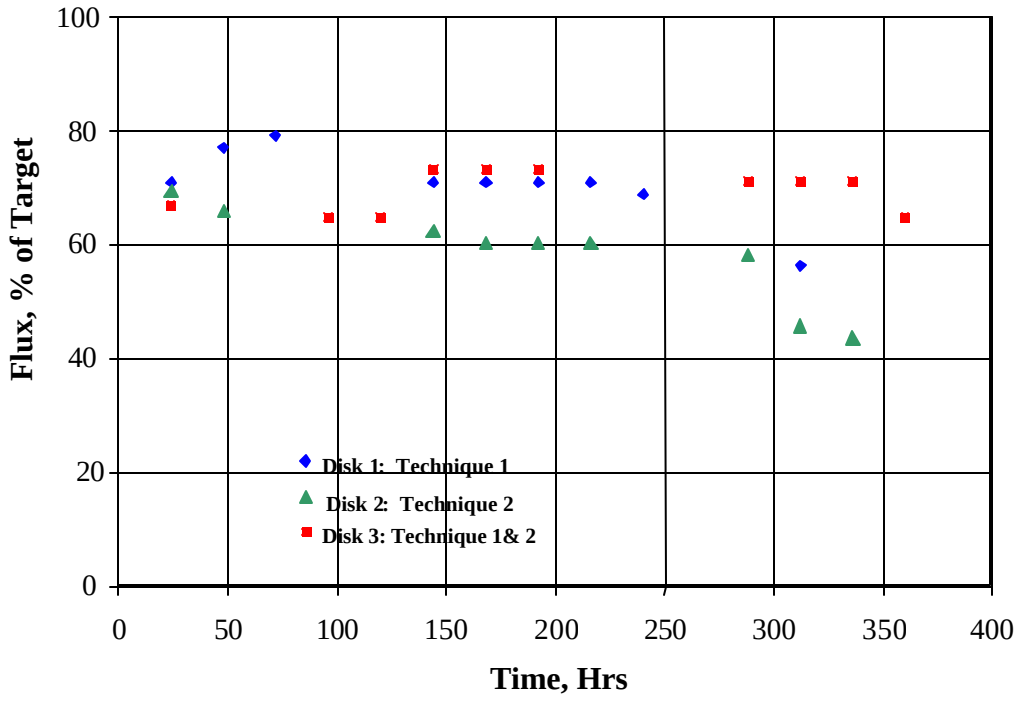

Figure 10: Performance of three LCM1/MM3 Composite Disks

Based on this and other learnings, another disk LCM1/MM3 disc was fabricated and tested in the same manner. Designated Disk 4, its test results are shown in Figure 11. The disk was tested at two temperatures, TT for the first ~ 100 hours and 1.1TT for another 220 hours. The disk was then slowly cooled to obtain flux data over a wider temperature range.

Flux and leak rate are plotted versus time on-stream in Figure 11. Flux is measured by two mass balance techniques; both methods are plotted as shown by the blue and red lines. Leak rate is measured as percentage of total fuel fed to the system. The calculated fluxes are normalized for the leak. (The error of the calculated flux rates will increase as the leak rate increases.)

This test showed that target fluxes can be obtained with this system at 1.1TT. Based on leak rate, the test also shows the system is relatively stable (over 300 hours). The leak rate jumped twice in this test; first when the temperature was increase by 10%, and second

time when the system was cooling down. The latter case may be caused by the disk contracting, increasing leakage around the seals.

After the test, the disk was removed and examined by SEM. This disk shows a slight improvement in flux when compared to Disks 1-3 at TT. However, the disk shows a significant improvement in stability, especially given the test was run at the higher temperature, 1.1TT.

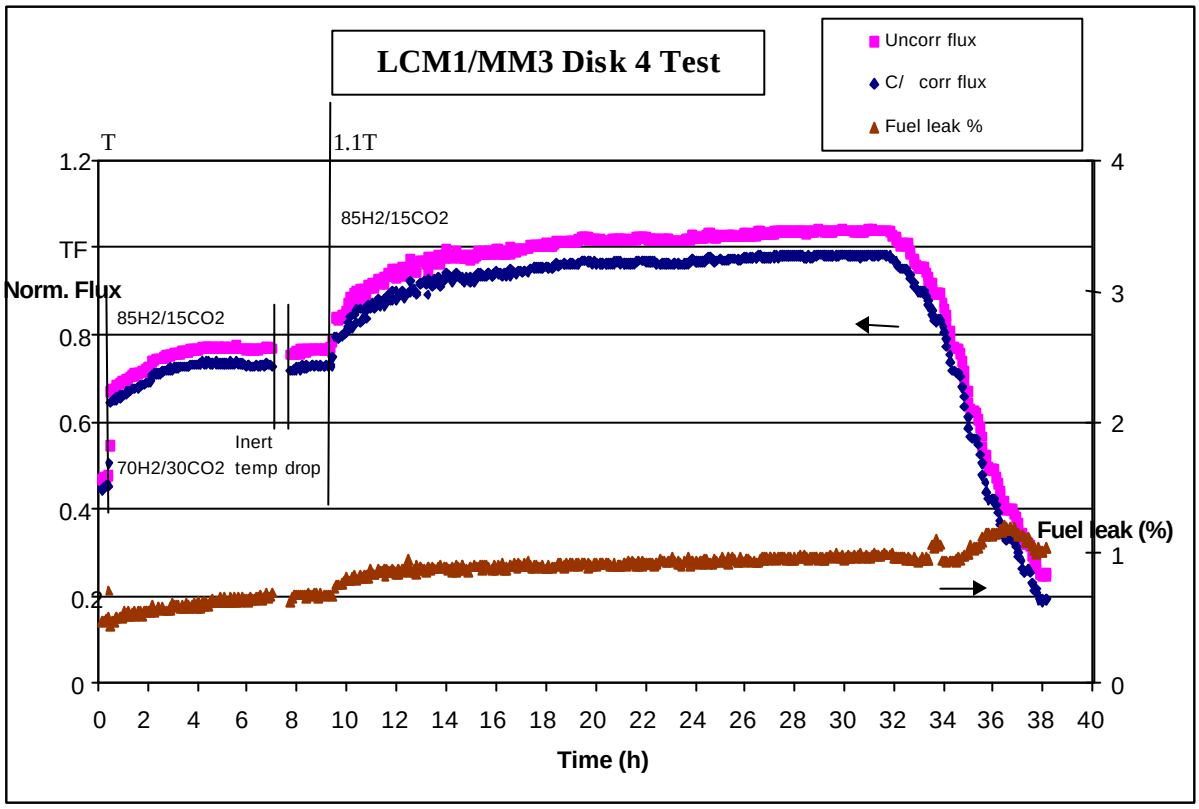

Figure 11: Performance of LCM1/MM3 Composite Disk 4

3.2.3.2.2 LCM1/MM1 System

The LCM1/MM1 system is intended for the very high temperature operating conditions that are expected in an OTM syngas reactor. An LCM1/MM1 disk was fabricated using techniques similar to those used to fabricate LCM1/MM3 Disk 4. This disk, designated LCM1/MM1 Disk 1 was tested for over 2000 hours as shown in Figure 12. The flux and temperature data are plotted versus time for the 2500-hour run. The reported fluxes on the left "Y" axis are relative to the composite target flux, TFc. The disk showed no significant degradation in flux after 2500 hours on stream and 10 thermal cycles. This satisfies a major milestone in demonstrating the viability of these types of systems.

Additional disk tests showed there was no effect of MM1 substrate thickness on flux. Nearly identical fluxes were measured for disks with 1.5 X and 0.5 X the substrate thickness of Disk 1.

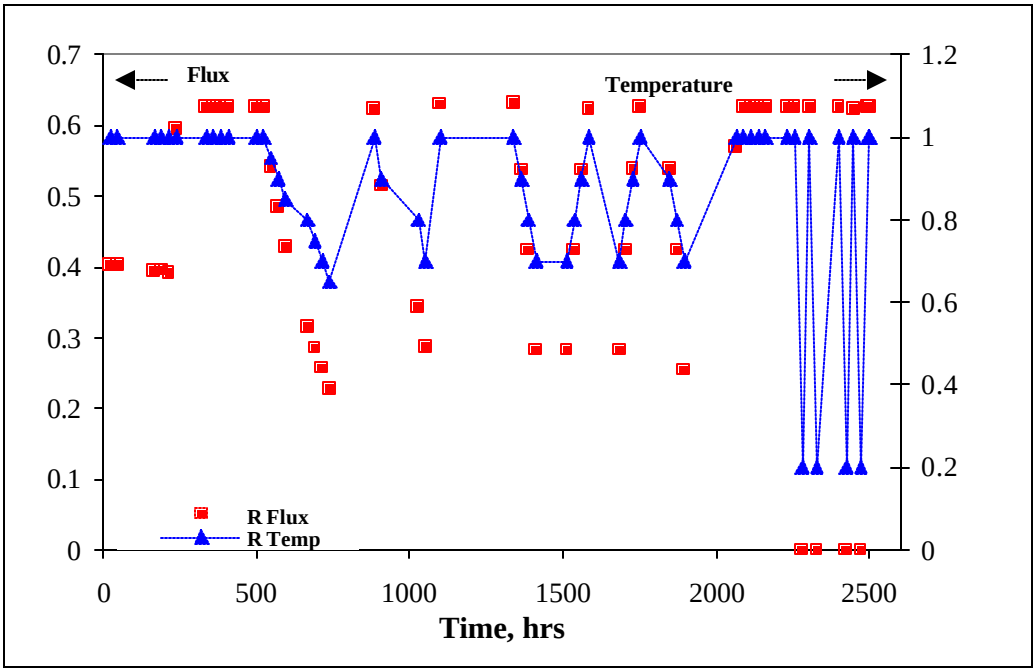

Figure 12: Performance of composite LCM1/MM1 Disk 1

In order to evaluate the effect of temperatures on the flux performance, the composite LCM1/MM1 Disk 1 was tested every 50 degrees from TT to 0.6TT until the flux data could no longer be recorded due to an increase in the leak rate on the air-side. The leak rate increases at low temperatures because the seals contract. The leak usually is abated when the temperature is ramped back up. As shown in Table 7, the flux decreased with temperature. At 0.65TT, the flux remained at 0.23TFc, which is still significant and may be adequate for some other applications, such as hydrogen.

Table 7. Flux test results of LCM1/MM1 Composite Disk 1 vs. temperature

Relative T	Relative Flux, TFc @ 85%H2:15%CO2
TT	0.63
0.95	0.54
0.9	0.48
0.85	0.43
0.8	0.31
0.75	0.28
0.7	0.26
0.65	0.23

Post mortem of the above disk showed some cracking in the dense film. This may have occurred during final cool-down or during one of the last few thermal cycles. Subsequently several architectural improvements for the LCM1/MM1 have been proposed. Two new architectures (Config. 1 and Config. 2) were fabricated and submitted for oven thermal cycle tests. Both test samples employed MM1 as a substrate and LCM1 as the dense membrane. Systems that survive this screening test are then advanced to disk tests, followed by pressurized tube tests.

The permeability test record for LCM1/MM1, Config. 1 is shown below in Figure 13. (The red line is a reference standard used to check the permeability apparatus.) The sample was leak tested before the sample was cycled (0 TC), then after the 3rd, 5th and 11th thermal cycle. In all cases the sample showed zero gas permeability over the pressure differential range tested (0 to 50 psi). This is very encouraging.

LCM1/MM1 Config. 2 is also undergoing thermal cycle tests by the same method. Config. 2 so far has survived one cycle; the test is on-going.

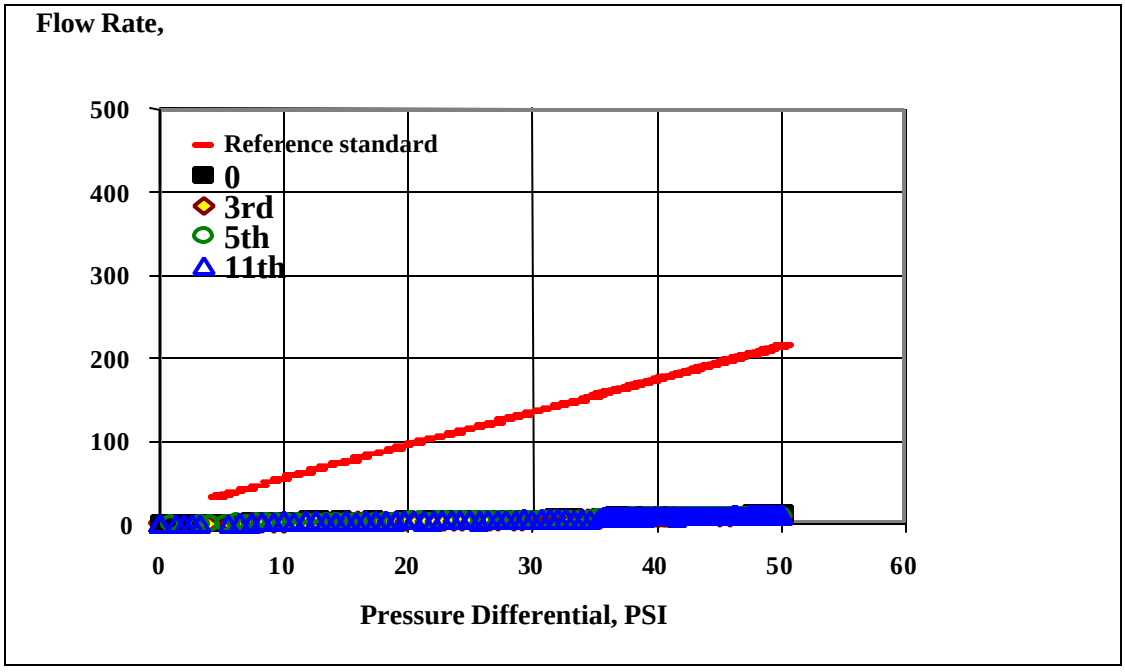

Figure 13: LCM1/MM1 Config. 1 thermal cycle permeability test results

It is expected that these architectural improvements in combination with the OTM material improvements discussed in Task 1, will lead to major advances in both performance and durability in the next program budget period.

3.3 Task 4: Reactor Design and Process Optimization

3.3.1 Goal - Task 4

Develop the commercial OTM syngas process including reactor design and catalyst deployment, reactor components (seals, internals, isolation devices, high temperature tube sheet, etc), and ancillary processes (feed pre-treatment, pre-heat, syngas cooling). This team shall develop and employ mathematical models to simulate process

conditions (reactor flow conditions, kinetics, heat and mass balances) and the mechanical, thermal and compositional stresses on the reactor components and elements. These models will enable evaluation of various conceptual designs and facilitate detailed design and evaluation of preferred options. Task 4 includes the operation of the small bench scale units, P-0, which are used to evaluate small OTM elements (6 inches long) and develop engineering data for reactor scale-up.

3.3.2 Experimental - Task 4

The experimental facilities and methods in Task 4 were described in detail in the Topical Report for the Period Jan. 1 through Oct. 31, 2001 [Ref. 1].

3.3.3 Results and Discussion

3.3.3.1 P-0 Test Results

P-0 reactors are small pressurized rigs capable of testing tubular elements up to 8 inches in length at pressures up to 0.6 TP. One reactor at BP was modified to operate safely at 2.2TP. Results of studies carried out in both types of rigs are discussed below. Except as noted, all P-0 test results are at 0.6TP.

3.3.3.1.1 High Pressure P-0 Test

A high-pressure test was carried out at the BP facility. A dense LCM1 tube was tested at 2.2TP. Flux was measured as a function of pressure and air flow rate. Air flow studies show that very high oxygen removal rates can be achieved at low air flow rates as shown in Figure 14 below.

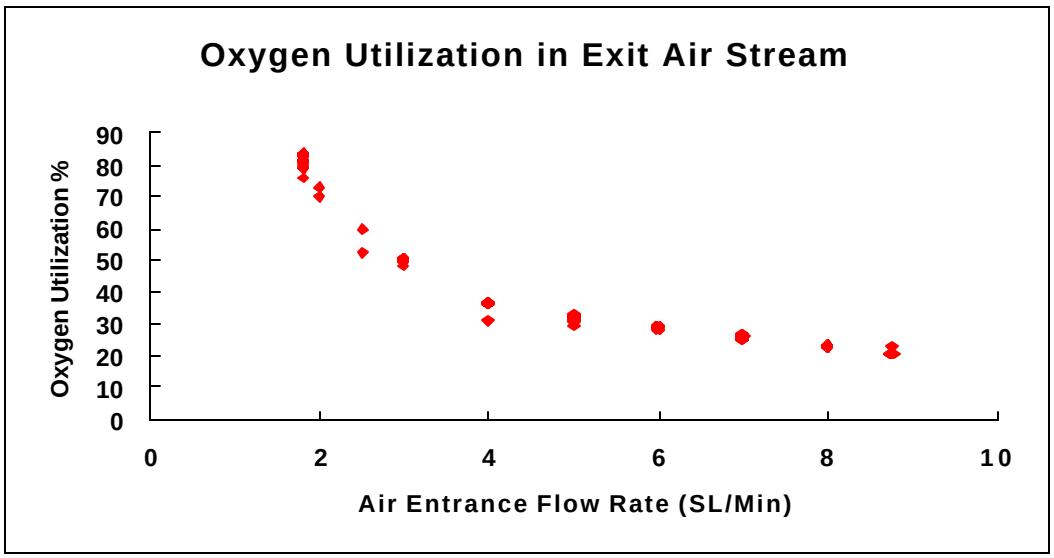

Figure 14: P-0 oxygen utilization test for a dense LCM1 tube at TT

Figure 15 shows the effect of high pressure on flux for the same LCM1 dense tube at TT. These tests confirmed the operability of the BP high Pressure reactor system. The data will be used to validate the P-0 process models.

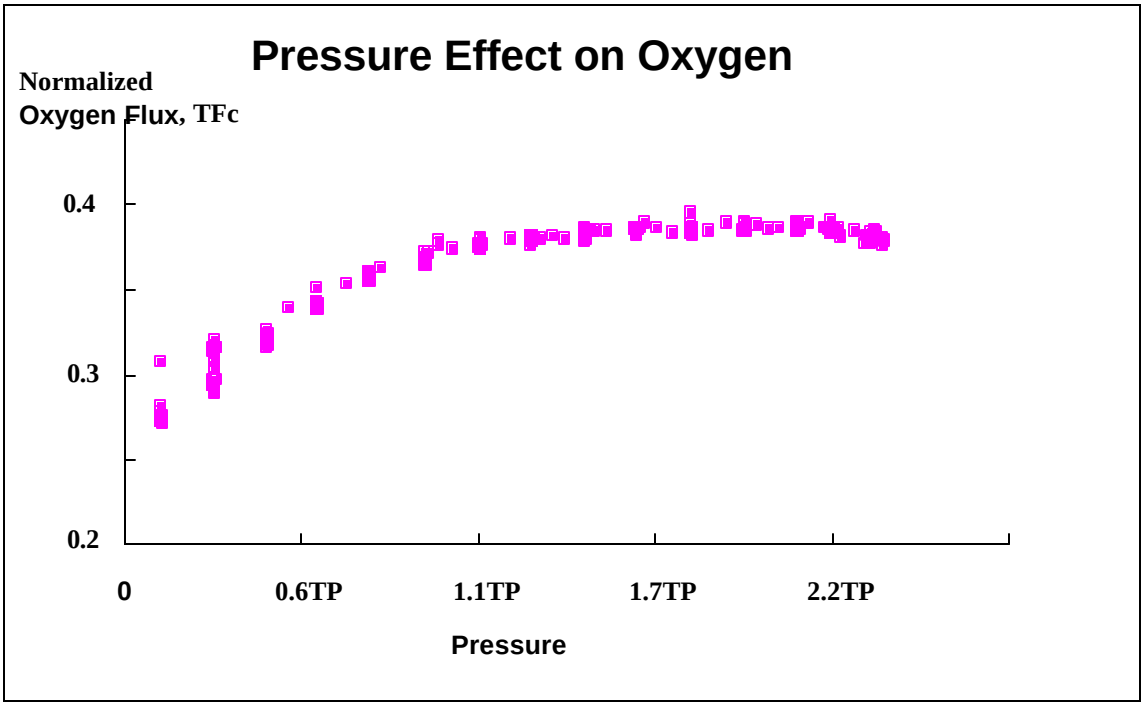

Figure 15: **Effect of pressure on flux in a P-0 reactor with an LCM1 dense tube**

3.3.3.1.2 New Tube Architecture Tests

Four tubes with different architectures (but all of the same LCM1 material) were prepared and tested in the Statoil P-0 rig. Oxygen flux was measured as a function of temperature and air flow rate. Results plotted in Figure 16 show an interesting insensitivity to element morphology--neither dense film nor substrate thickness appear to have a significant effect on the measured oxygen flux of the tube. Flux appears to be affected by airflow rate, suggesting that oxygen diffusion at the boundary layer may be limiting in this particular test rig. These data will be used to validate the fundamental oxygen transport model and the P-0 models.

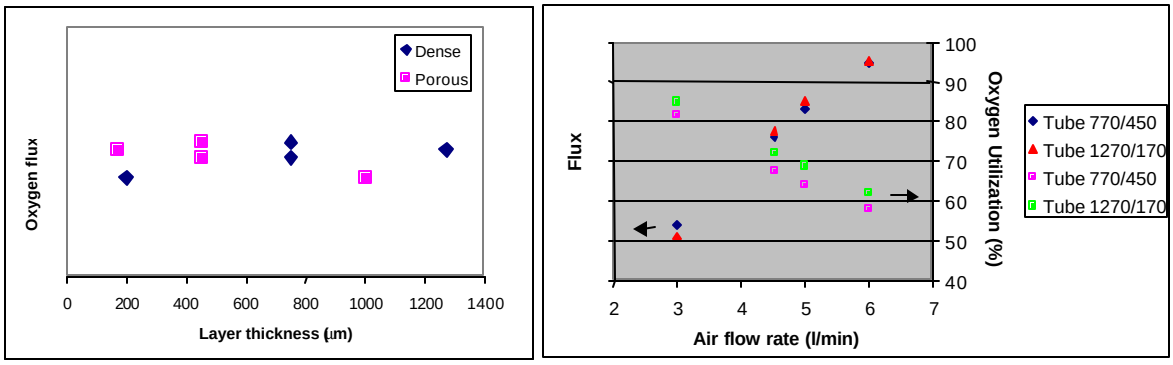

Figure 16: Results of LCM1 composite tube P-0 tests

3.3.3.1.3 LCM1/MM1 Composite Tube Test

An LCM1/MM1 substrate composite tube was prepared and loaded into a BP high-pressure P-0 reactor. Unfortunately the tube developed a leak during heat-up and the test could not be completed.

3.3.3.2 Process and Reactor Design Studies

3.3.3.2.1 Evaluation of a Novel Reactor System

A process study of an OTM reactor to allow use of less expensive was completed. The study showed cost savings of about 18% can be realized. Consequently, the novel reactor design has been adopted as the lead reactor design for the OTM syngas technology.

In addition, it was noted that the operating conditions are also suitable for making hydrogen. Thus, a flexible OTM plant could be envisaged, which could produce syngas for liquids production, hydrogen for fuel, or a combination of the above .

3.3.3.3 Architecture and Process Modeling Results

A proprietary study determined targets for the creep rates of substrate materials by evaluating the effect of element geometric parameters (tube ID and wall thickness) on time to buckle/collapse. Results are presented Figure 17.

The two main factors that affect the time to buckle are the creep rate of the material and the tube geometry (diameter and thickness) as shown in Figure 17. The high creep rate of LCM1 (~10^{-7} s^{-1} at 110% of target temperature) was the main reason last year to focus on thin membranes on improved substrates.

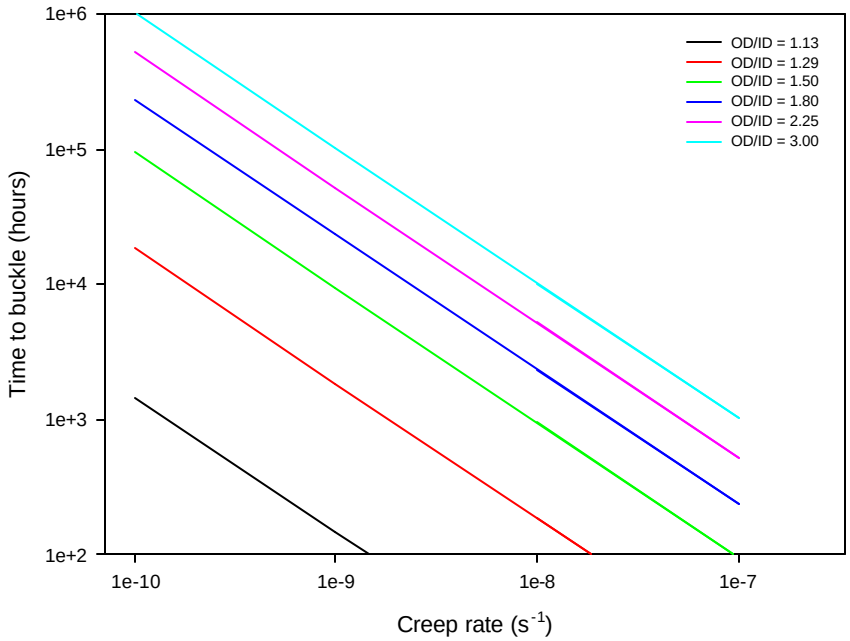

Figure 17: Time to Buckle vs. Tube Geometry and Creep Rate

A creep rate of LCM29 in the region $4x10^{-10}$ - $9x10^{-10}$ s^{-1} was measured at 110% of target temperature in air. However, examination of the creep behavior of the silicon nitride fixtures alone yields similar values for strain. Regardless, the creep rate of LCM29 is low enough to indicate that 10 years life (10^5 h) is an attainable goal for ceramic composite tubes

A second proprietary study evaluated the impact of porosity, tortuosity and wall thickness on flux rate. In addition, it determined design ranges for tube internal diameter, porosity, tortuosity and material creep rate that satisfy both creep/buckling lifetime targets and oxygen flux targets.

A third proprietary study utilized CFD modeling to assess oxygen transport through a more robust alternative architecture design. The study concluded that the porous substrate must have very large pore sizes and high porosity to provide sufficient permeability to meet oxygen flux targets.

3.4 Task 8: Fuels and Engine Testing

A matrix of UCTFs will be prepared for testing at each engine (International Truck and Engine) or fuel cell developer (Nuvera Fuel Cells). The fuel matrix will include a base stock of syngas derived Fischer Tropsch liquids and will study the addition of advanced oxygenates supplied by BP. The study will quantify the impact of fuel properties on emissions and engine (or fuel cell) system performance.

3.4.1 Diesel Engine and Exhaust Treatment

3.4.1.1 Goal - Diesel Engine and Exhaust Treatment

The goal of this task is to understand the relationship between ultra-clean fuel properties and their impact on the emissions and performance of an advanced CIDI and exhaust treatment system under development at International Truck and Engine.

3.4.1.2 Experimental - Diesel Engine and Exhaust Treatment

Detailed discussion of the test methodology used in establishing this baseline fuel database has been provided in the 4Q01 Report [Ref. 3]. Pictures and description of the SCTE are shown in the Topical Report for the Period Jan. 1 through Oct. 31, 2001 [Ref. 1].

3.4.1.3 Results and Discussion - Diesel Engine and Exhaust Treatment

3.4.1.3.1 SCTE evaluation of fuel ultra-clean diesel fuel formulations.

Two ultra-clean diesel fuels were evaluated in this budget period utilizing the SCTE rigs at International truck and Engine. The first set of tests (Set 1) compared Fischer Tropsch diesel fuel (FT diesel) supplied by Sasol, LTD to a conventional No. 2 diesel fuel. The second set of tests evaluated the effect of BP oxygenate (BPO) on a petroleum based ultra-low sulfur diesel fuel (ULS). Properties of these fuels are shown in Table 8. Results of both tests are discussed below. Complete test results for both campaigns are provided in Appendix 1.

Table 8. Characterization of diesel fuels tested in the SCTE

		Set 1		Set 2	
Fuel Property		**Baseline No. 2 Diesel**	**FT GTL Diesel**	**Baseline ULS**	**ULS + BPO**
API Gravity		**36.0**	**49.9**	**36.5**	**34.8**
Distillation, IP	**Deg F**	**370**	**327**	**364**	**317**
10%		**434**	**367**	**401**	**359**
30,%		**474**	**419**	**459**	**437**
50%		**503**	**480**	**488**	**502**
70%		**537**	**546**	**510**	**551**
90,%		**589**	**638**	**588**	**607**
End pt		**642**	**672**	**666**	**646**
Flash point, F		**167**	**135**	**170**	**133**
Viscosity @ 40 C,	**cSt**	**2.4**	**2.1**	**2.5**	**2.13**
Aromatics	**Vol. %**	**30.2**	**0.4**	**12.5**	**~11.2**
Sulfur	**PPM**	**370**	**<5**	**<10**	**6**
H/C atomic ratio		**1.82**		**1.98**	**2.05**
Carbon content	**Wt.%**				**76.7**
Hydrogen content	**Wt. %**				**13.1**
Oxygen content	**Wt. %**	**0**	**0**	**0**	**10.2**
Net heat of comb.	**Btu/Lb**	**18457**	**18884**	**18667**	**16458**
Cetane number		**47.6**	**>70**	**65**	**68**

Set 1: No. 2 Diesel versus FT Diesel

Emission performance comparisons between the FT and baseline test fuel are presented as trade-offs between NOx and soot as well as between NOx and HC in Appendix 1.1. This is the customary way to present and analyze data engine combustion data in development work. These trade-offs have been generated by changes in combinations of settings of major combustion control parameters such as injection pressure, injection timing (represented by start of combustion SOC), air/fuel ratio and concentration of EGR in intake air. Comparison between emission performance of both investigated fuels have been conducted at four points of the engine operating map designated as Mode 4, 6, 7 and 8 and considered to be the significant overall contributors to result of the HD FTP emission certification cycle. The actual data are summarized graphically in Appendix 1.1, Figures 1 through 8, and numerically in Tables 1 through 3. Tables also include definitions of operating conditions at each of the test points as well as the information on specific combinations of control settings driving obtained emission trade-offs.

As it can be seen from the presented results, the FT fuel tested in International's SCTE demonstrates potential for significant emission reduction over the baseline No.2 diesel fuel, however its actual advantages are specific to both the operating point and the parameter calibration specific. In general, the relative emission performance of the FT diesel fuel vs. the baseline No. 2 diesel fuel can be summarized as follows:

Mode 4 (1500rpm/10 bar BMEP):

- Range of Soot: from 8% reduction to 57% increase
- Range of NOx: reduction from 3 to 7%
- Range of HC: reduction from 15 to 53%

Mode 6 (3170rpm/3.8 bar BMEP):

- Range of Soot: reduction from 13 to 45%
- Range of NOx: reduction from 2 to 32%
- Range of HC: reduction from 26 to 43%

Mode 7 (3170rpm/7 bar BMEP):

- Range of Soot: reduction from 12 to 32%
- Range of NOx: reduction from 13 to 26%
- Range of HC: reduction from 33 to 67%

Mode 8 (3010rpm/10.5 bar BMEP):

- Range of Soot: from 40% reduction to 8% increase
- Range of NOx: reduction from 23 to 37%
- Range of HC: reduction from 73 to >90%

Set 2: Ultra-low sulfur fuel and BP oxygenate

In the second test campaign, an ultra-low sulfur diesel fuel was blended with a proprietary BP oxygenate, BPO, to yield a blend with 10% oxygen by weight. The 10% oxygen blend has a net heating value about 13% lower than the base feedstock, complicating interpretation of the test data. To ensure a meaningful and comprehensive comparison of both emission and fuel consumption performance for these fuels, the standard test matrix based on the abbreviated AVL 8-Mode test had to be run twice.

- In the first run (referred later as "constant fuel" case) the fueling rates and corresponding A/F ratios (as well as other engine settings and operating parameters) have been kept the same between baseline fuel and oxygenated fuel tests, resulting in lower torques and deteriorated fuel economy.

- In the second run (referred later as "constant torque" case) the fueling rates have been adjusted to achieve baseline level of engine torques as well as some adjustment of A/F fuel ratios applied to account for a higher energy transfer to the turbo in the real engine. Effects of those adjustments on emission and potential improvement of fuel economy were evaluated.

As in the previous discussions of the engine investigation, the results of the emission and fuel consumption performance comparisons between the ultra -low sulfur baseline fuel and the heavily oxygenated test fuel are presented here as the trade-offs between the NOx and soot as well as between the NOx and BSFC. These trade-offs have been generated by changes in combinations of settings of major combustion control parameters such as injection pressure, injection timing (represented by start of combustion SOC), air/fuel ratio and concentration of EGR in intake air. Comparison between performance of both investigated fuels have been conducted at four points of the engine operating map designated as Modes 4, 6, 7 and 8 and considered to be the significant overall contributors to result of the HD FTP emission certification cycle. The actual data are summarized graphically and tabulated numerically in Appendix 1.2. The tables include definitions of operating conditions at each of the test points as well as information on specific combinations of control settings driving obtained emission trade-offs. In addition, the tables also include the comparison of performance results obtained in a "constant fuel" runs for both the baseline and the oxygenated fuel. The results obtained from the "constant torque" case are only presented on graphs. When reviewing the full scope of presented data, an observation can be made that there is a limited amount of data for the Mode 7 "constant torque" case as well as for all the cases of Mode 8. Reason for the limited test data was due to the amount of fuel available for testing. This limitation, however, did not obscure the overall conclusions regarding the effects of investigated test fuel on engine emission and performance.

The heavily oxygenated fuel tested in International SCTE demonstrates a very significant smoke emission reduction at all operating conditions and calibration points over the baseline low sulfur fuel. The other very interesting finding is a consistent and quite substantial reduction in NOx, which persist for both "constant fuel" and "constant

torque" cases. As expected, due to reduced calorific value of oxygenated fuel, the fuel mass based BSFC is increased. This increase, although somewhat mitigated in the "constant torque" case, seems to be higher than it could be explained by a lower calorific value of the fuel itself. Additional reasons of such significant deterioration in fuel economy related to specific combustion chemistry or otherwise, are not clear at this point. In general, the relative emission /BSFC performance of the oxygenated fuel vs. the base low sulfur fuel can be can be summarized as follows:

Mode 4 (1500rpm/10 bar BMEP):

- Range of Soot reduction: from 50% reduction to 80%
- Range of NOx: reduction: from 6 to 19%
- Range of BSFC increase: from 12 to 18%

Mode 6 (3170rpm/3.8 bar BMEP):

- Range of Soot reduction: from 49 to 67%
- Range of NOx: reduction: from 15 to 22%
- Range of BSFC increase: from 25 to 45%

Mode 7 (3170rpm/7 bar BMEP):

- Range of Soot reduction: from 61 to 78%
- Range of NOx reduction: from 13 to 34%
- Range of BSFC increase: from 13 to 36%

Mode 8 (3010rpm/10.5 bar BMEP):

- Range of Soot reduction: from 70 to 74%
- Range of NOx: reduction: from 8 to 9%
- Range of BSFC increase: from 20 to 23%

The highly oxygenated fuel seems to lower NOx by reducing local flame temperature, similarly to the exhaust gas recycle (EGR) mechanism. The benefit of BPO must be weighed against the increase in fuel consumption.

These tests (Set 1 and Set 2) indicate that both FT diesel and BPO can substantially reduce NOx and soot emissions.

To further explore the impact of BPO, two more SCTE tests are scheduled in 1Q03: a 5% BPO in FT diesel blend and 5% BPO in ULS. This test work will then conclude the SCTE test campaign.

3.4.1.3.2 MCTE Campaign

For a NOx reduction device to be a viable solution for future emissions regulations, the problem of NOx Adsorber poisoning by sulfur components (SO_2/SO_3) must be addressed. Apparently, periodic desulfation is one of the critical ways to purge SO_2/SO_3 out and recover the catalyst activity. A desulfation test apparatus, shown in Figure 18, has been built to study this process and gauge the effects of fuel

components on its operation. An experimental campaign is underway to develop the best desulfation strategy to regenerate the NOX adsorber. One possible solution is to raise the catalyst inlet temperature to adequate levels (~600°C) while maintaining a rich exhaust stream (A/F ~13). This protocol was tested in a preliminary experiment. Conditions for the experiment were: mid-speed/mid-load condition of 1500 RPM, and 210ft-lbs. at steady state.

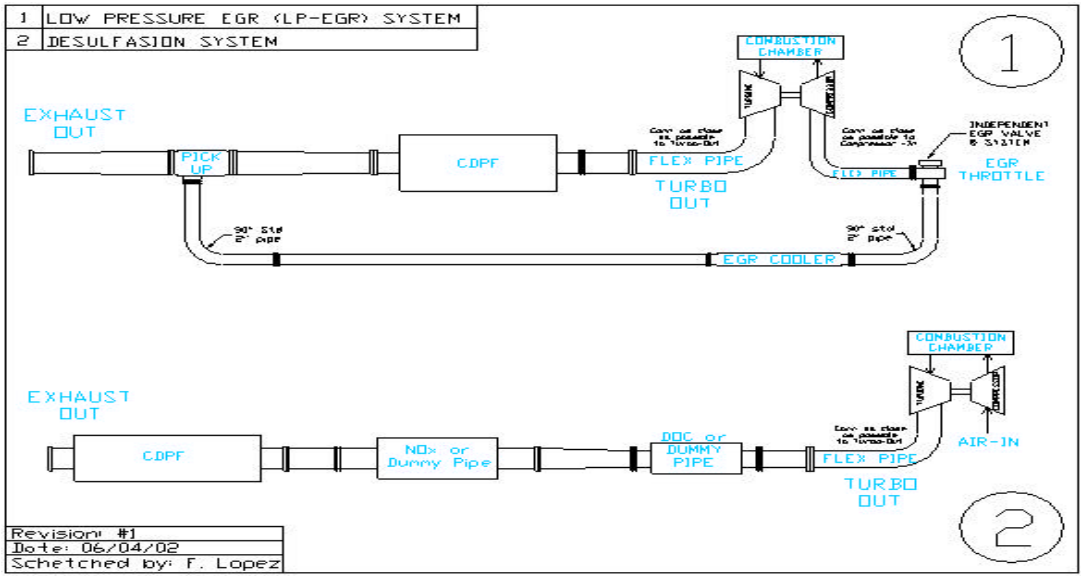

Figure 18: Desulfation test apparatus

At these engine conditions it was found that:

- ITH, EGR, and post injection are the key components to reduce A/F ratio to 13.
- Post injection is necessary to generate high HC levels (~8000 ppm) and the pre-catalyst seems critical to burn off HC and raise up the inlet temperature to >600°C.

A relatively clean NOx absorber was used to test the above desulfation protocol. The clean NOx adsorber yielded a baseline efficiency of 80% over the HD FTP cycle using the latest L/R strategy. It was then poisoned for 14 hours using a conventional No. 2 diesel fuel. After sulfur poisoning, the NOx reduction efficiency of the catalyst dropped down to 48%. The desulfation conditions were then run for 15 minutes, and the NOx absorber efficiency recovered to near 80%, indicating the preliminary desulfation process is effective.

The next step is to evaluate potential benefits of the modified fuels on the desulfation process, such as by-products control, sulfur purge efficiency and fuel penalty, etc.

3.4.2 Nuvera Fuel Cells

3.4.2.1 Goal - Nuvera Fuel Cells

The goal is to understand effect of UCTF on the fuel cell system and possibly reduce emissions on a per mile basis. The scope of phase II in the current program is to study and compare emissions produced by three alternative fuels in fuel processing / fuel cell power plant. The fuels chosen for the study were Naphtha from Sasol/Chevron, California Phase II Gasoline from Chevron Phillips and Oxygenated Naphtha blended at BP.

3.4.2.2 Experimental

Nuvera's Burner facility comprises of Nuvera's Burner module, gas and condensate sampling system, and all the process streams required for clean processing of different fuels. The experimental layout of burner facility is shown in Appendix 2.

3.4.2.3 Results and Discussion

Three fuels – GTL Naphtha, oxygenated GTL Naphtha/BPO and California Phase II RFG, were successfully processed in Nuvera's Burner Module for start-up emission study. Physical property data for these fuels are shown below in Table 9.

Table 9. Properties of fuel used in Nuvera's Burner Module for startup emission study

Fuel Properties	GTL Naphtha/BPO	GTL Naphtha	California Phase II RFG
API Gravity	71.86	73.4	60.57
Specific Gravity, 60F/60F	0.6958	0.6906	0.7367
Density, kg/m^3	695.8	690.6	736.7
C, m%	82.44	84.1	84.96
H, m%	15.82	15.9	13.02
O, m%	1.74	0	2
N, ppm	<1	<1	<1
S, ppm	1	0	32.9
Lower heating value LHV, kJ/kg	43946	44357	40983
(Air/Fuel)$_{stoich}$	14.79	15.08	14.12
Estimated molecular weight, gm/gm-mol	99.4	101.0	100.95

Exhaust gas composition was analyzed for bulk components such as carbon dioxide, water vapors and oxygen, and traces of species, such as NOx, carbon monoxide (CO) and total hydrocarbons (THC), that are governed by emission standards from the Environmental Protection Agency (EPA). In addition, process condensates were collected for analysis of water contaminants in the burner exhaust. The fuels under

study were compared in terms of burner module operating conditions, exhaust compositions, start-up and steady state emissions.

To ensure repeatability of the experiments, the burning cycle of each fuel was conducted at least three times starting with the fuel ignition through the startup and steady state phase and ending with cooling burner to initial temperature.
All fuels show spikes of THC and carbon monoxide emissions at the burner startup. This is attributed to unburned fuel skipping through the module when it is lit initially. The CO spike occurred due to incomplete fuel combustion. No spikes in NOx emissions were recorded for any fuel at the startup conditions. Concentration of NOx is much less than the concentration of CO and THC

There are two principal sources of nitrogen oxide (NOx) formed during combustion: one is oxidation of atmospheric (molecular) nitrogen and another is oxidation of nitrogen-containing compounds in the fuel. During combustion of studied "clean" fuels, containing no nitrogen compounds, under lean or stoichiometric conditions the thermal mechanism is the principal source of nitrogen oxide emissions.

Integrated startup emissions for all three fuels tested are shown in Table 10. The integrated values were calculated using total amount of startup emissions divided by the amount of fuel used during respective startup time.

Table 10. Emissions at Startup

Fuel	mg/gfuel		
	CO	THC	NOx
GTL Naphtha	7.34	110.78	0.57
GTL Naphtha/BPO	5.61	78.07	0.23
Cal Phase II RFG	6.28	92.24	0.79

Table 10 shows that GTL Naphtha/BPO has the lowest CO, THC, and NOx startup emissions among all fuels tested. This can be attributed to the oxygen added to the fuel. GTL Naphtha and GTL Naphtha/BPO have almost the same fuel blend except GTL Naphtha/BPO contains 1.74% oxygen. It seems that adding oxygen to the fuel results in more complete fuel combustion and, subsequently, reducing tailpipe emissions. Oxygenated fuel also tends to provide more complete combustion of its carbon into carbon dioxide (CO_2), thereby reducing emissions of hydrocarbons and carbon monoxide. Even though both GTL Naphtha/BPO fuel and California Phase II RFG gasoline have similar oxygen concentration in the fuel (1.74 and 2 % respectively), emissions from gasoline burning are higher than emissions from GTL Naphtha/BPO. This could be explained by high percentage of aromatic compounds in California Phase II RFG, which satisfies its high octane rating.

Table 11 shows steady state emissions of three fuels averaged throughout the single burning cycle.

Table 11. Emissions throughout steady state

Fuel	mg/gfuel		
	CO	THC	NOx
GTL Naphtha	0.42	0.61	0.57
GTL Naphtha/BPO	0.41	0.61	0.23
Cal Phase II RFG	0.55	0.52	0.79

Addition of oxygen to the Naphtha blend did not affect steady state emissions of hydrocarbons and carbon monoxide as shown in Table 11. However, NOx emissions are decreased in the oxygenated Naphtha fuel blend that may be attributed to the oxygen presence in the fuel. Table 11 indicates that California Phase II RFG is the worst fuel blend among all three fuels at steady state conditions. This can be attributed to high-octane aromatics presence.

Table 12 shows average values of oxygen and carbon dioxide emissions of the three fuel blends.

Table 12. Oxygen and carbon dioxide emissions

Fuel	vol. %	
	O_2	CO_2
GTL Naphtha	13.85	6.04
GTL Naphtha/BPO	13.72	5.76
Cal Phase II RFG	11.85	10.8

Table 12 shows that GTL Naphtha and GTL Naphtha/BPO have almost the same oxygen and carbon dioxide concentrations in the burner exhausts. This is expected since both fuels have almost the same fuel compositions. It seems that adding oxygen to the Naphtha blend did not influence oxygen and carbon dioxide emissions significantly.

3.5 Task 10: Program Management

3.5.1 Goal - Task 10

The recipient shall provide technical leadership and management direction to ensure that the program delivers its goals on time, within budget and in a safe and environmentally acceptable manner. Good communications with the DOE, participants, and subcontractors will be maintained.

3.5.2 Milestones - Task 10

A detailed briefing shall be presented within (60) days of the end of the budget period. The briefings shall be given by the Recipient to explain the plans, progress, and results of the project effort, both technical and administrative.
Status:

- The Quarterly Reports for the Second Budget Period, 1st, 2nd, 3rd and 4th Quarters were completed and issued on time.
- Nuvera completed all Phase 2 experiments and the final report on time and within budget.
- A delay has been encountered in the preparation of BPO, an oxygenate supplied by BP. This fuel blending component is required to complete the SCTE test program.
- The HCCI engine tests have been delayed due to availability of certain test rigs.
- A kick-off meeting for the Second Budget Period was held on May 2, 2002 at Praxair's Tonawanda, NY research center.
- An end of the year briefing was presented to the DOE on December 12, 2002 at Praxair's Tonawanda, NY research center.
- The program remains under budget through the fourth quarter.
- A no cost extension has been requested to carry the program into 2003.

3.5.3 Discussion - Task 10

The OTM syngas program is under budget but behind schedule in some tasks. The Nuvera fuel cell testing is complete. The International diesel engine work is progressing well, but is about 4 to 6 months behind schedule due to the hiatus between completion of the 1st budget period in November, 2001 and approval of this (2nd) budget period in April, 2002. The single cylinder engine test work should be completed early next year. Thirteen drums of FT diesel fuel were obtained for the diesel engine development work. Additional quantities of BPO are also being manufactured. The production of BPO was scheduled to be completed by the end of this quarter, but a technical problem was encountered in the manufacturing process. The HCCI work at International has been delayed due to availability of the single cylinder test engine, which will be modified for HCCI studies. This should be corrected in the next budget period.

Overall, costs remain under budget. A no cost extension for the program has been requested. This should allow continuation of the program through early 2003.

4.0 Conclusions

- Two robust substrate systems (MM1, LCM29) show great promise for achieving long-term life and performance targets. Life tests on both systems are on-going.
- A suite of OTM materials have been developed that approximate the thermal expansion properties of the new substrates.
- Target flux has almost been achieved with a new, more robust composite (LCM29/LCM38) system. Architectural improvements should allow this system to achieve target flux.
- Thermal and chemical expansion properties of both membrane and substrate materials can be engineered to a certain degree by compositional manipulation.

- Several new architectures (Config.1 and 2) for the MM system appear promising based on preliminary thermal cycle tests.
- Target flux has been achieved for an MM3/LCM1 system at 1.1TT.
- The temperature boundaries of these systems are being mapped by new test procedures, including operations at 10% above the target temperature. Preliminary high temperature tests of LCM29 and MM3 substrates are very encouraging.
- A new high-pressure test rig was successfully operated at TT and 2.2TP with a dense LCM1 tube. This shows that high-pressure operations are feasible.
- A novel reactor design has been developed that lowers capital costs, improves operability, and has the flexibility to produce hydrogen as well as syngas.
- Fischer Tropsch diesel fuel shows a clear advantage in reducing NOx and soot in comparison to conventional No. 2 diesel fuel.
- The BP oxygenate show significant reductions in both NOx and soot in comparison to an ultra low sulfur petroleum derived diesel fuel.
- The lower heating value of the highly oxygenated fuel requires more fuel to achieve constant torque. Sometimes the fuel consumption is more than expected by calorific value of the fuel, suggesting other inefficiencies are being created in the combustion process.
- In the Nuvera fuel cell burner system, burning GTL Naphtha/BPO fuel resulted in the least amount of emissions among the three fuels studied
    - Adding BPO to the naphtha fuel blend reduced start-up emissions of carbon monoxide, NOx and hydrocarbons.
    - Adding oxygen to the Naphtha fuel blend did not affect the steady state emissions of carbon monoxide and hydrocarbons but resulted in reducing NOx emissions.
- Based on test results reported by both Nuvera and International, the BPO has real value for reducing emissions (hydrocarbons, NOx) from both open flame burners and internal combustion diesel engines.

5.0 References

1. Robinson et al, Topical Report for “Development of OTM Syngas Process and Testing of Syngas-Derived Ultra-clean Fuels in Diesel Engines and Fuel Cells”, US DOE Award No. DE-FC26-01NT41096, Budget Period 1, October 2001.
2. Robinson et al, Quarterly Project Status Report for Period ending September 30, 2002 for “Development of OTM Syngas Process and Testing of Syngas-Derived Ultra-clean Fuels in Diesel Engines and Fuel Cells”, US DOE Award No. DE-FC26-01NT41096, December 2002.
3. Robinson et al, Quarterly Project Status Report for Period ending December 31, 2001 for “Development of OTM Syngas Process and Testing of Syngas-Derived Ultra-clean Fuels in Diesel Engines and Fuel Cells”, US DOE Award No. DE-FC26-01NT41096, March 2002.

Appendix 1

International Truck and Engine SCTE Fuel Results

Appendix 1.1 -- No.2 Diesel versus FT Diesel

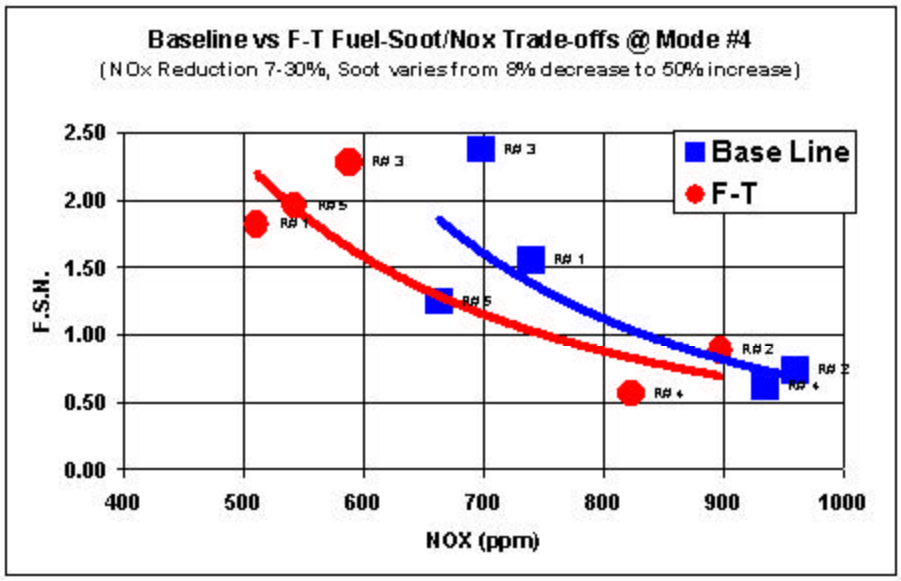

Figure 1. Baseline vs. F-T Fuel - Soot/NOx Trade-offs @ Mode 4

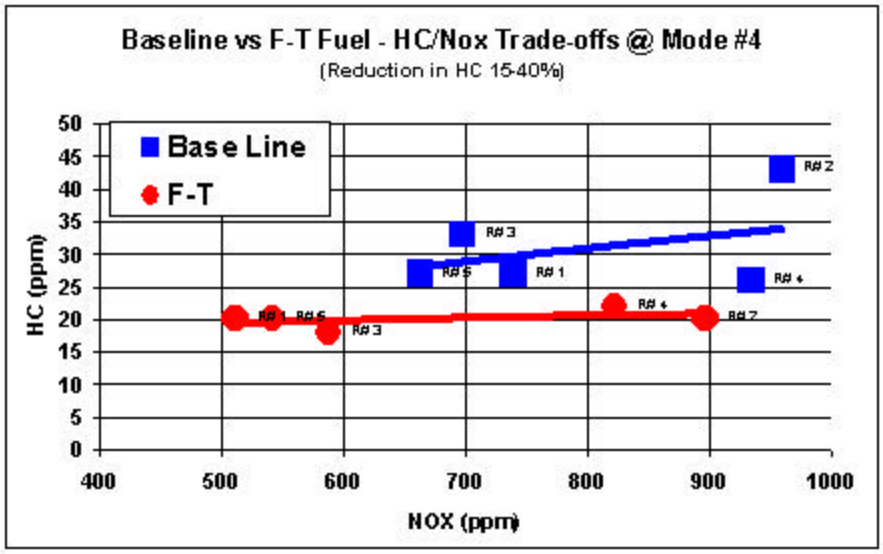

Figure 2. Baseline vs. F-T Fuel - HC/NOx Trade-offs @ Mode 4

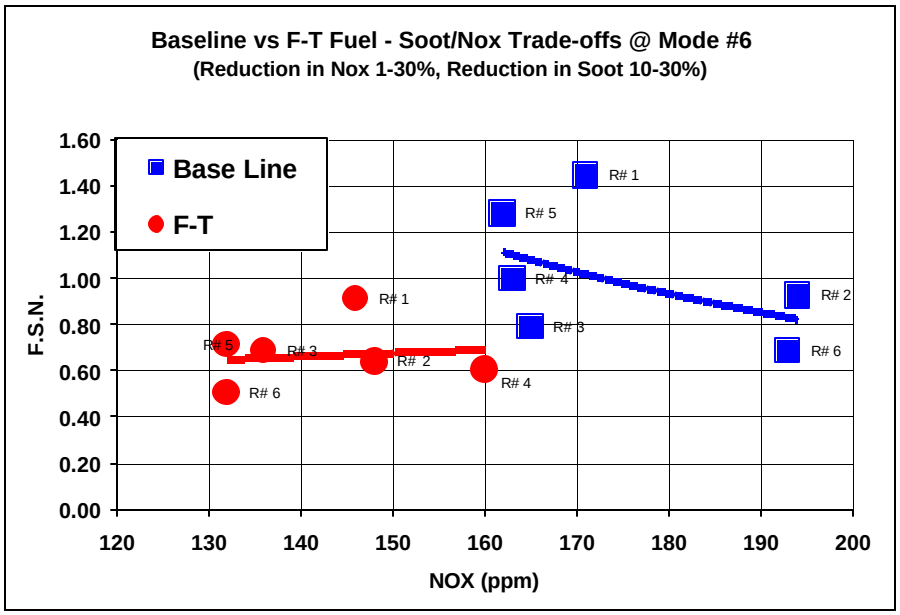

Figure 3. Baseline vs. F-T Fuel - Soot/NOx Trade-offs @ Mode 6

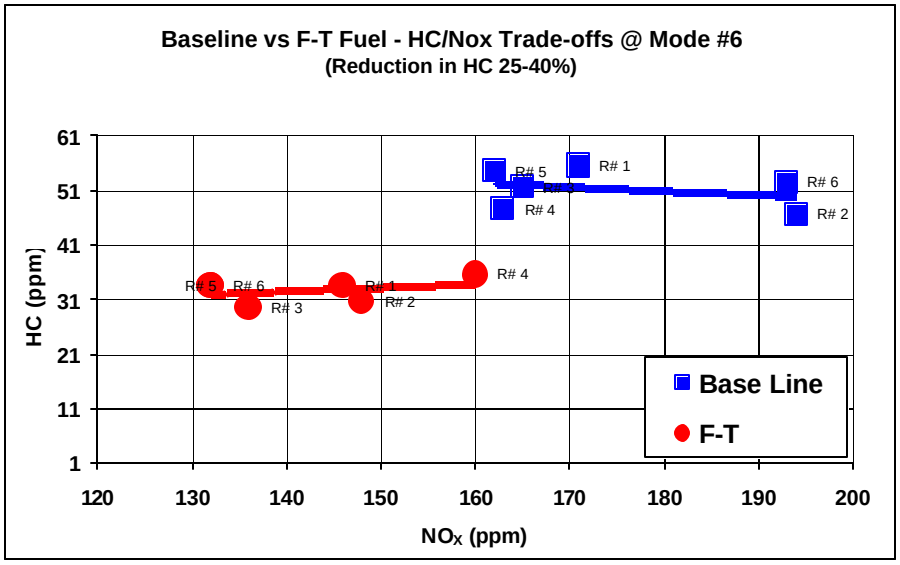

Figure 4. Baseline vs. F-T Fuel - HC/NOx Trade-offs @ Mode 6

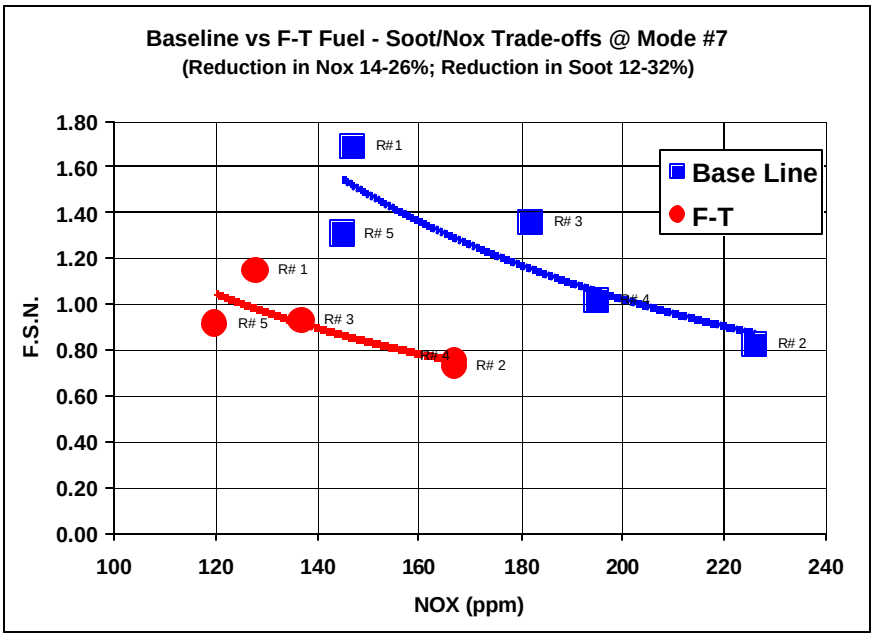

Figure 5. Baseline vs. F-T Fuel - Soot/NOx Trade-offs @ Mode 7

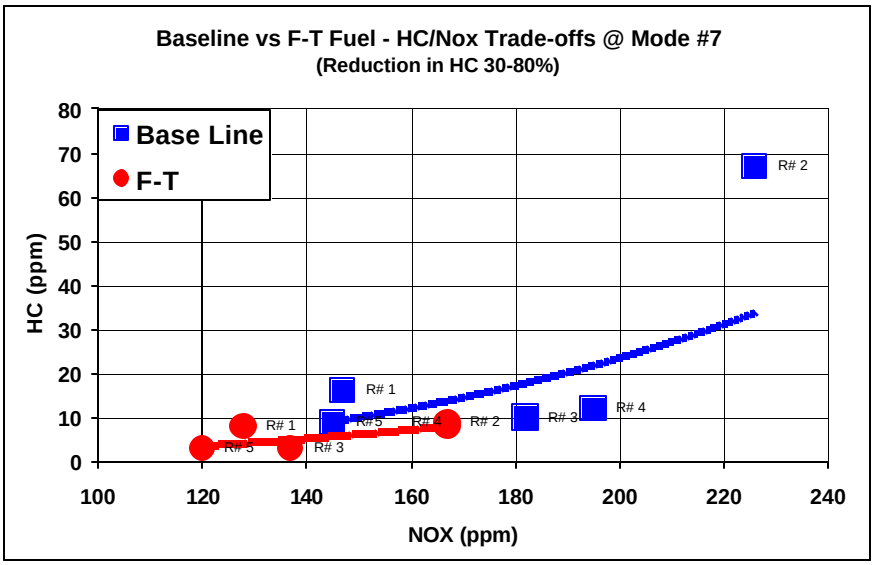

Figure 6. Baseline vs. F-T Fuel - HC/NOx Trade-offs @ Mode 7

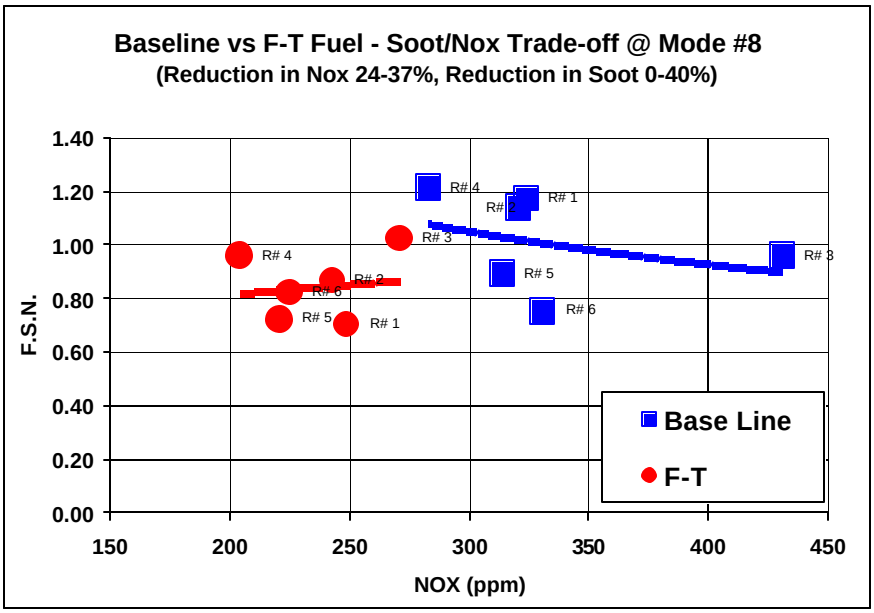

Figure 7. Baseline vs. F-T Fuel - Soot/NOx Trade-off @ Mode 8

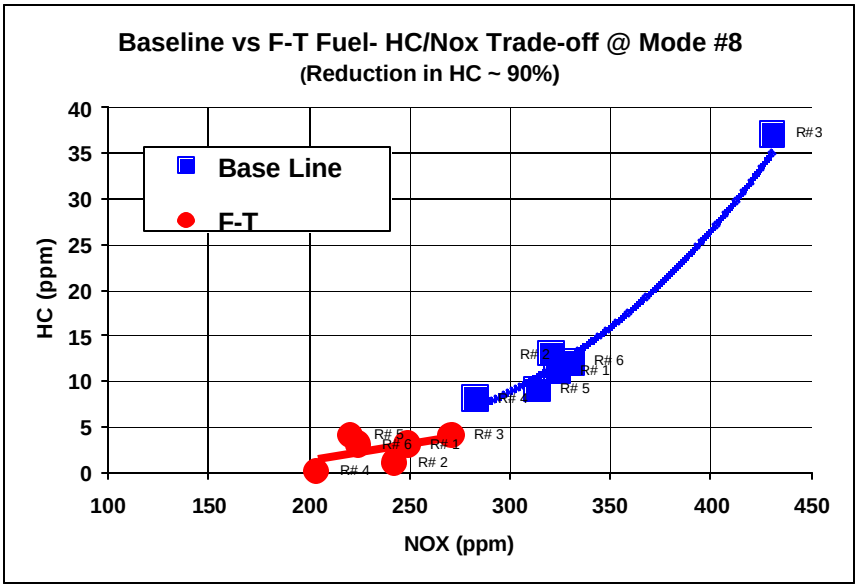

Figure 8. Baseline vs. F-T Fuel - HC/NOx Trade-off @ Mode 8

Table 1. Test Data at Mode 4

Mode #4																
Run#		1	1	d%	2	2	d%	3	3	d%	4	4	d%	5	5	d%
Fuel		BL	FT		BL	FT		BL	FT		BL	FT		BL	FT	
Engine Speed	rpm	1493	1498		1503	1497		1510	1497		1496	1496		1503	1507	
Torque	lb-ft	47.1	47.5		43.7	49.4		44.5	45.4		46.2	48.2		44.8	45.6	
NOx	ppm	740	511	-31	960	897	-7	698	588	-16	935.0	823.0	-12	663	542.0	-18
HC	ppm	27	20	-26	43	20	-53	33	18	-45	26.0	22.0	-15	27	20.0	-26
AVL smoke	FSN	1.55	1.82	17	0.7	0.9	20	2.4	2.3	-4	0.6	0.6	-8	1.24	2.0	57
ICP	Mpa	11	11		10.7	10.7		10.6	10.7		12.0	12.1		12	12.1	
Air Fuel Ratio		21.7	21.5		24.3	24.3		21.6	21.5		23.8	23.5		21.0	20.9	
EGR	%	5.5	5.7		0.7	0.6		3.1	3.0		4.1	3.9		5.8	6.1	
SOC-main	deg CA ATDC	4	4		4.0	4.0		8.0	8.0		4.0	0.4		6	6.0	
BSFC	lb/hp-hr	0.367	0.372	1	0.399	0.359	-10	0.388	0.394	2	0.362	0.360	-1	0.382	0.373	-2
Fuel Flow	lb/hr	5.43	5.41		5.39	5.41		5.51	5.49		5.29	5.30		5.45	5.42	

Table 2. Test Data at Mode 6

Mode #6																			
Run#		1	1	d%	2	2	d%	3	3	d%	4	4	d%	5	5	d%	6	6	d%
Fuel		BL	FT		BL	FT		BL	FT		BL	FT		BL	FT		BL	FT	
Engine Speed	rpm	3168	3171		3168	3170		3170	3170		3169	3171		3169	3171		3169	3172	
Torque	lb-ft	17.0	17.7		14.6	16.1		15.4	15.8		15.6	15.6		15.1	15.7		14.6	15.7	
NOx	ppm	171	146	-15	194	148	-24	165	136	-18	163.0	160.0	-2	162	132.0	-19	193	132.0	-32
HC	ppm	55	33	-40	46	30	-35	51	29	-43	47.0	35.0	-26	54	33.0	-39	52	33.0	-37
AVL smoke	FSN	1.44	0.91	-37	0.9	0.6	-31	0.8	0.7	-13	1.0	0.6	-39	1.28	0.7	-45	0.69	0.5	-27
ICP	Mpa	17	17		17.1	17.1		17.1	17.1		19.2	19.1		17	17.1		19	19.1	
Air Fuel Ratio		30.7	30.8		33.5	33.6		29.9	29.5		32.8	32.0		29.5	29.7		32.4	32.5	
EGR	%	16.4	16.1		9.3	10.1		12.8	12.1		14.6	14.0		13.0	13.5		8.6	8.9	
SOC-main	deg CA ATDC	6	6		8.0	8.0		10.2	10.0		6.0	6.0		8	8.5		10	10.0	
BSFC	lb/hp-hr	0.563	0.546	-3	0.594	0.594	0	0.624	0.609	-2	0.594	0.594	0	0.614	0.599	-2	0.639	0.604	-5
Fuel Flow	lb/hr	7.43	7.44		7.53	7.53		7.64	7.62		7.43	7.43		7.42	7.43		7.61	7.62	

Table 3. Test Data at Mode 8

Mode #8																			
Run#		1	1	d%	2	2	d%	3	3	d%	4	4	d%	5	5	d%	6	6	d%
Fuel		BL	FT		BL	FT		BL	FT		BL	FT		BL	FT		BL	FT	
Engine Speed	rpm	3010	3009		3009	3012		3008	3012		3010.4	3010.5		3010	3009		3010	3009	
Torque	lb-ft	45.6	46.6		48.2	49.6		49.2	51.1		45.0	45.6		44.5	46.2		46.2	47.0	
NOx	ppm	324	249	-23	321	243	-24	431	271	-37	283.0	204.0	-28	314	221.0	-30	331	225.0	-32
HC	ppm	11	3	-73	13	1	-92	37	4	-89	8.0	0.0	-100	9	4.0	-56	12	3.0	-75
AVL smoke	FSN	1.17	0.70	-40	1.1	0.9	-24	1.0	1.0	7	1.2	1.0	-21	0.89	0.7	-19	0.75	0.8	9
ICP	Mpa	24	24		24.0	24.1		24.0	24.3		26.2	26.2		28	27.1		28	26.9	
Air Fuel Ratio		24.2	24.3		24.6	24.8		24.5	24.6		24.2	24.2		25.6	26.1		26.0	26.0	
EGR	%	6.3	6.1		9.3	10.0		11.3	12.2		10.6	11.0		9.0	9.7		11.6	12.1	
SOC-main	deg CA ATDC	6	7		3.0	3.0		0.0	0.0		6.0	6.0		6	6.0		3	3.0	
BSFC	lb/hp-hr	0.525	0.485	-8	0.485	0.447	-8	0.469	0.428	-9	0.532	0.487	-9	0.525	0.474	-10	0.491	0.451	-8
Fuel Flow	lb/hr	14.59	14.62		14.20	14.24		14.08	14.03		14.68	14.49		14.28	14.32		13.80	13.91	

Appendix 1.2 – ULS Diesel and ULS with 10% Oxygen

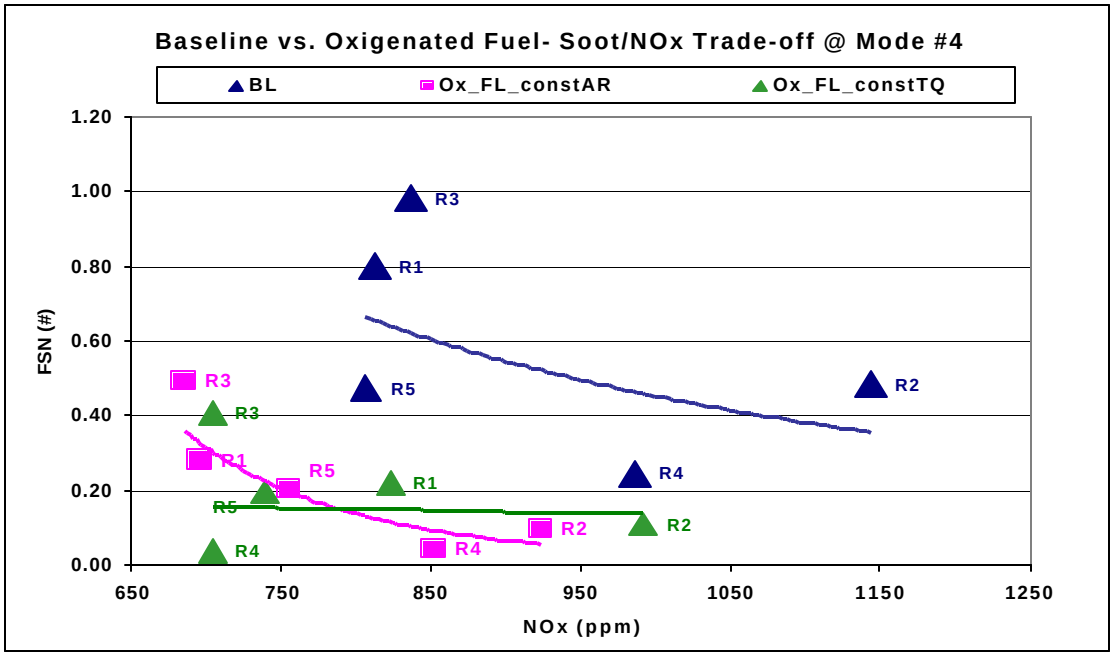

Fig 1

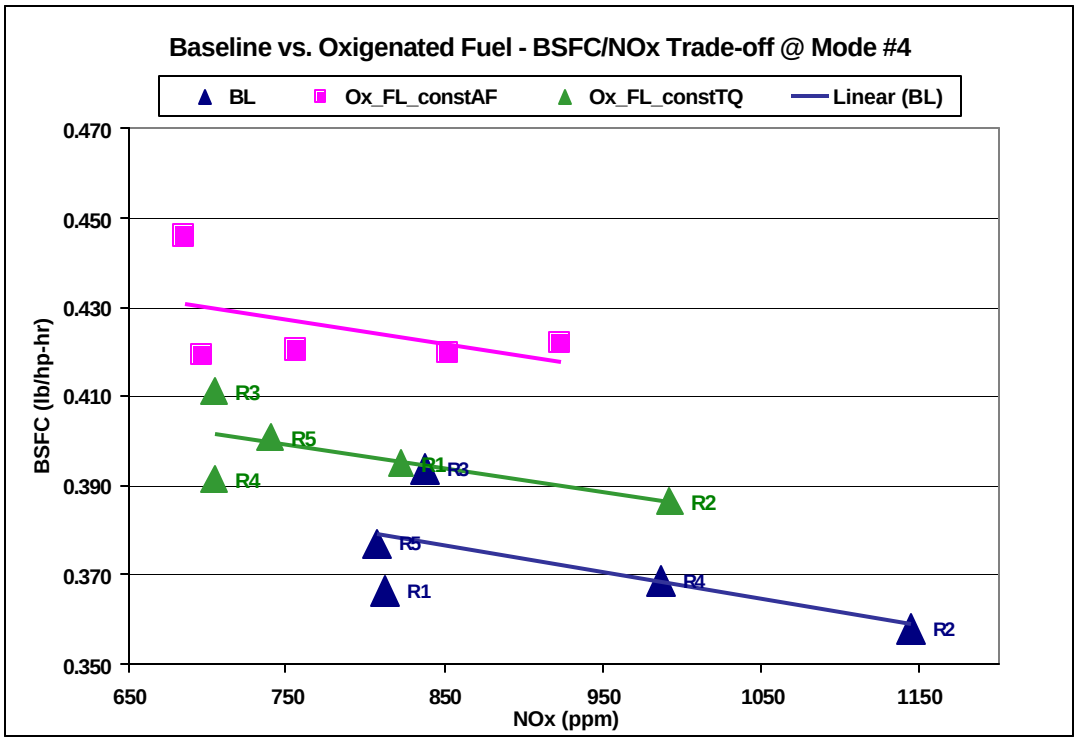

Fig 2

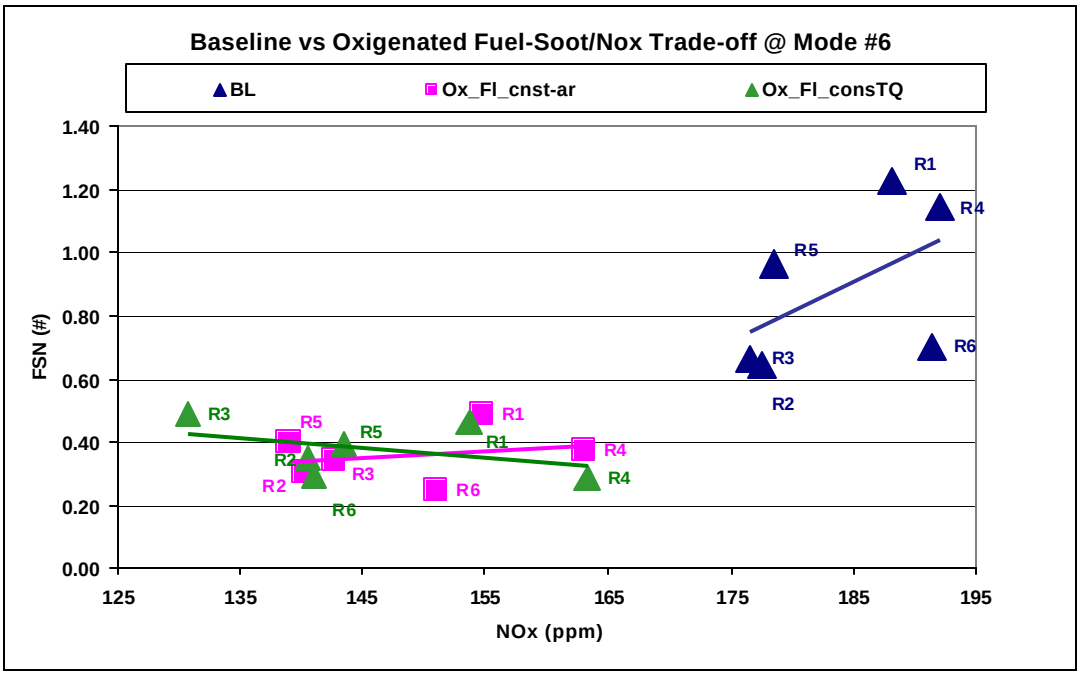
Baseline vs Oxigenated Fuel-Soot/Nox Trade-off @ Mode #6
BL
Ox_Fl_cnst-ar
Ox_Fl_consTQ
FSN (#)
NOx (ppm)
1.40
1.20
1.00
0.80
0.60
0.40
0.20
0.00
125
135
145
155
165
175
185
195
R1
R4
R5
R6
R3
R2

Fig. 3

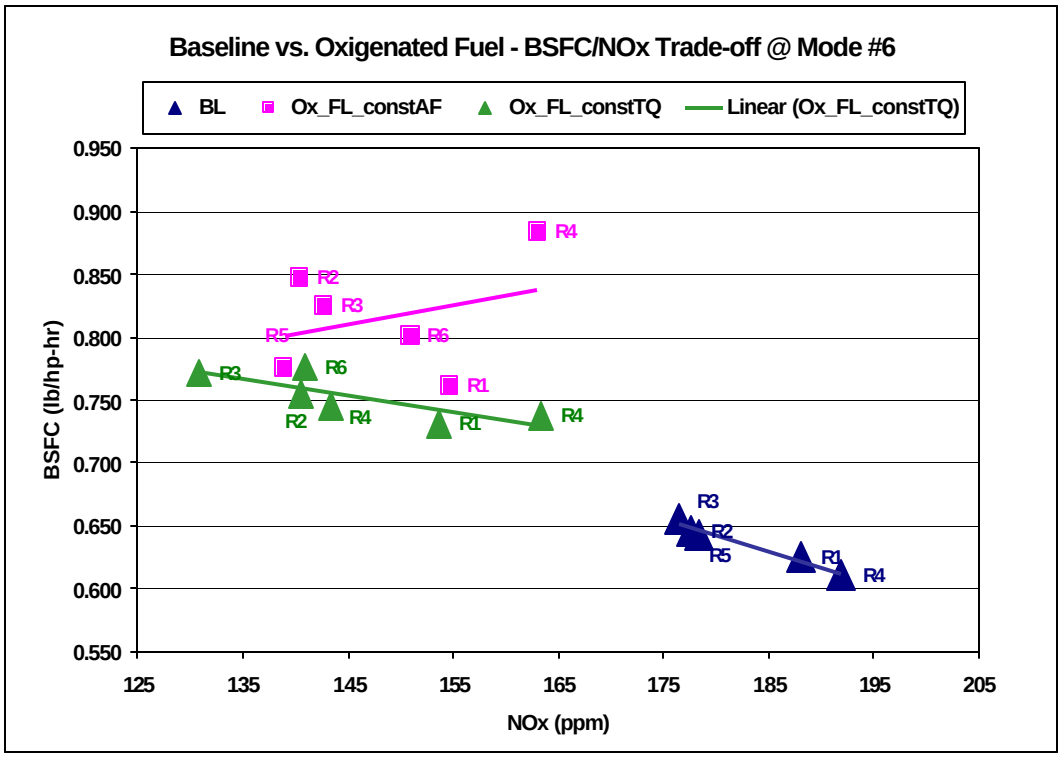
Baseline vs. Oxigenated Fuel - BSFC/NOx Trade-off @ Mode #6
BL
Ox_FL_constAF
Ox_FL_constTQ
Linear (Ox_FL_constTQ)
BSFC (lb/hp-hr)
NOx (ppm)
0.950
0.900
0.850
0.800
0.750
0.700
0.650
0.600
0.550
125
135
145
155
165
175
185
195
205
R4
R2
R3
R5
R6
R1

Fig. 4

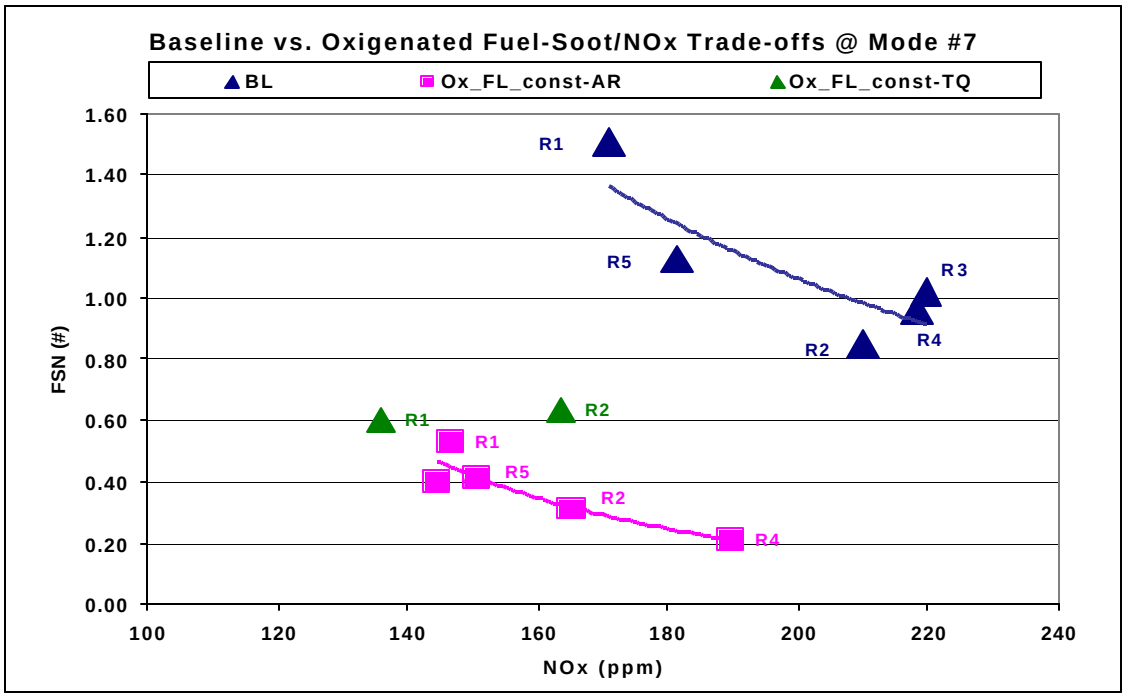
Baseline vs. Oxigenated Fuel-Soot/NOx Trade-offs @ Mode #7
BL
Ox_FL_const-AR
Ox_FL_const-TQ
FSN (#)
NOx (ppm)
1.60
1.40
1.20
1.00
0.80
0.60
0.40
0.20
0.00
100
120
140
160
180
200
220
240
R1
R5
R3
R4
R2
R1
R2
R1
R5
R2
R4

Fig. 5

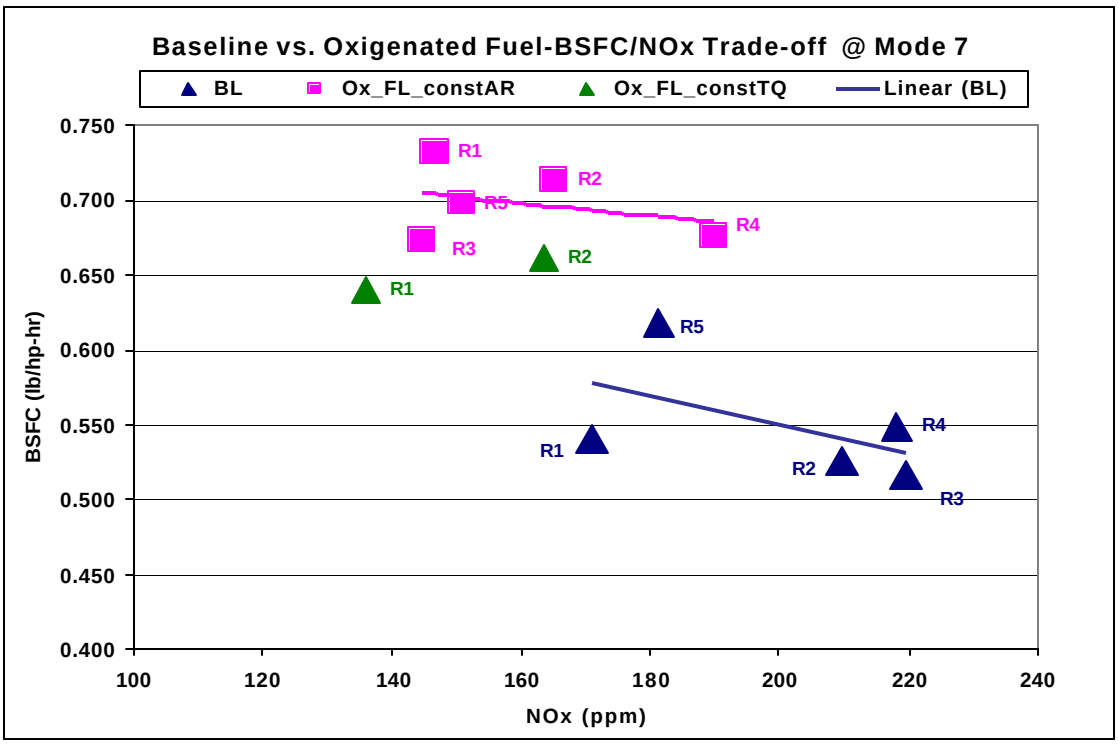
Baseline vs. Oxigenated Fuel-BSFC/NOx Trade-off @ Mode 7
BL
Ox_FL_constAR
Ox_FL_constTQ
Linear (BL)
BSFC (lb/hp-hr)
NOx (ppm)
0.750
0.700
0.650
0.600
0.550
0.500
0.450
0.400
100
120
140
160
180
200
220
240
R1
R2
R5
R4
R3
R2
R1
R5
R1
R4
R2
R3

Fig. 6

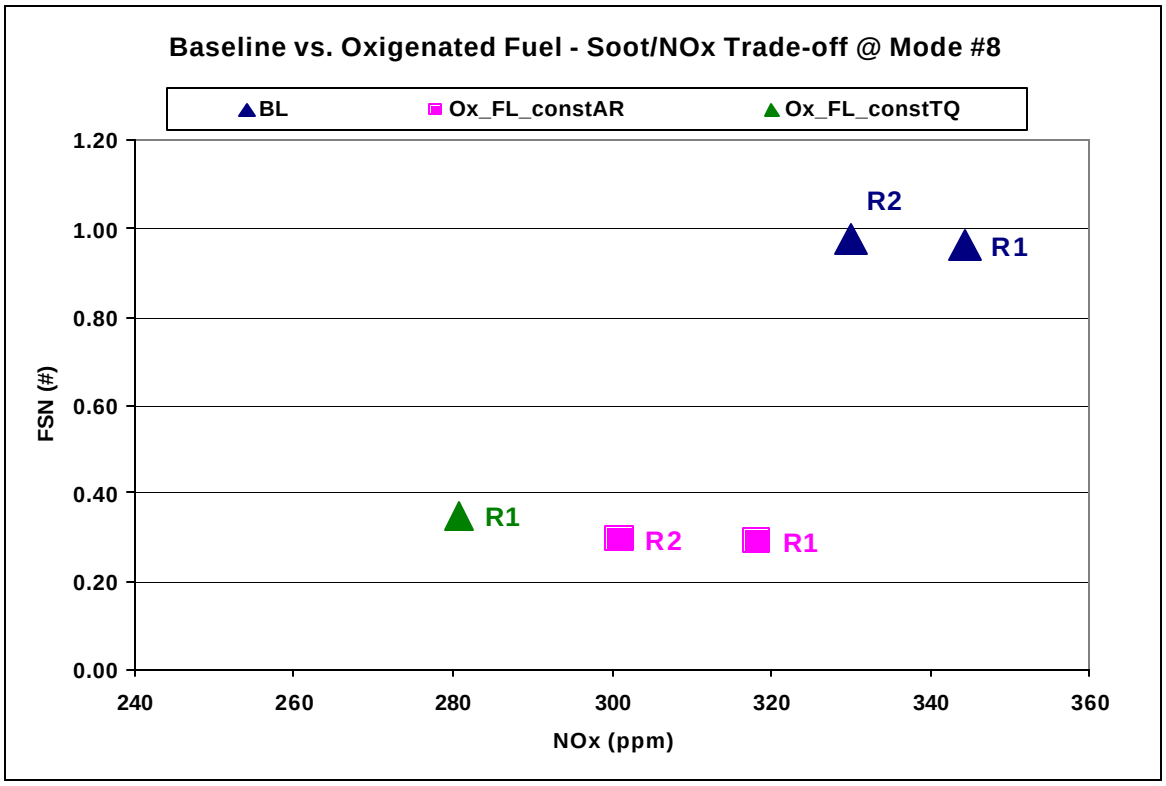
Baseline vs. Oxigenated Fuel - Soot/NOx Trade-off @ Mode #8
BL
Ox_FL_constAR
Ox_FL_constTQ
1.20
1.00
0.80
0.60
0.40
0.20
0.00
FSN (#)
R2
R1
R1
R2
R1
240
260
280
300
320
340
360
NOx (ppm)

Fig.7

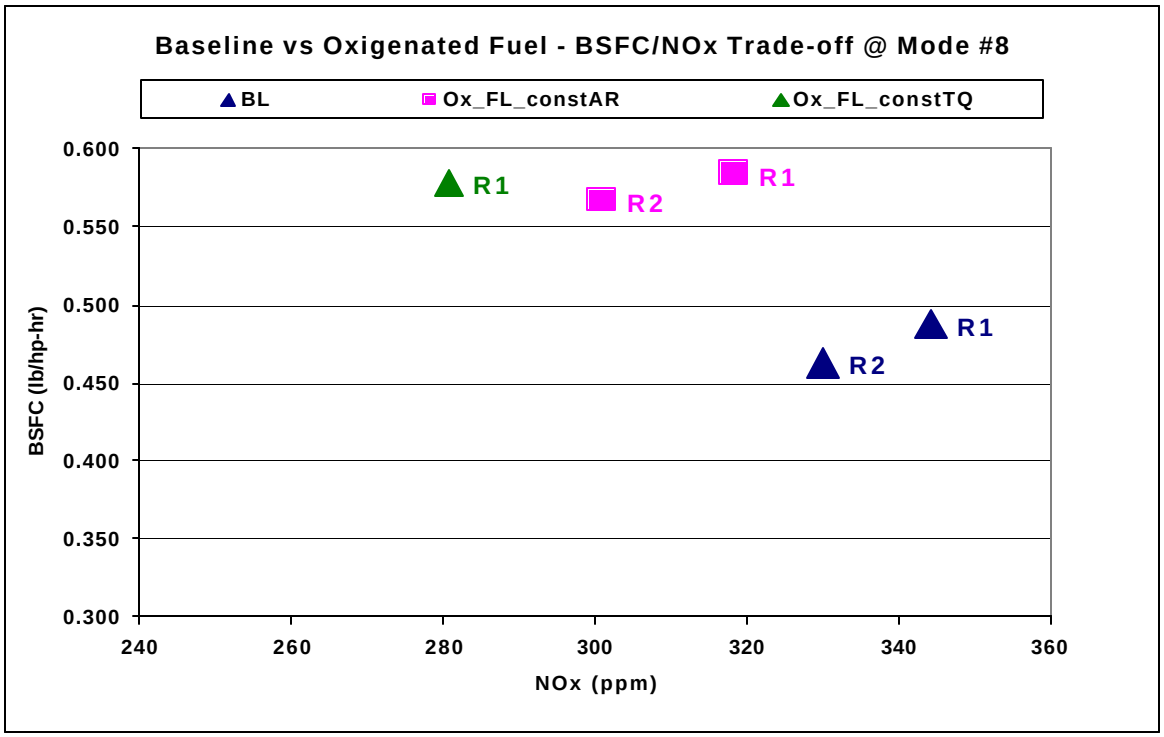
Baseline vs Oxigenated Fuel - BSFC/NOx Trade-off @ Mode #8
BL
Ox_FL_constAR
Ox_FL_constTQ
0.600
0.550
0.500
0.450
0.400
0.350
0.300
BSFC (lb/hp-hr)
R1
R2
R1
R1
R2
240
260
280
300
320
340
360
NOx (ppm)

Fig. 8

Table 1

Mode #4

Run#		1	1	d%	2	2	d%	3	3	d%	4	4	d%	5	5	d%
Fuel		BL	OX		BL	OX		BL	OX		BL	OX		BL	OX	
Engine Speed	rpm	1503	1507		1503	1497		1510	1497		1496.5	1496.5		1503	1507.4	
Torque	lb-ft	47.0	40.4	-14	48.1	40.3	-16	44.5	38.7	-13	45.9	39.3	-14	45.2	40.5	-10
NOx	ppm	812	696	-14	1144	923	-19	837	685	-18	985.7	852.0	-14	807	755.3	-6
HC	ppm	62	24	-61	60	22	-63	54	27	-51	42.7	26.5	-38	52	28.3	-45
AVL smoke	FSN	0.80	0.28	-65	0.5	0.097	-80	0.98	0.49	-50	0.25	0.043	-82	0.47	0.203	-57
ICP	Mpa	11	11		10.7	10.7		10.6	10.7		12.0	12.1		12	12.1	
Air Fuel Ratio		21.7	21.7		24.5	24.4		21.7	21.8		23.8	24.0		20.8	20.6	
EGR	%	6.1	6.1		0.6	0.9		3.0	3.8		4.8	4.7		6.0	6.1	
SOC-main	deg CA ATDC	4	4		4.0	4.0		8.0	8.0		4.0	0.4		6	6.0	
BSFC	lb/hp-hr	0.366	0.419	14	0.358	0.422	18	0.394	0.446	13	0.369	0.420	14	0.377	0.420	12
Fuel Flow	lb/hr	5.44	5.45		5.43	5.46		5.55	5.55		5.35	5.32		5.40	5.47	

Table 2

Mode #6

Run#		1	1	d%	2	2	d%	3	3	d%	4	4	d%	5	5	d%	6	6
Fuel		BL	OX		BL	OX		BL	OX		BL	OX		BL	OX		BL	OX
Engine Speed	rpm	3170	3169		3170	3168		3169	3168		3169	3167		3172	3167		3169	3166
Torque	lb-ft	14.9	11.3	-24	14.4	9.8	-32	14.4	10.4	-27	15.1	8.8	-42	14.3	11.0	-23	14.1	10.6
NOx	ppm	188	155	-18	178	140	-21	177	143	-19	192.0	163.0	-15	178	139.0	-22	191	151.0
HC	ppm	70	33	-53	69	30	-57	65	29	-55	54.8	35.0	-36	56	33.0	-41	59	33.0
AVL smoke	FSN	1.23	0.49	-60	0.6	0.3	-53	0.7	0.3	-49	1.1	0.4	-67	0.96	0.4	-59	0.70	0.2
ICP	Mpa	17	17		17.1	17.1		17.1	17.1		19.2	19.1		17	17.1		19	19.1
Air Fuel Ratio		30.1	30.3		33.2	33.1		30.0	29.9		32.6	32.7		29.7	29.8		32.6	32.6
EGR	%	15.8	15.7		10.1	10.3		12.3	12.2		14.1	14.2		13.2	13.4		9.8	9.4
SOC-main	deg CA ATDC	6	6		8.0	8.0		10.2	10.0		6.0	6.0		8	8.5		10	10.0
BSFC	lb/hp-hr	0.625	0.762	22	0.646	0.847	31	0.656	0.824	26	0.611	0.884	45	0.643	0.776	21	0.659	0.801
Fuel Flow	lb/hr	7.47	7.46		7.53	7.53		7.63	7.62		7.46	7.44		7.45	7.42		7.64	7.63

Table 3

Mode #7

Run#		1	1	d%	2	2	d%	3	3	d%	4	4	d%	5	5	d%
Fuel		BL	OX		BL	OX		BL	OX		BL	OX		BL	OX	
Engine Speed	rpm	3168	3167		3169	3166		3169	3168		3170.2	3168.9		3169	3169	
Torque	lb-ft	31.1	21.6	-31	31.4	21.7	-31	32.8	23.8	-27	28.8	22.1	-23	26.2	22.6	-14
NOx	ppm	171	147	-14	210	165	-21	220	145	-34	218.3	189.7	-13	181	150.7	-17
HC	ppm	31	21	-32	29	23	-21	19	25	30	21.0	21.0	0	33	21.0	-37
AVL smoke	FSN	1.51	0.53	-65	0.85	0.31	-63	1.02	0.40	-61	0.96	0.21	-78	1.13	0.41	-63
ICP	Mpa	22	22		24.0	24.1		24.1	24.0		26.1	26.2		26	26.0	
Air Fuel Ratio		28.7	28.5		29.9	29.9		27.8	27.8		28.7	28.8		28.2	28.0	
EGR	%	13.4	13.2		8.2	8.8		12.4	12.0		13.2	13.2		12.3	11.9	
SOC-main	deg CA ATDC	9	9		9.0	9.0		9.0	9.0		7.1	7.0		11	11.0	
BSFC	lb/hp-hr	0.541	0.732	35	0.526	0.714	36	0.516	0.674	31	0.549	0.676	23	0.618	0.698	13
Fuel Flow	lb/hr	11.95	11.97		11.81	11.83		12.03	12.04		11.55	11.52		12.02	12.07	

Table 4

Mode #8

Run#		1	1	d%	2	2	d%
Fuel		BL	OX		BL	OX	
Engine Speed	rpm	3008	3009		3009	3007	
Torque	lb-ft	46.4	37.6	-19	47.7	37.9	-21
NOx	ppm	344	318	-8	330	301	-9
HC	ppm	17	39	133	13	23	79
AVL smoke	FSN	0.96	0.29	-70	1.1	0.30	-74
ICP	Mpa	24	24		24.0	24.1	
Air Fuel Ratio		24.1	24.1		24.2	24.2	
EGR	%	6.4	6.0		9.6	10.2	
SOC-main	deg CA ATDC	6	7		3.0	3.0	
BSFC	lb/hp-hr	0.487	0.584	20	0.462	0.567	23
Fuel Flow	lb/hr	14.63	14.61		14.24	14.24	

Appendix 2

Nuvera Fuel Cells Final Report

PRAXAIR INC./
NUVERA FUEL CELLS

FINAL REPORT

Development of OTM Syngas Process and Testing of Syngas Derived Ultra-clean Fuels in Diesel Engines and Fuel Cells.

Re: DE-FC26-01NT41096

Nuvera Fuel Cells

Nuvera Fuel Cell, Inc.
Acorn Park
Cambridge,
Massachusetts
02140-2390

Project Liaison James Cross
Project Manager Olga Polevaya
Project Engineers Rafey Khan, Piyush Pilaniwalla

Date December, 23, 2002

Summary.

Nuvera Fuel Cells conducted fuel testing within the scope of subcontract to Praxair Inc as a part of DOE initiated and funded Ultra Clean Transportation Fuel (UCTF) program in the area of alternative transportation fuel formulation, emissions and fuel cell power system demonstration. Growing interest in PEM fuel cells as a potential propulsion system for transportation vehicles initiated development of the advanced fuel-making technologies for improving environment and meeting fuel vehicles emission targets. These technologies will enable production of ultra-clean transportation fuels, alternative to gasoline but utilizing it's infrastructure and being cost competitive at the same time. Nuvera Fuel Cells have been investigating autothermal reforming for the series of fuels such as gasoline, methanol, ethanol, diesel and naphthas. Previous efforts were concentrated on the parametric study of syngas production efficiencies and reforming operating conditions. The purpose of the current project was to understand effect of UCTF on the fuel cell system and possibly reduce emissions on a per mile basis.
Funding schedule suggested conducting the program in two phases.

- Phase I commenced in 2001 and was purposed to demonstrate DC power in Nuvera's state-of-art disintegrated fuel cell power train with autothermal (ATR) fuel reforming. Single ultra-clean synthetic fuel was selected for this task and then compared to conventional California Phase II Gasoline fuel for hydrogen and power production efficiency.
- Phase II was completed in 2002 and scoped testing selected fuels in Nuvera's state-of-art burner module. Three fuels including two synthetic fuels and conventional gasoline were compared in terms of start-up and steady state emissions to the environment.

The current report summarizes work conducted within the scope of both phases. Performance of all synthetic fuels tested was referenced to the performance of conventional gasoline fuel, which served the benchmark in the current program and in Nuvera's automotive state-of-art fuel processors. All studied fuels were successfully processed in Nuvera's Modular Pressurized Reactor (MPR) facility and resulted in electrical power produced by the fuel cell stack. The fuels under study were compared in terms of process efficiencies, operating conditions, reformate compositions along the power train and potential emissions to the environment. The reformate gas was analyzed for bulk composition and traces of species, representing poisons to the fuel cell stack and environment. The fuel cell stack polarization curves were recorded and the derating factors on fuel reformates were estimated relatively to operation on pure hydrogen and air. The process condensates have been analyzed at different locations for understanding potential emissions and contaminants to fuel cells and environment.

Phase I. Evaluation of hydrocarbon based fuels in the disintegrated fuel cell power train.

Phase I objectives.
Demonstrate power production and evaluate selected fuels in Nuvera's state-of-art disintegrated fuel cell power plant for hydrogen and DC power production efficiency and emissions to the environment.

Experimental.
Two fuels were selected for the studies. California Phase II certified Gasoline was obtained from Chevron Phillips. This commercially available fuel meets the current strict emission standards of the state of California. The second fuel was a Fischer Tropsch naphtha obtained from the Sasol-Chevron joint venture. This is highly paraffin fuel with essentially no sulfur, nitrogen or aromatics, as presented in Table 1.

Table 1. Fuels specifications.

Characteristics	GTL Naphtha	California Phase II RFG
Hydrogen/Carbon ratio	2.25	1.8
Sulfur, ppm	<1	35
Aromatics, Vol. %	0.5	28.1
Olefins, Vol. %	0.5	7.5
Specific gravity at 60 F, g/l	0.6906	0.7377
Lower Heating Value, LHV, BTU/LB	19130	18553

Both fuels under study were processed into hydrogen containing reformates in Nuvera's disintegrated Modular Pressurized facility (MPR), shown in Fig. 1.

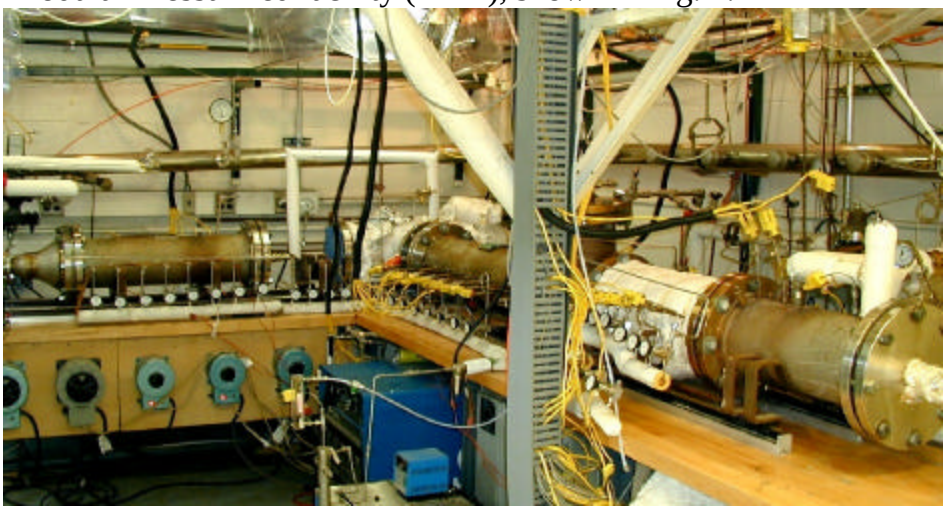

Figure 1. Modular Pressurized Facility (MPR). The upstream section, including ATR and WGS sections.

This pilot plant facility comprises the totality of fuel cell based power-producing functionality, including temperature management modules, fuel reforming spool, high-

and low-temperature Water-Gas-Shifts (WGS), optional sulfur capture module, two-stage preferential-oxidation based CO cleanup, and flexible PEM fuel cell test stand shown in Fig. 2.

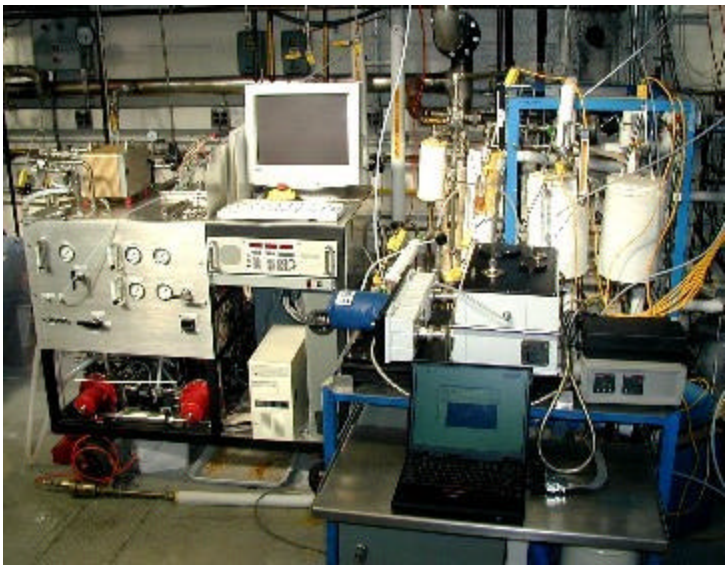

Figure 2. MPR Downstream Section, including reformate clean up and fuel cell test stand.

The maximum firing rate for the front-end assembly, including preheat, ATR and WGS sections are 140 kWth (based on the Lower Heating Value (LHV) of the fuel; for the downstream assembly, they are 40 kWth of hydrogen flowrate. Because of the differences in ratings between the upstream and downstream sections, provisions for bypassing the excess of reformate flow to the exhaust manifold have been incorporated into the assembly – a flow diagram illustrating this is shown in Figure 3.

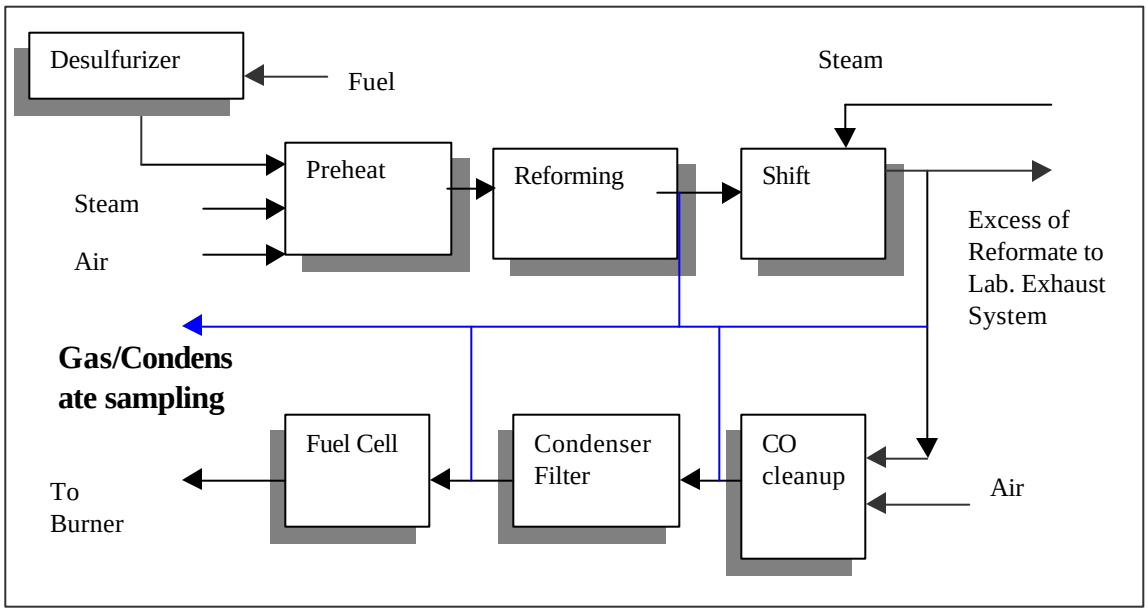

Figure 3. Experimental layout of the disintegrated power train.

Nuvera's custom desulfurization module, external to the MPR, was installed to decrease the initial concentration of sulfur in gasoline from 35 parts per million to less than 1 ppm,

which is tolerated by the catalyst modules the fuel processing train comprises of. Gasoline was desulfurized prior to inletting reforming section of the MPR train. The sulfur level before and after the adsorption traps were measured in real time during the experimental runs using the UV fluorescence sulfur detector with a lower detection limit of 200 ppb of sulfur. Sampling ports for sulfur analysis were located at the desulfurizer exit and at the exit of CO clean-up section. Resulting concentration of sulfur at the exit of desulfurization module was recorded below the referenced detection limit.

Results and discussion.

The fuel specifications were analyzed and a matrix of operating conditions for fuel reforming suggested. In all the experiments the operating pressure was maintained constant at 30 psig at the reformer inlet, while fuel cell stack operating downstream pressure was maintained at 22 psig allowing pressure decrease along the fuel processor, fuel cell and clean-up reactors.

Each fuel was mixed with the steam, preheated for vaporization and sent to the ATR section, containing Nuvera's proprietary catalytic module. In all the experiments the fuel thermal input has been maintained at 60 KW based on the lower heating value (LHV) of the fuel with the fixed equivalence ratio and steam-to-carbon ratio. Equivalence ratio (ϕ) is calculated as
ϕ = (actual fuel flow/ actual air flow)/ (stoichiometric fuel flow/ stoichiometric air flow).
Steam-to-carbon (S/C) ratio is calculated as
S/C = molar steam flow/ molar carbon flow.

Increasing both ϕ and steam-to-carbon ratio result in higher hydrogen yield but require higher process heat input in case of high steam-to carbon ratio and risk of carbon formation at the catalyst or high methane slip in case of increasing equivalence ratio. Higher ϕ also yields less process heat release to satisfy the entire system heat balance requirements and results in lowering temperature profile inside the reformer risking to elevated methane slip or potential poisons to all catalytic modules and the fuel cell.

Equivalence ratio of air to fuel was originally planned to maintain at 3.65 for both fuels to maximize the hydrogen yield. In case of naphtha processing we were able to maintain the equivalence ratio close to the designed value and satisfy the required temperature profile in the fuel processor at the same time. During gasoline fuel processing ϕ had to be lowered to 3.36 to maintain the required temperature profile in the reactor and avoid skipping non-converted aromatics. Steam-to-carbon ratio was maintained at 3.4 in all the experiments. The reformate gas has been further processed in the WGS reactors followed by the cleanup from carbon monoxide. Both fuels were successfully processed in Nuvera's MPR facility and the reformates were considered "clean" and contained no poisons to the fuel cell stack.

Maintaining designed temperature profile in multiple reactors, required to process sulfur containing gasoline, is a complicated task, and additional restrictions were imposed on the controls and operating strategy. Stability of the operating regime reflected consistency

of the reformate composition data, recorded over the running time, through the wider deviation of bulk gas concentrations from the average values in case of gasoline reforming,

shown in Table 2. Another source of the measurement error in the experiment was gas chromatograph (GC). All the steady state concentrations recorded by GC are reproduced within the GC measurement error.

Table 2. Fuel Processing data of Naphtha vs. Gasoline.

Reformate bulk composition	**Naphtha Reformate composition**	**Gasoline Reformate composition**
Hydrogen, Vol.%, dry base	43.4 +/- 0.49	40.78 +/- 1.91
Nitrogen, , Vol.%, dry base	35.8 +/- 0.68	36.87 +/- 2.32
Carbon dioxide, Vol.%, dry base	20.0 +/- 0.16	20.37 +/- 0.30
Methane, Vol.%, dry base	0.18 +/- 0.01	0.22 +/- 0.08

Analysis of carbon mass balance based on GC measurements of reformate composition allowed comparing amount of carbon processed into CO, CH_4 and CO_2 to the initial amount of carbon inletting the processor as a fuel. The carbon balance is calculated for every processed fuel at each load point during the steady state operation to verify that no carbon formation occurred. Another direct indication of carbon formation is pressure drop along the reformer. Significant carbon formation would result in increase of pressure drop, which was not observed in any of studied cases. Multiple samples were collected at the steady state to ensure repeatability. Collected samples were conditioned and sent to a specially configured GC. Detection limit of oxygen concentration measured by GC was 0.1 mol.%. No oxygen was detected at any point beyond the low detection limit.

Hydrogen production efficiency η_{HP} is calculated as

$$\eta_{HP} = H_2 \text{ flow} * LHV_{H2} / \text{Fuel flow} * LHV_{Fuel}$$

The above expression is well suited for hydrogen production efficiency of entire fuel processor. To estimate hydrogen production efficiency of each section of the fuel processor, the above expression can be converted into equation

$$\eta_{HP} = 201.63\ (Y^{d}_{H2}/\Sigma Y^{d}_{Ci})*(Cw\%/ LHV_{Fuel}) * X_f,$$

where

Cw% is the carbon weight percentage of the fuel,
Y^{d}_{H2} is the hydrogen dry volume concentration from GC data,
ΣY^{d}_{Ci} is the sum of hydrogen dry volume concentrations of CO, CH_4 and CO_2 from GC data,
LHV_{Fuel} is the lower heating value of the fuel, kJ/kg
X_f is the conversion ratio of the fuel defined as $(N_{CO}+N_{CH4} + N_{CO2})/m*N_{fuel}$
N_{ii} – is the mole flow rate of component i, m is the carbon number of the fuel defined as $C_mH_nO_o$.

Nuvera's model takes into account both material balance and chemical reaction equilibrium to predict the outcome of fuel processing at the designed operating conditions. The model, implemented in Hysis software, calculates theoretical equilibrium composition of all reaction species at the temperature values experimentally verified in the MPR power train.
GTL Naphtha fuel processing resulted in the highest hydrogen yield and hydrogen production efficiency, which was predicted by model calculations and could be attributed to its highest H/C ratio. The increasing trend in hydrogen production with increasing H/C ratio is obtained experimentally for both fuels studied and confirmed by the model prediction shown in Figure 4 and 5. Methane slip was slightly higher in case of gasoline processing affected by lower operating temperature profile.

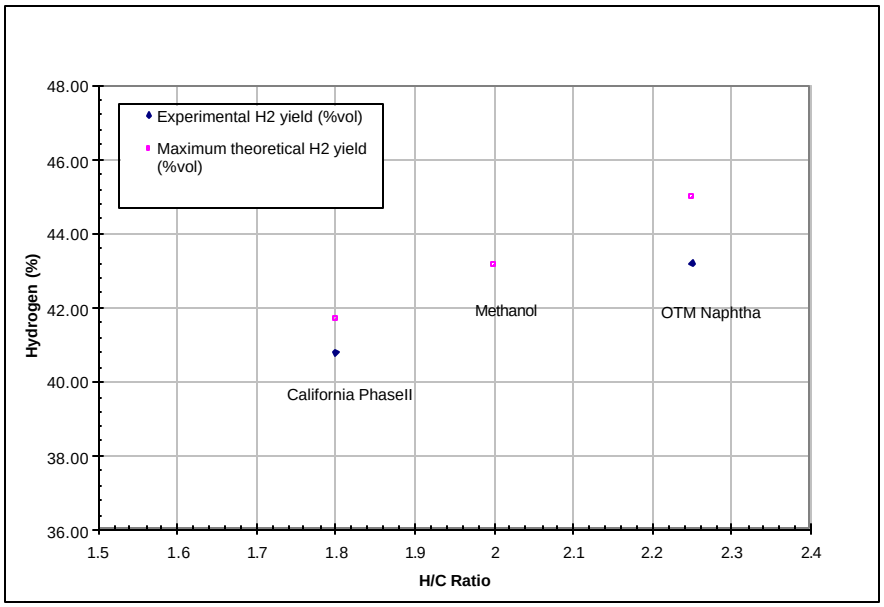

Figure 4. Hydrogen yield (experimental vs. theoretical) data at the entrance to fuel cell stack for fuels with different hydrogen-to-carbon ratios. Oxygen concentration in the fuel is accounted in methanol case for comparison.

The difference between theoretical and experimental points for gasoline fuel is about 0.8 volumetric percents of hydrogen , which is within the experimental error of 1.9 vol.%, this point was obtained with, as shown in Table 2.The difference between theoretical and experimental points for naphtha fuel is about 1.5 vol. % of hydrogen , which is higher than the experimental error of 0.49, this point was obtained with, as shown in Table 2. Higher difference between experimental and theoretical values recorded in naphtha processing versus gasoline was attributed to operating strategy of the clean-up section purposed to decrease the concentration of carbon monoxide below 20 ppm. This strategy was sacrificial to the concentration of hydrogen in the reformate stream. Since the current study was purposed on characterization of the entire power train, it was very important to balance all the subsystems within certain operating ranges, close to optimal to specific section but without sacrificing performance of another section of the power train at the same time, including the fuel cell stack.

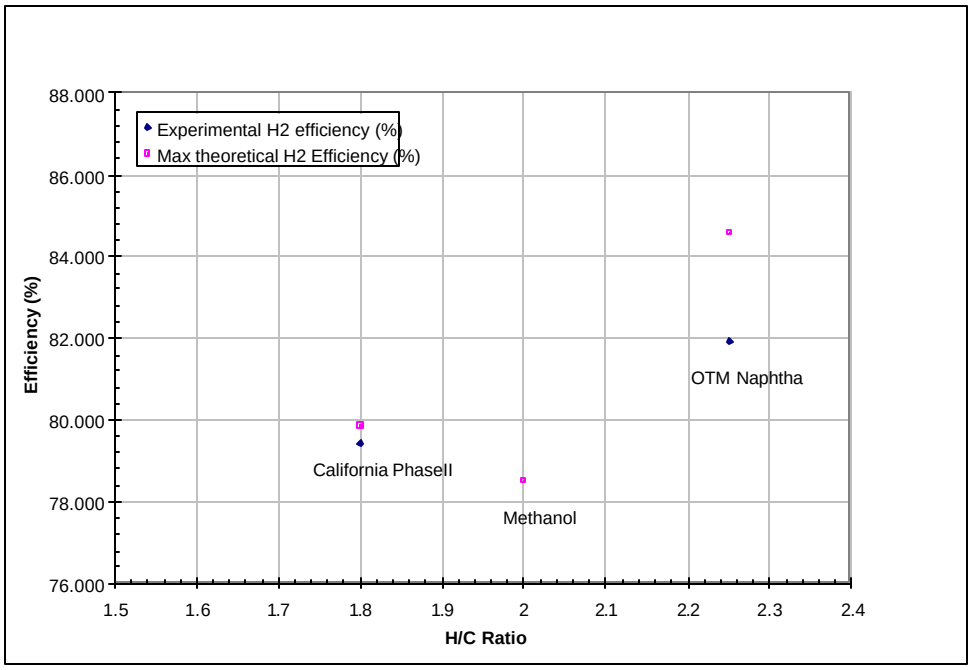

Figure 5. Hydrogen production efficiency (experimental vs. theoretical) at the entrance to fuel cell stack for fuels with different hydrogen-to-carbon ratios. Oxygen concentration in the fuel is accounted in methanol case for comparison.

To prove the good fuel conversion – close to equilibrium of the shift reaction- we compared the theoretical model to the experimental data at the exit of LTS section, presented below in Figures 6 and 7. For both studied fuels experimental data are close to the data predicted by modeling within the error ranges.

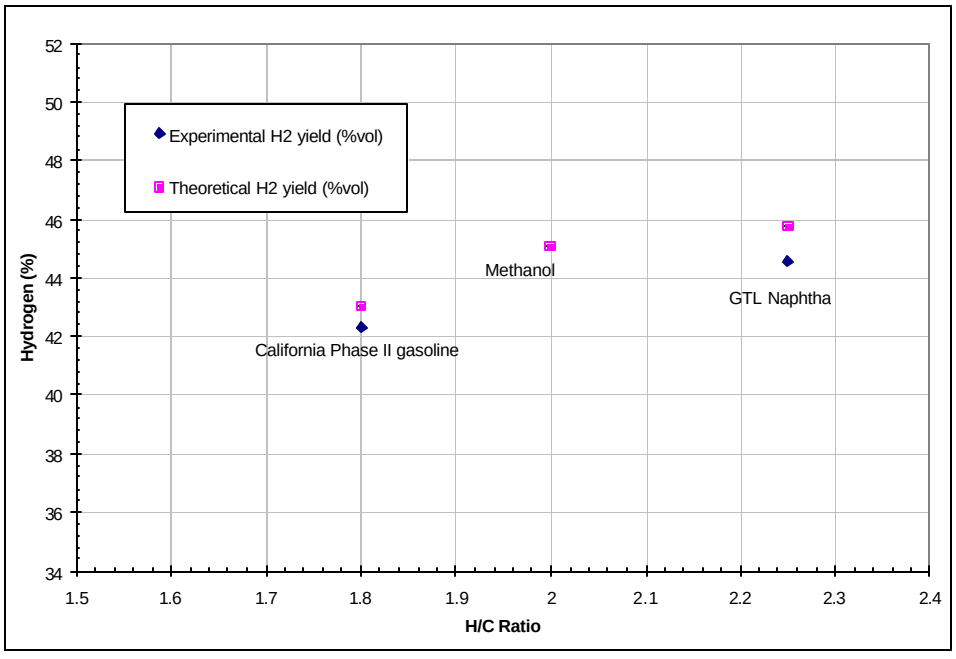

Figure 6. Hydrogen yield at the exit of LTS section (experimental vs. theoretical) data.

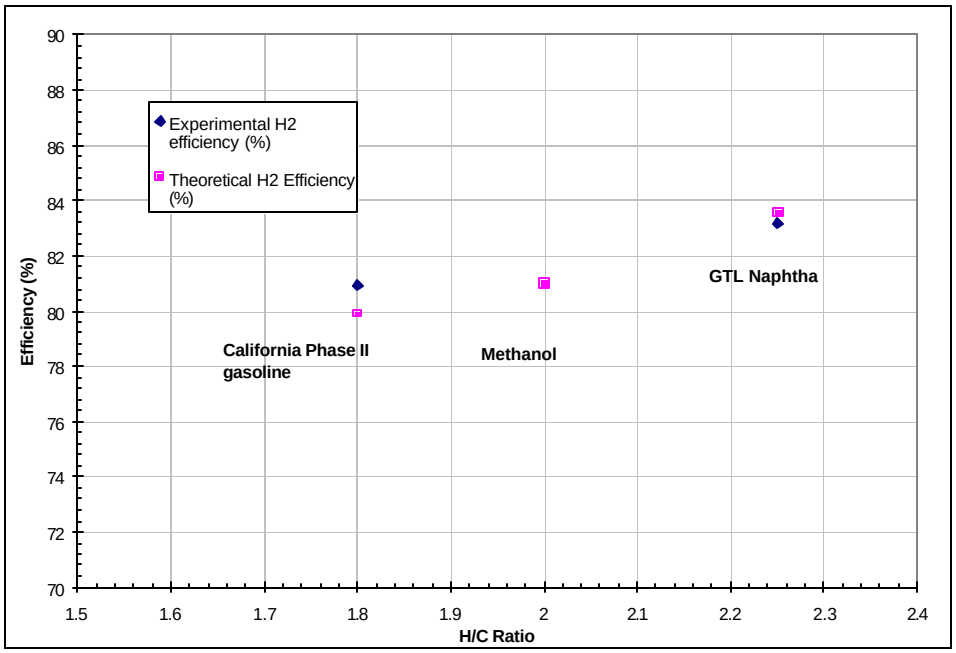

Figure 7. Hydrogen production efficiency at the exit of LTS section (experimental vs. theoretical) data.

Reformate flow was split after the LTS section of the fuel processor, in order to adhere to the maximum PROX throughput specification of 40 kW_{th}. Actual flow sent through the PROX was maintained at about 12 kW_{th}, based on the fuel cell stack size selected and the objective of running at realistic conditions (anode stoichiometries from 1.4-1.8). Carbon monoxide concentration at the PROX exit was varying in time, but consistently below 20 ppm in all fuel experiments.

The FTIR technique (model MIDAC 2001) had been used to detect species at low concentrations in both fuel reformates in the gas phase. The FTIR had been calibrated for aromatic species and ammonia. The sample to the FTIR was collected at the exhaust of clean-up section of the reforming process, which was the entrance to the fuel cell stack. In both studied reformates concentrations of above species were below detection limit of the FTIR.

As a complement to gas-phase analysis, process condensate was collected and analyzed for water-soluble species in the reformate streams, including volatile organic compounds (VOC), ammonia, metal ions and other potential contaminants. Samples were collected at two different locations:
(1) at the exit of CO cleanup section – fuel cell anode entrance
(2) at the fuel cell anode exhaust

At the exit of CO cleanup section low concentrations of aromatic compounds have been detected in the reformate condensates. The detected levels were close to the detection

limit, varied from 25 to 100 ppbv depending on sample dilution. Ammonia concentration in the condensate of the gasoline reformates after CO cleanup section was detected under 3 ppm. The total organic carbon (TOC) level varied below 5 ppm at the end of the power train for both fuel reformates. No above species have been detected in the condensates at the exit of the fuel cell stack operated on gasoline or naphtha reformates. For those species found elevated above the detection limit in the condensate analysis, but not detected in the gas phase, an estimation of the level in the gas phase was made based on partitioning equilibrium (Henry's Law). At a temperature of 25°C, the coefficient between the gas and liquid phases for ammonia is ~2.7. This means that 1-2 mg NH3/liter of water in the liquid phase would correspond to approximately less than one ppm of ammonia in the gas phase. This calculated concentration is difficult to detect even using FTIR due to the low detection limit.

The fuel cell stack used is shown in Figure 2, consisted of 30 cells and produced more than 3.25 KW of electrical DC power operating on pure hydrogen and air.
The difference in hydrogen concentration in gasoline and naphtha reformates was insignificant to change the polarization characteristics of the fuel cell, shown in Figure 8. The same stack was used for power generation on both fuel reformates. The base line polarization curve was recorded on hydrogen/air before introducing reformates to the stack and between the expriments with different fuels. There was no signs of short-term performance degradation caused by feeding the stack anode with neither of the reformate streams. The reformate flow entering the stack was maintained constant and equivalent to 12 kW of the fuel thermal input.

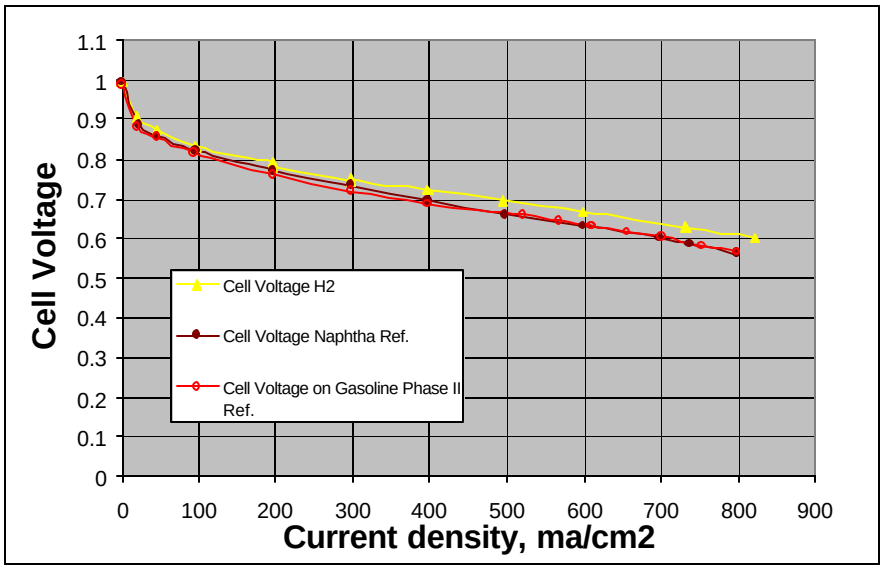

Figure 8. Polarization curves recorded on Naphtha and Gasoline Phase II ATR reformates vs. hydrogen/air performance.

It is possible to estimate the gross efficiency, denoted $\eta_{DC,gross}$, experimentally recorded at the MPR-fuel cell setup, as a ratio of the gross electrical power produced by the fuel cell to the calculated fuel input equivalent to the fuel processor (12 kWe, as previously stated).

$$\eta_{DC,gross} = 3.25 \text{ kWe} / 12 \text{ kWth} = 27\% \quad \text{(LHV basis)}$$

For a laboratory demonstration with no process optimization as in this study, this number is reasonable. In an integrated system, higher efficiencies would be achieved effected by anode hydrogen utilization and supplementing fuel to the burner. The specific operating conditions of the stack were as follows:

- Cathode stoichiometry of 2 was maintained constant at all the points on polarization.
- Anode flow was maintained constant at all the points on polarization chart equivalent to anode stoichiometry of ~1.5 at the highest current density reached.
- The stack temperature was maintained at 70ºC measured at the cathode exhaust. The cathode air inletting the stack was humidified at the temperature of 65ºC above 80 % of relative humidity using external to the stack Nuvera's humidification module. The stack has an internal cooling loop utilizing deionized water as a coolant.
- The DC power produced by the stack was recorded and sustained by the electronic Dynoload operated in the constant current mode.
- Both anode and cathode of the stack were maintained at 2.5 bara of downstream pressure in all the fuel reformate experiments.
- The fuel cell had been running on every fuel reformate for about one hour to allow stabilization of cell voltages at the current density up to 800 mamp/cm^2 and recording fuel cell utilization confirmed by GC analysis of inlet and outlet anode flow composition. GC measurement also served as a confirmation of total amount of hydrogen presented in the incoming reformate flow after PROX and condenser units. At the end of each fuel cell run the polarization curve shown in Figure 8 was recorded.

The derating factor on fuel reformates versus operation on pure hydrogen is calculated as the difference between voltage sustained by the fuel cell on pure hydrogen and fuel reformate at the same operating current density. This approach defines the performance or voltage derate, denoted ? $_V$, and, on both reformates, is estimated at 4.5% of power at 400 mA/cm2 of current density and about 7% at 600 mA/cm^2 versus power production on pure hydrogen at the corresponding current densities. The power production curves are shown in Fig.9.

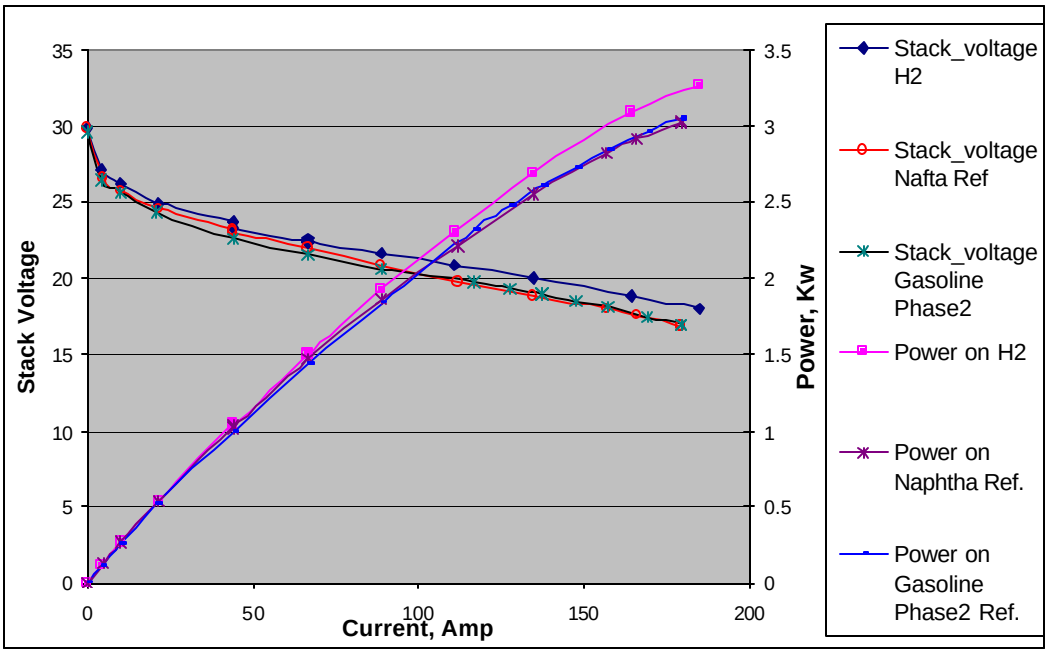

Figure 9. Power production of 30 cell stack on Naphtha and gasoline reformates vs. pure hydrogen.

Maintaining high hydrogen utilization at the fuel cell anode at the elevated current densities is a technical challenge associated with the decreased concentration of hydrogen along it's consumption and increased dilutants – nitrogen, carbon dioxide and water- at the exit of the stack. Maintaining water balance to avoid stack flooding represent current state-of-the art technology along with the insights of the fuel cell stack , adding complexity to the issue of reformate utilization and ,finally, efficiency. Mapping hydrogen utilization by the fuel cell stack operating on fuel reformate to the current density would result in the stack sizing tradeoff issues versus operating efficiency and would be the subject of separate study.

Conclusions of Phase I.

- GTL Naphtha and California Phase II RFG were successfully processed into fuel cell quality reformate in Nuvera's ATR based modular pressurized facility.
- DC power production was demonstrated in Nuvera's fuel cell stack on both fuel reformates studied.
- Both fuels were studied for hydrogen yield and reforming efficiency and experimental data were compared to the theoretical simulation data.
- Hydrogen yield and reforming efficiency demonstrated by naphtha processing were higher than for gasoline fuel, which was predicted by system analysis of both fuels. Since gasoline contained sulfur, the power train configuration had an increased complexity and maintaining stable temperature profile became a challenging task in comparison to naphtha processing.
- The power production in the fuel cell stack was not effected by operating on different fuel reformates, since hydrogen partial pressure in the reformate streams varied insignificantly.
- The gross efficiency of the power production in fuel cell is estimated at 27%, considering 3.25 kW electrical output of the stack and the fuel thermal input of 12 kW. In the stand-alone fuel cell power plant more parameters affect efficiency. Hydrogen utilization at the anode and necessity of fuel supplement in the burner would strongly influence the overall power plant efficiency.
- Both fuel reformates were considered equivalent in terms of containing no carbon monoxide emissions in the fuel cell exhaust stream to the burner, however, reformate condensates contain micro quantities of "potential bad actors" such as ammonia and aromatics in both fuels studied. Longevity of the fuel cell operation and effects of potential contaminants at micro levels should be the subject of a separate study.

Phase II. Testing of Syngas-Derived Ultra-Clean Fuels in Nuvera's burner module for start-up emission study.

Phase II objectives.

Evaluate selected fuels: GTL naphtha, oxygenated GTL naphtha and California Phase II RFG in Nuvera's burner module and compare emissions produced in the fuel processing/fuel cell power plant. The GTL naphtha was oxygenated with a proprietary oxygenate compound, designated BPO, provided by BP.

Experimental.

Nuvera's Burner facility comprises of Nuvera's Burner module, gas and condensate sampling system, and all the process streams required for clean processing of different fuels. The experimental layout of burner facility is shown in Figure 10.

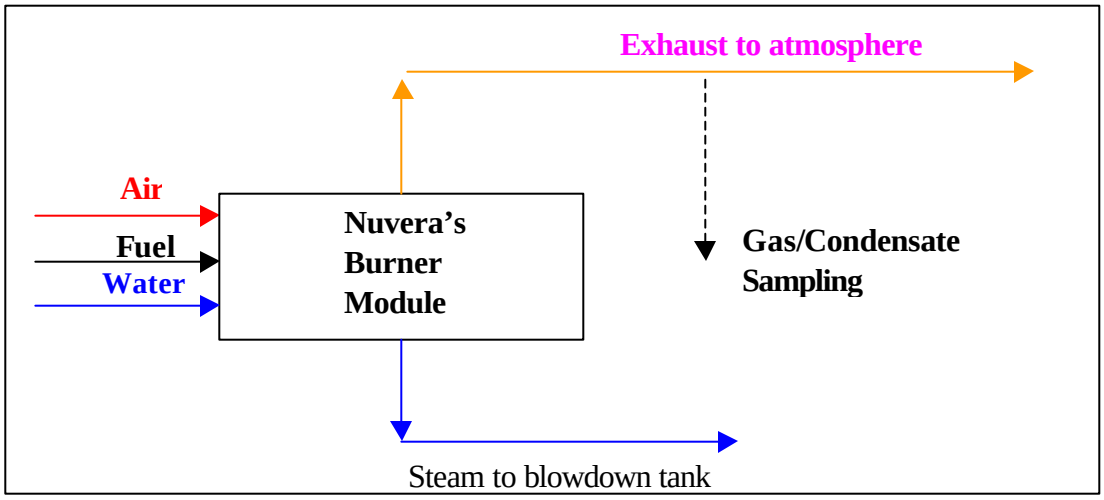

Figure 10: Experimental layout of Nuvera's Burner Module.

Table 3 below contains some characteristics of the fuels studied**.**

Table3: Properties of fuel used in Nuvera's Burner Module for startup emission study.

Fuel Properties	Oxygenated GTL Naphtha	GTL Naphtha	California Phase II RFG
API Gravity	71.86	73.4	60.57
Specific Gravity, 60F/60F	0.6958	0.6906	0.7367
Density, kg/m^3	695.8	690.6	736.7
C, m%	82.44	84.1	84.96
H, m%	15.82	15.9	13.02
O, m%	1.74	0	2
N, ppm	<1	<1	<1
S, ppm	1	0	32.9
Lower heating value LHV, kJ/kg	43945.89	44357.44	40983.13
(Air/Fuel)$_{stoich}$	14.79	15.08	14.12
Estimated molecular weight, gm/gm-mol	99.4	101.0	100.95

Table 4 below shows operating conditions of the burner module on all studied fuels. To start fuel ignition a slightly rich mixture of fuel and air (air-to-fuel equivalence ratio between 1.2 to 1.4) is introduced to the burner. As soon as the burner is lit, the equivalence ratio is decreased to a lean condition (typically below 0.95) to minimize hydrocarbon emissions.

Table 4: Operating parameters of Nuvera's Burner Module on three fuels studied.

Operating Parameters	GTL Naphtha	Oxygenated GTL Naphtha	California Phase II RFG
Thermal input, based on LHV, kW	12	12	12
Start-up air-to-fuel equivalence ratio	1.39	1.4	1.41
Steady state air-to-fuel equivalence ratio	0.95	0.95	0.95
Operating pressure, bars	1.01325	1.01325	1.01325

Details of Nuvera's gas sampling system and analyzers used in the study are collected in Table 5, showing ranges of concentrations the burner exhaust gas was analyzed for.

Table 5: Emission species and concentrations analyzed.

Emissions Species	Units	Maximum Analysis Range	Analyzer Unit
CO	ppm	1000 ppm	Horiba infrared analyzer model number VIA-510
CO	vol %	50%	Horiba infrared analyzer model number VIA-510
CO2	vol %	25%	Horiba infrared analyzer model number VIA-510
NOx	ppm	2000 ppm	Horiba chemiluminescence analyzer model number CLA-510SS
O2	vol %	50%	Horiba magnetic pressure analyzer model number MPA-510
THC	ppm	30000 ppm	Horiba flame ionization analyzer model number FIA-236

Results and discussion.

All studied fuels were successfully processed in Nuvera's Burner Module for start-up emissions. Exhaust gas composition was analyzed for bulk components such as carbon dioxide, water vapors and oxygen, and traces of species, such as NOx, carbon monoxide (CO) and total hydrocarbons (THC) that are governed by emission standards from the Environmental Protection Agency (EPA). In addition, process condensates were collected for analysis of water contaminants in the burner exhaust. The fuels under study were compared in terms of burner module operating conditions, exhaust compositions, start-up and steady state emissions. In order to compare emissions from Nuvera's Burner module to the EPA standards, recorded concentrations of emission species in parts per million (ppm) are presented in milligrams per gram of fuel (mg/gfuel) units in Figure 11, 12, and 13 for naphtha, oxygenated naphtha and California Phase II RFG respectively.

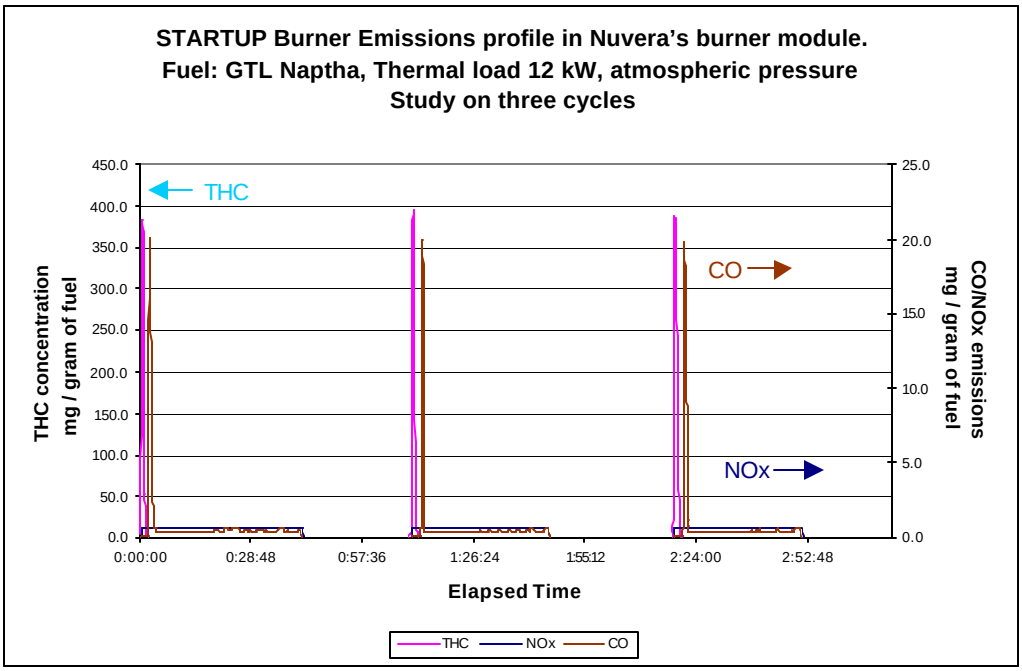

Figure 11: Burner emissions on GTL Naphtha.

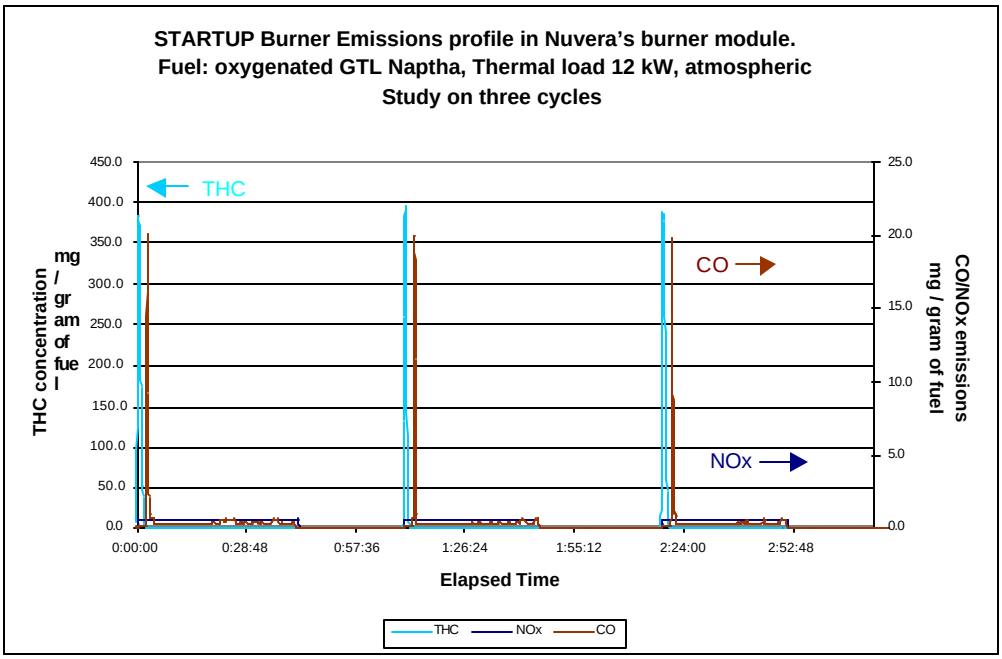

Figure 12: Burner emissions on oxygenated GTL naphtha.

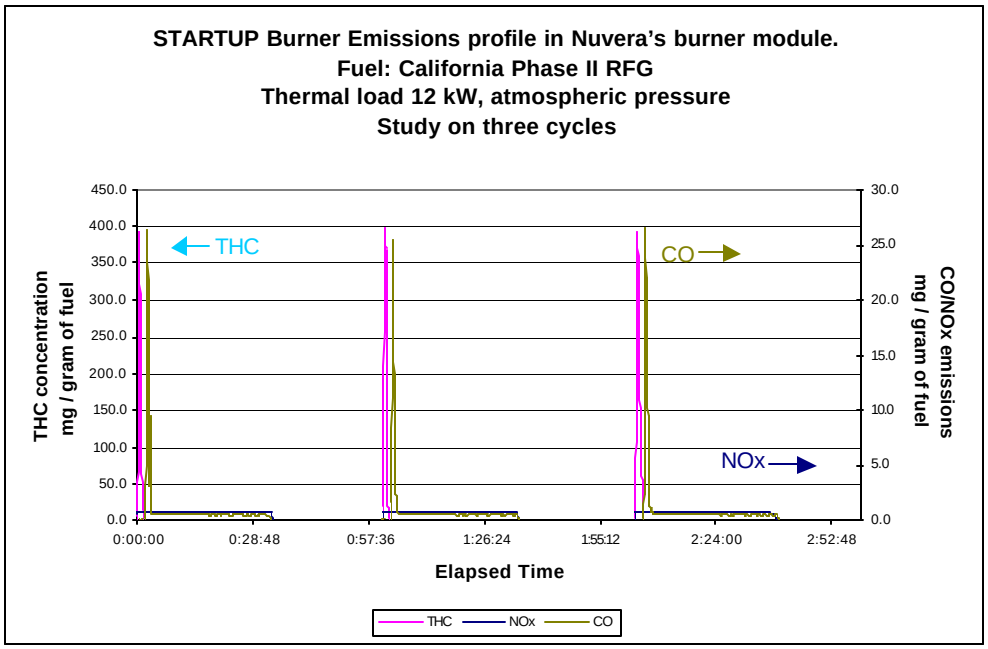

Figure 13: Burner emissions on California Phase II RFG.

To ensure repeatability of the experiments, the burning cycle of each fuel was conducted at least three times starting with the fuel ignition through the startup and steady state phase and ending with cooling burner to initial temperature. All concentration profiles are highly repeatable for each fuel as shown in Figures 11,12 and 13.

All fuels show spikes of THC and carbon monoxide emissions at the burner startup. This is attributed to unburned fuel skipping through the module when it is lit initially. The CO spike occurred due to incomplete fuel combustion. No spikes in NOx emissions were recorded for any fuel at the startup conditions. Concentration of NOx is much less than the concentration of CO and THC as shown in Figure 11,12 and 13. Comparison of NOx concentration profiles at the startup conditions is shown in Figure 14 for all fuels studied.

There are two principal sources of nitrogen oxide (NOx) formed during combustion: one is oxidation of atmospheric (molecular) nitrogen and another is oxidation of nitrogen-containing compounds in the fuel. During combustion of studied "clean" fuels, containing no nitrogen compounds, under lean or stoichiometric conditions the thermal mechanism is the principal source of nitrogen oxide emissions.

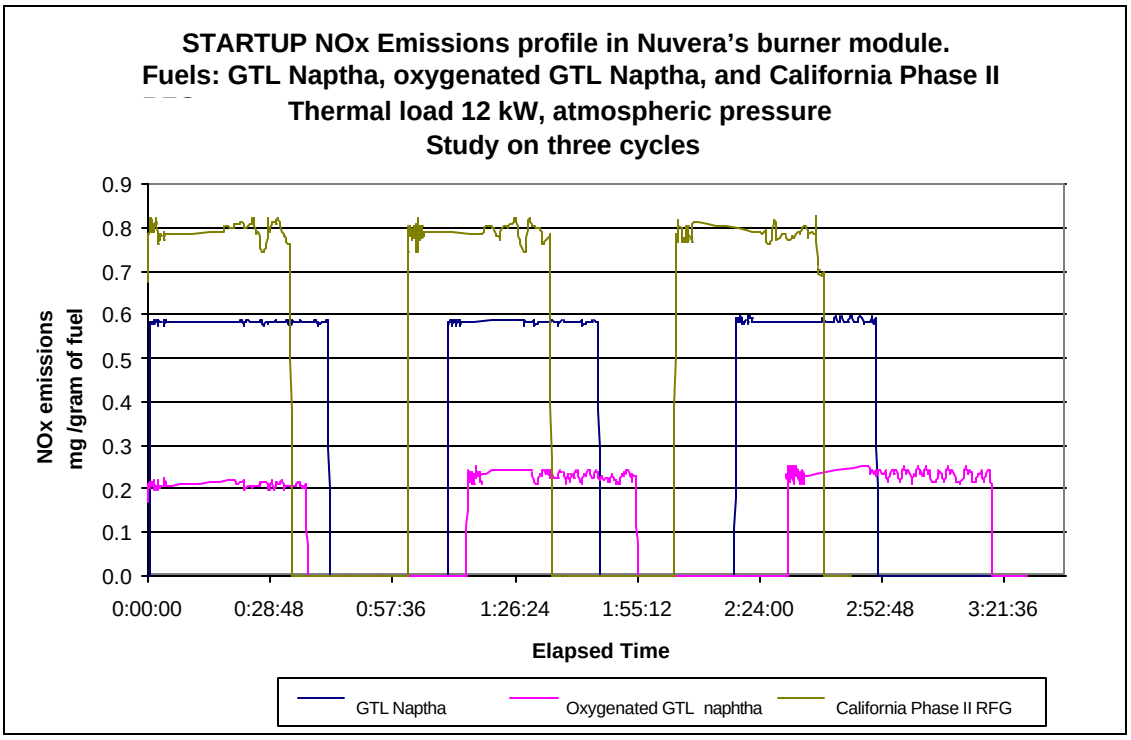

Figure 14: NOx emissions profile of studied fuels.

Integrated startup emissions for all three fuels tested are shown in Table 6 and are reported on the mass basis in milligrams per gram of every fuel and in gram of emission species per driving mile. To present the recorded data in the latter units, the current Corporate Average Fuel Economy (CAFÉ) standard of 27.5 miles per gram of fuel was used in calculation. The integrated values were calculated using total amount of startup emissions divided by the amount of fuel used during respective startup time.

Table 6: Emissions at startup.

FUEL	mg per gram of fuel			gram per mile		
	CO	THC	NOx	CO	THC	NOx
GTL Naphtha	7.34	110.78	0.57	0.70	10.53	0.05
Oxygenated GTL Naphtha	5.61	78.07	0.23	0.54	7.48	0.02
California Phase II RFG	6.28	92.24	0.79	0.64	9.35	0.08

Table 6 shows that oxygenated GTL naphtha has the lowest CO, THC, and NOx startup emissions among all fuels tested. This can be attributed to the oxygen added to the fuel. GTL naphtha and oxygenated GTL naphtha have almost the same fuel blend except oxygenated GTL naphtha contains 1.74% oxygen. It seems that adding oxygen to the fuel results in more complete fuel combustion and, subsequently, reducing tailpipe emissions. Oxygenated fuel also tends to provide more complete combustion of its carbon into carbon dioxide (CO_2), thereby reducing emissions of hydrocarbons and carbon monoxide. Even though both oxygenated GTL naphtha fuel and California Phase II RFG gasoline have similar oxygen concentration in the fuel

(1.74 and 2 % respectively), emissions from gasoline burning are higher than emissions from oxygenated GTL naphtha. This could be explained by high percentage of aromatic compounds in California Phase II RFG, which satisfies it's high octane rating.
Emissions recorded during steady state combustion are shown respectively for all fuels studied in Figures 15, 16, and 17.

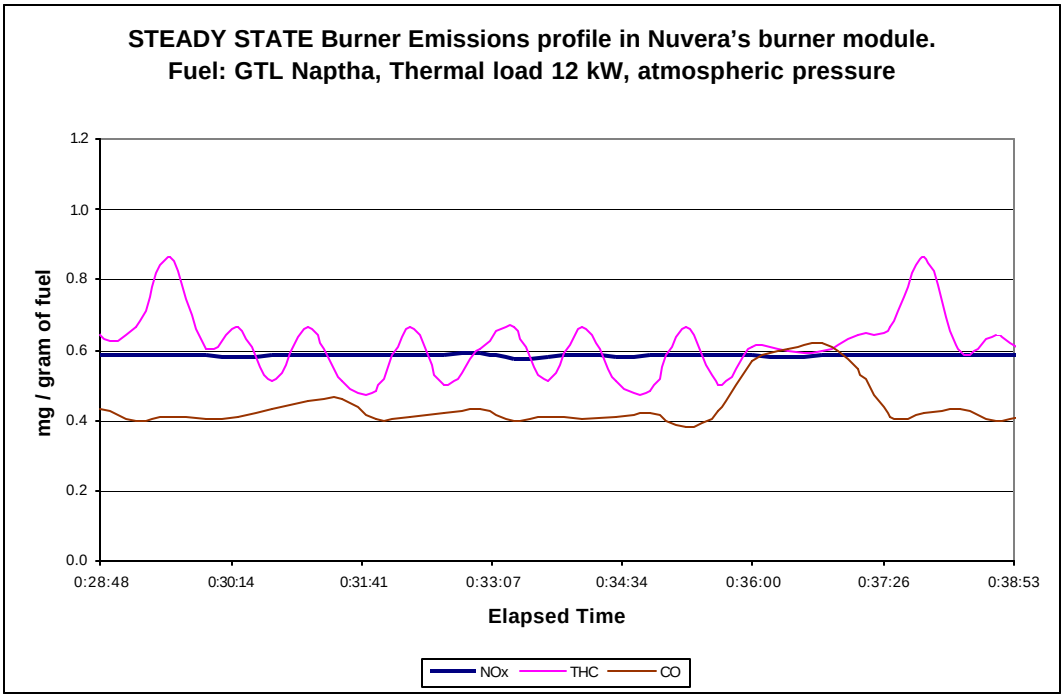

Figure 15. Steady state burner emission on GTL naphtha.

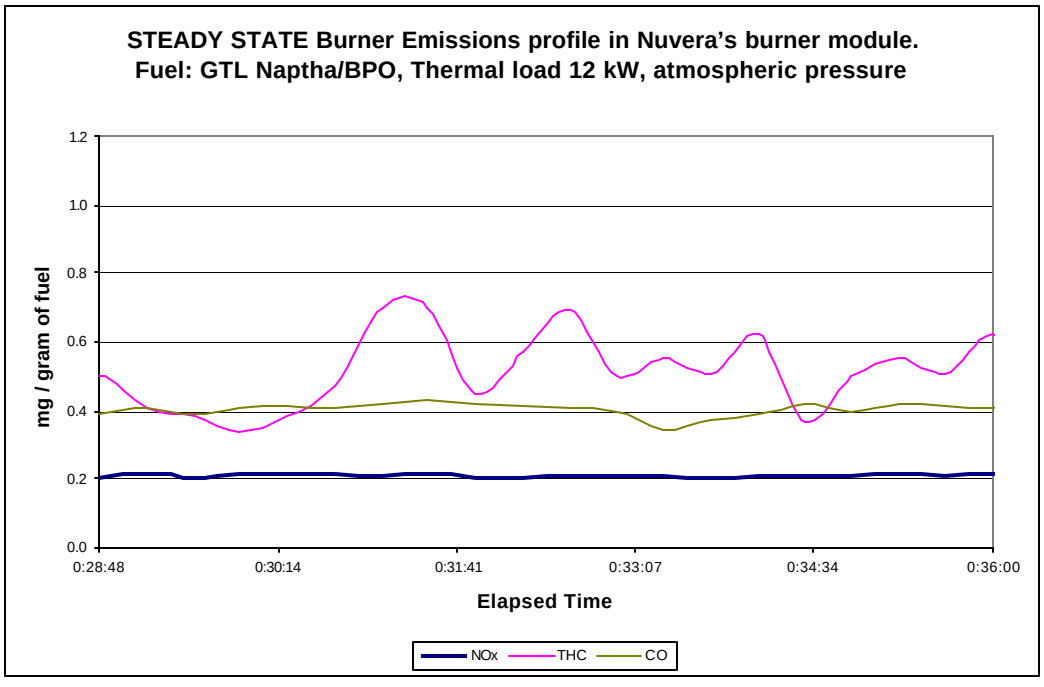

Figure 16. Steady state burner emissions on oxygenated GTL naphtha.

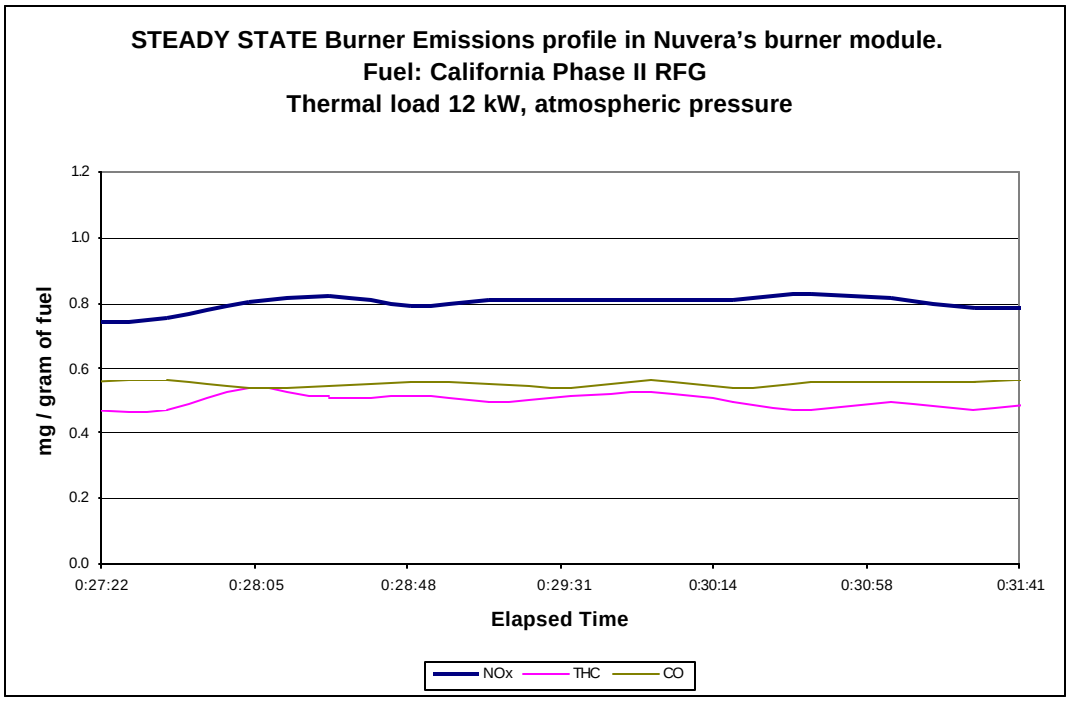

Figure 17. Steady state burner emissions on California Phase II RFG.

Table 7 shows steady state emissions of three fuels averaged throughout the single burning cycle. Note, that quality of Nuvera's burner exhaust gas satisfied all the Federal standards for light duty vehicles including ULEV requirements for CO and Nox, as shown below.

Table 7. Emissions throughout steady state.

FUEL	mg per gram of fuel			gram per mile		
	CO	THC	NOx	CO	THC	NOx
Federal Standard for Light Duty Vehicle – Tier 1				4.2	0.31	0.6
Federal Standard for Light Duty Vehicle – Ultra Low Emission Vehicles (ULEV)				2.1	-	0.3
GTL Naphtha	0.42	0.61	0.57	0.040	0.058	0.054
oxygenated GTL Naphtha	0.41	0.61	0.23	0.039	0.058	0.022
California Phase II RFG	0.55	0.52	0.79	0.056	0.053	0.080

Addition of oxygen to the naphtha blend did not effect steady state emissions of hydrocarbons and carbon monoxide as shown in table 7. However, NOx emissions are decreased in the oxygenated naphtha fuel blend that may be attributed to the oxygen presence in the fuel. Table 7 indicates that California Phase II RFG produced the highest amount of poisons to the environment on the absolute mass basis, and from this point could be considered the worst fuel blend among all three fuels at the steady state conditions. This can be attributed to high-octane aromatics presence. At the same time gasoline produced less total hydrocarbons than synthetic fuel blends.

Nuvera developed specific FTIR technique to get insights on what hydrocarbon species were released from the burner. The FTIR was calibrated for methane at 15 ppm. The FTIR spectra of the burner exhaust gas showed levels of methane close to the recorded by flame ionization detector concentrations of THC for all three fuels studied. The found phenomenon could be specific to the performance of the catalyst in the burner rather than fuel inherited, since fuels of different structure were burned resulting in dominating amount of methane in the THC emissions. Table 8 shows average concentrations of bulk gases in the burner exhaust: oxygen and carbon dioxide for all three fuel blends.

Table 8. Oxygen and carbon dioxide emissions.

Fuel	vol. %	
	O_2	CO_2
GTL Naphtha	13.85	6.04
Oxygenated GTL Naphtha	13.72	5.76
Cal Phase II RFG	11.85	10.8

GTL naphtha and oxygenated GTL naphtha have almost the same oxygen and carbon dioxide concentrations in the burner exhausts. This is expected since both fuels have almost the same fuel compositions. It seems that adding oxygen to the Naphtha blend didn't influence oxygen and carbon dioxide emissions significantly.

In addition to the gas phase analysis process condensates were collected at the burner exhaust and analyzed for volatile organic compounds, metal ions, ammonia, aldehydes and other poisons to the environment, results are shown in Table 9. All condensates had been collected in steady state condition, while running fuels through the burner in the steady state. Several condensate samples were collected from the same operating regime to ensure repeatability.

Table 9. Condensate analysis.

Fuel	Ammonia, ppmv	Acet aldehyde, ppmv	Formaldehyde, ppmv	Benzene, ppbv	Toluene, ppbv	Ethyl Benzene, ppbv	Xylenes, total, ppbv
GTL naphtha	1.8-2.1	0.13	1.35	Below detection limit (Bdl)	Bdl	Bdl	Bdl
Oxygenated GTL naphtha	1.1-1.5	0.05	1.29	Bdl	Bdl	Bdl	Bdl
California phase II gasoline	1.2	0.0002	0.0057	6-7	33-38	12-16	53-68

All fuel condensates contained ammonia and aldehydes, while no aromatic compounds were detected in naphtha's condensates as expected from the fuel structure. Presence of micro quantities of ammonia and aldehydes in the liquid phase suggests that these species are presented in the gas phase as well according to the equilibrium. Example of partitioning between gas and liquid phase for ammonia is described in the phase I of the current report. Analogically this analysis is applicable to aldehydes.

Condensate analysis of volatile organic compounds served an indirect confirmation that most of the THC emissions were not of organic origin but rather methane recognized by the FTIR analysis. Even in the case of gasoline condensates the total concentration of VOC found was around hundreds of parts-per-billion, corresponding through Henry's law to low part-per-million levels of VOC in the gas phase, which was significantly less than the levels of THC recorded by flame ionization detector and methane found by the FTIR.

Conclusions of Phase II.

- GTL naphtha, oxygenated GTL naphtha and California Phase II gasoline were successfully tested in Nuvera's Burner Facility for start-up and steady state emissions.
- Exhaust gases from all fuels tested were analyzed for bulk gases such as carbon dioxide and oxygen and emissions of CO, NOx, and total hydrocarbons.
- Burner condensates were collected for analysis of potential contaminants to the environment in the liquid state.
- Adding oxygen to the naphtha fuel blend reduced start-up emissions of carbon monoxide, NOx and hydrocarbons.
- Adding oxygen to the naphtha fuel blend did not effect the steady state emissions of carbon monoxide and hydrocarbons but resulted in reducing NOx emissions.
- Adding oxygen to the naphtha fuel blend did not affect the oxygen and carbon dioxide emissions.
- Burning oxygenated GTL naphtha resulted in the least amount of emissions among the three fuels studied due to oxygen presence and lack of high-octane aromatics.
- Hydrocarbon emissions consisted of mostly methane, not VOC compounds.
- All processed fuels produced fewer emissions than Federal standards require for Light Duty Vehicles on a per mile basis in the steady state conditions. Oxygenated naphtha resulted in the least absolute amount of emissions on a per mile basis. California phase II gasoline proved to yield the highest emissions in the steady state.
- Oxygenated naphtha was mostly clean among all fuels at the startup conditions, while GTL naphtha produced higher emissions than gasoline fuel.
- All fuel after-burner condensates contain micro levels of ammonia and aldehydes. Gasoline fuel condensate also contained ppb levels of aromatic compounds. It is possible to speculate on the level of micro contaminants found in the liquid phase for the gas phase, however, it would be the subject of further research beyond the scope of the current program.